

**Experimental therapeutic approaches against
hyperglycemia-induced mitochondrial injury
in endothelial cells**

PhD thesis

Domokos Gerő M.D.

Doctoral School of Basic and Translational Medicine
Semmelweis University



Consultant: Miklós Mózes, M.D., Ph.D.

Official reviewers: János Nacsa, M.D., Ph.D.
Ákos Zsembery, M.D., Ph.D.

Head of the Complex Exam Committee:
Anikó Somogyi, M.D., D.Sc.

Members of the Complex Exam Committee:
György Jermendy, M.D., D.Sc.
György Nádasy, M.D., Ph.D.
Éva Szőke, D.Sc.

Budapest
2018

TABLE OF CONTENTS

LIST OF ABBREVIATIONS	4
1. SCIENTIFIC BACKGROUND	8
1.1. Introduction.....	8
1.2. Characteristics of the damage.....	8
1.2.1. Glucose and oxidative stress in diabetic vascular damage	8
1.2.2. Target cells of hyperglycemia.....	10
1.2.3. Time course of hyperglycemic injury	11
1.3. Triggers of endothelial dysfunction and damage.....	12
1.3.1 Hyperglycemia and ‘glucose memory’	12
1.3.2. Downstream molecules responsible for the injury.....	15
1.4. Mechanisms of ROS production in hyperglycemia	15
1.4.1. Glucose-induced oxidative stress pathways.....	15
1.4.2. Unifying hypothesis: the role of mitochondrial oxidants	19
1.4.3. The mechanism of glucose-induced mitochondrial superoxide generation..	20
1.5. Mechanism of damage: Cell damaging responses to ROS production in hyperglycemia	26
2. AIMS	30
3. MATERIALS AND METHODS	32
3.1. Compound libraries and commercially available drugs	32
3.2. Synthesis of mitochondrial H₂S donors (10-(4-Carbamothioylphenoxy)-10-oxodecyl) triphenylphosphonium bromide (AP123) and (10-Oxo-10-(4-(3-thioxo-3H-1,2-dithiol-5-yl)phenoxy) decyl)triphenylphosphonium bromide (AP39)	32
3.3. H₂S release detection in solution and <i>in situ</i> in endothelial cells	34

3.4. Cell culture and cell-based screening for inhibitors of hyperglycemia induced mitochondrial ROS production.....	35
3.5. Measurement of cytoplasmic ROS generation.....	36
3.6. <i>In situ</i> detection of ROS generation	37
3.7. Mitochondrial ROS measurement in isolated mitochondria.....	37
3.8. Xanthine-oxidase assays	38
3.9. Viability assays: MTT and LDH assays, ATP measurement.....	38
3.10. Mitochondrial membrane potential measurement	39
3.11. Gene expression array	40
3.12. siRNA mediated gene silencing and real-time PCR measurements.....	40
3.13. Mitochondria isolation and western blotting	41
3.14. Detection of oxidative nucleic acid and protein damage.....	42
3.15. Detection of oxidative damage of the mitochondrial DNA (mtDNA).....	43
3.16. Respiratory complex II/ III activity assay	43
3.17. Extracellular Flux Analysis.....	44
3.18. Vascular studies of <i>in vitro</i> hyperglycemia	45
3.19. Vascular studies of streptozotocin-induced diabetes.....	45
3.20. Statistical analysis	45
4. RESULTS	46
4.1. Characterization of the hyperglycemic endothelial cell injury model.....	46
4.2. Cell-based screening for inhibitors of hyperglycemia-induced mitochondrial ROS production in endothelial cells.....	49
4.3. Characterization of the mode of action of hit compounds	53

4.3.1. The mechanism of action of paroxetine: mitochondrial superoxide scavenging in hyperglycemic endothelial cells.....	53
4.3.2. Paroxetine protects against oxidative damage: prevents the hyperglycemia- and diabetes-induced endothelial dysfunction in vascular rings.....	60
4.3.3. Glucocorticoids inhibit the mitochondrial ROS production in microvascular endothelial cells	63
4.3.4. The mode of action of glucocorticoids: restoration of the mitochondrial potential via UCP2 induction.....	66
4.3.5. The mode of action of mitochondria-targeted H ₂ S-donor compounds against mitochondrial ROS production in hyperglycemic endothelial cells	75
5. DISCUSSION	84
5.1. Cell-based screening identifies currently approved drugs with repurposing potential and novel chemotypes as inhibitors of hyperglycemic endothelial ROS production.....	84
5.2. The mode of action of select hit compounds.....	89
5.2.1. Paroxetine acts as mitochondrial superoxide scavenger	89
5.2.2. Glucocorticoids block the mitochondrial ROS production via UCP2 induction in microvascular endothelial cells.....	91
5.2.3. H ₂ S donors act as electron donors to the respiratory chain in endothelial cells	93
6. CONCLUSIONS	98
7. SUMMARY	99
8. REFERENCES.....	101
9. BIBLIOGRAPHY OF THE CANDIDATE’S PUBLICATIONS.....	132
10. ACKNOWLEDGEMENTS	140
11. SUPPLEMENTARY MATERIAL	141

List of abbreviations

ADP adenosine diphosphate
ADT-OH desmethyl anethole dithiolethione
AGEs advanced glycation end products
AMP adenosine monophosphate
AMPK AMP-activated protein kinase
ANOVA one-way analysis of variance
AP123 (10-(4-Carbamothioylphenoxy)-10-oxodecyl) triphenylphosphonium bromide
AP39 (10-Oxo-10-(4-(3-thioxo-3H-1,2-dithiol-5-yl)phenoxy) decyl)triphenylphosphonium bromide
ATP adenosine triphosphate
ATP5A1 ATP synthase subunit alpha
AzMc 7-azido-4-methylcoumarin
BCA bicinchoninic acid assay
BCAA branched chain amino acid
BER base excision repair
BSA bovine serum albumin
CCD charge-coupled device
cDNA complementary DNA
cGMP cyclic guanosine monophosphate
CM-H₂DCFDA 5-(and-6)-chloromethyl-2',7'-dichlorodihydrofluorescein diacetate
CN-POBS N-cyclohexyl-4-(4-nitrophenoxy)benzenesulfonamide
CoQ coenzyme Q, ubiquinone
COX3 cytochrome c oxidase III
CTL control
Cyt C cytochrome C
DADS diallyldisulfide
DAMP damage-associated molecular patterns
DATS diallyltrisulfide
DC protein assay detergent compatible protein assay
DETAPAC diethylenetriaminepentaacetic acid
DHAP dihydroxyacetone phosphate

DMEM Dulbecco's modified Eagle's medium
DMSO dimethyl-sulfoxide
DNA deoxyribonucleic acid
ECAR extracellular acidification rate
EDTA ethylenediaminetetraacetic acid
eNOS endothelial nitric oxide synthase
EXOG *exo*/endonuclease G
Ex/Em excitation/emission
F6P fructose-6-phosphate
FAD/FADH₂ flavin adenine dinucleotide
FBS fetal bovine serum
FCCP carbonyl cyanide *p*-trifluoromethoxyphenylhydrazone
FOXO1 forkhead-box O1 protein 1
GAPDH glyceraldehyde-3-phosphate dehydrogenase
G6PDH glucose-6-phosphate dehydrogenase
GLUT1 glucose transporter 1
GR glucocorticoid receptor
GRE glucocorticoid response element
GSH/GSSG reduced/oxidized glutathione
GTP guanosine triphosphate
H₂O₂ hydrogen peroxide
H₂S hydrogen sulfide
HbA1c glycated hemoglobin
HEPES (4-(2-hydroxyethyl)-1-piperazineethanesulfonic acid)
HMGB1 high-mobility group box 1
hnRNP-K heterogeneous nuclear ribonucleoprotein-K
hOGG1 8-oxoguanine DNA glycosylase
HTB 4-hydroxythiobenzamide
INT 2-(4-Iodophenyl)-3-(4-nitrophenyl)-5-phenyl-2*H*-tetrazolium chloride
Keap1 Kelch-like erythroid cell-derived protein with Cap 'n' collar (CNC) homology (ECH)-associated protein 1
LDH lactate dehydrogenase
LKB1 tumor suppressor liver kinase B1
miRNA microRNA

MnSOD manganese-dependent superoxide dismutase
mtDNA mitochondrial DNA
MAO monoamine oxidase
mitoKATP mitochondrial ATP-sensitive potassium channel
MitoQ mitochondria-targeted ubiquinol
mitoTEMPO mitochondria-targeted piperidine nitroxide TEMPO
MTCO1 Cytochrome c oxidase subunit I
mTOT mitochondrial target of TZDs
MTT thiazolyl blue tetrazolium bromide
NAD⁺/NADH nicotinamide adenine dinucleotide
NADP⁺/NADPH nicotinamide adenine dinucleotide phosphate
NamPRT nicotinamide phosphoribosyltransferase
NaSH sodium hydrosulfide
Na₂S sodium sulfide
NDUFB8 NADH dehydrogenase (Ubiquinone) 1 beta subcomplex 8
NF-κB nuclear factor kappa B
NO• nitric oxide
NOD mice non obese diabetic mice
Nrf2 nuclear factor E2-related factor 2
NSAIDs non-steroidal anti-inflammatory drugs
O₂•⁻ superoxide
OCR oxygen consumption rate
OD optical density
ONOO•⁻ peroxynitrite
OXPHOS oxidative phosphorylation
p66SHC 66-kDa Src homology 2 domain-containing protein
PARP poly(ADP-ribose) polymerase
PBS phosphate-buffered saline
PCR polymerase chain reaction
PDE5 cGMP phosphodiesterase
PGC-1 PPAR-γ coactivator 1-α
PKC protein kinase C
PMS N-methylphenazonium methyl sulfate

Poly DNA polymerase gamma
PPAR- γ peroxisome proliferation activating receptor- γ
PPR proton production rate
RAGE receptor of AGEs
RET reverse electron transfer
RIPA buffer radio immunoprecipitation assay buffer
ROS reactive oxygen species
RNA ribonucleic acid
S3QELs (“sequels”) selective suppressors of site III_{OQ} electron leak
SDHB Succinate dehydrogenase [ubiquinone] iron-sulfur subunit
sGC soluble guanylate cyclase
siRNA silencing RNA
SIRT1 sirtuin 1
SOD superoxide dismutase
SOD2 superoxide dismutase 2
SQR sulfide:quinone oxidoreductase
SSRI selective serotonin reuptake inhibitor
STZ streptozotocin
TC₅₀ toxic concentration for the 50% of the cells
TCA cycle tricarboxylic acid cycle
TFAM mitochondrial transcription factor A
Tris tris(hydroxymethyl)aminomethane
TPP⁺ triphenylphosphonium
TZD thiazolidinedione
UCP1 uncoupling protein 1
UCP2 uncoupling protein 2
UCP3 uncoupling protein 3
UKPDS United Kingdom Prospective Diabetes Study
UV ultraviolet
VEGF vascular endothelial growth factor
V_{max} maximum velocity
WHO World Health Organization

1. Scientific background

1.1. Introduction

The significance of hyperglycemia-induced endothelial damage is underlined by its pathogenic role in diabetes complications and the associated costs of diabetes management. The global prevalence of diabetes among adults over 18 years of age has risen from 4.7% in 1980 to 8.5% in 2014 with a steep increase over the age of 50, reaching the peak prevalence of 25% above 80 years of age [1, 2]. The (direct and indirect) medical costs for patients with diabetes are double the amount compared to expenses for non-diabetic individuals and three times higher in case of cardiovascular diseases such as myocardial infarction or stroke [3]. Currently, diabetes-related healthcare expenditure accounts for 10% of the total healthcare costs and it is estimated to increase by 70% over the next 25 years leading to a serious societal and economic burden [4]. Diabetes complications are responsible for the majority of the associated costs and excess costs gradually increase with the duration of the disease leading to substantially higher expenses after 8-10 years [5, 3]. Hyperglycemia-induced endothelial dysfunction is the major contributor to the development of vascular disease in diabetes mellitus [6]. While insulin resistance may be present in patients with no increase in plasma glucose level and it may contribute to endothelial dysfunction, the major pathway that is responsible for endothelial damage is glucose-induced oxidative stress in diabetes [6, 7].

1.2. Characteristics of the damage

1.2.1. Glucose and oxidative stress in diabetic vascular damage

Endothelial dysfunction is a pathological state of the endothelium and can be defined as an aberration of the normal endothelial function of vascular relaxation, blood clotting and immune function. In general, it means impaired endothelium-dependent vasodilation as a result of imbalance between vasodilating and vasoconstricting substances produced by (or acting on) the endothelium. Endothelial dysfunction can be a significant predictor of coronary artery disease and atherosclerosis and it increases the risk of stroke and heart attack [8]. In basic science and in clinical research, endothelial function is commonly assessed by the use of the acetylcholine-

mediated vasodilatation test or by flow-mediated vasodilation, and this methodology is considered the 'gold standard' at this moment [9, 8]. Endothelial dysfunction is primarily responsible for the impaired vasorelaxation in diabetes but it is closely followed by the development of vascular smooth muscle cell dysfunction [10, 11]. Impaired relaxation may be caused by diminished production or increased destruction of vasodilating factors or impaired response to them in diabetes. Oxidative stress is considered as one of the major underlying mechanisms that leads to endothelial dysfunction in hyperglycemia, since the therapeutic supplementation of antioxidants or antioxidant enzymes can restore the endothelium-dependent vasodilation in experimental models of diabetes [10].

Glucose-induced damage is apparently controversial: glucose is a major source of energy and a small increase in blood glucose, that have no obvious ill effect on the short term, can cause serious long-term complications in diabetes. Glucose uptake is non-insulin dependent in endothelial cells and it occurs via GLUT1 (glucose transporter 1), thus high blood glucose level results in similarly high intracellular glucose concentration in endothelial cells [12, 13]. Endothelial cells have few mitochondria and primarily use glycolysis to produce ATP molecules, which suggests low oxygen consumption and relatively low level of oxidant production [14]. Furthermore, higher glucose concentration would allow even higher rate of anaerobic metabolism to produce the necessary amount of ATP and limit aerobic metabolism, oxygen consumption and reactive oxygen species (ROS) production in the cells. Still, hyperglycemia is associated with the activation of various ROS producing pathways and increased oxidant production in endothelial cells [15, 16]. Oxidants play a significant role in the destruction of nitric oxide and other signaling molecules and result in impaired vasoreactivity [17, 10, 18]. Inflammatory pathways may be implicated in the early stages of the injury and they are typically involved in the later stages of the disease and contribute to oxidant production and inflammatory cytokine secretion, which can also change the vascular function [19]. Oxidative stress also induces DNA damage that triggers endothelial cell senescence that might have an impact on vascular function in the later stages of the injury [20]. There are approximately 2-10 trillion ($2-10 \times 10^{12}$) endothelial cells in the human body and they form the endothelial surface of 500 m² of blood vessels and require constant renewal [21-23]. Mostly, the resident stem cells (located in the vessel wall) take part in the

repair processes but also circulating progenitor cells that arise from the bone marrow are involved in the process [22]. In diabetes, endothelial cell turnover is impaired and it might be a consequence of accelerated aging or reduced renewal of cells [24, 25]. While ROS-mediated injury dominates in the earlier stages of hyperglycemia-induced damage, cell senescence and impairment of endothelial cell turnover may play the leading part in the later stages.

1.2.2. Target cells of hyperglycemia

Hyperglycemia induces damage in a select cell population in the body, including mainly the mesangial cells in the kidney, neurons and Schwann cells in peripheral nerves and a subset of endothelial cells: only the microvascular and the arterial endothelial cells show impairment [26]. Interestingly, this dichotomy in the vulnerability is often preserved in *in vitro* experiments: microvascular endothelial cells are more susceptible to glucose-induced injury, whereas venous endothelial cells show reduced oxidant production and damage. This suggests that differences in the pressure, blood flow or vessel function in various parts of the circulation may not be accounted for the susceptibility. It is rather an inherent difference between the cells that explain the vulnerability of the microvasculature [27]. There are differences in the protein and RNA expression patterns, including the miRNA expression profiles, and the different responses of micro- and macrovascular endothelial cells to various metabolic stimuli may be attributed to this difference [28].

Differences in glucose uptake may be partially responsible for the susceptibility: most cells tightly regulate the glucose transport rate and prevent the unrestricted uptake, but endothelial and mesangial cells are unable to decrease the transport rate [29, 30]. Glucose overload induces a gradual increase in the mitochondrial membrane potential and the elevated protonic potential increases the superoxide generation by the respiratory chain [31]. The mitochondrial membrane potential is regulated by uncoupling proteins in the cells: these channels release excess protons from the intermembrane space to the matrix and protect against mitochondrial hyperpolarization. Endothelial cells express uncoupling protein 2 (UCP2) and its transport capacity is controlled by oxidative stress: high levels of oxidants open the channel, while the absence of oxidants closes the channel [32, 33]. In venous endothelial cells, hyperglycemia upregulates the expression of UCP2 and it

effectively protects against mitochondrial hyperpolarization and ROS production [34, 35]. This process does not work in microvascular endothelial cells: there is no change in UCP2 expression in response to elevated glucose concentration resulting in mitochondrial hyperpolarization with a simultaneous rise in mitochondrial superoxide generation [35]. In many cases, endothelial cells were found to produce excess levels of mitochondrial oxidants in response to hyperglycemia only in the presence of pro-inflammatory cytokines suggesting further mechanisms to be involved in the hyperglycemia-induced cell-damaging processes but the potential implication of inflammatory pathways has not been clarified [36].

1.2.3. Time course of hyperglycemic injury

At cellular level hyperglycemic damage occurs within a few days and induce compensatory and repair mechanisms that may have consequences in the cell population. Vascular endothelium covers a huge surface in the body and possesses a huge capacity to compensate for any damage that occurs over longer periods, thus changes in vascular function may occur with a delay.

In experimental models glucose levels are often above 20-30 mmol/L and vascular dysfunction develops over weeks or within a few months [37]. The development of hyperglycemia-induced endothelial cell damage is neither instantaneous *in vitro*, it usually takes a few days of exposure to high glucose levels to induce a significant increase in the mitochondrial membrane potential and oxidant production [38, 35]. Hyperglycemia-induced ROS production induce RNA and DNA damage that may be responsible for the reduced proliferation rate observed in endothelial cells [39]. Reduced proliferation and senescence occur after more than 10 doublings of endothelial cells exposed to 25 mmol/L glucose *in vitro* [25].

On the other hand, diabetic vascular complications occur after years of hyperglycemic exposure and poor glycemic control accelerates the development of the disease [40, 41]. Although, complications usually first appear some years after clinical diagnosis, retinopathy and nephropathy were often present (in 10-37% of patients) at the time of clinical diagnosis or within the first year after diagnosis [42]. Glucose levels that induce endothelial damage are moderately elevated in most patients due to improved diabetes care and diabetes self-management education and support (DSME/S) [43, 44].

Endothelial cell senescence and reduced proliferation are the dominant features in diabetes, still pathological proliferation of blood vessels occurs in diabetic retinopathy [45]. This controversy is explained by the fact that progressive retinal angiogenesis is preceded by a series of events that is characterized by reduced cell proliferation and stimulates neovascularization in the retina [45]. Proliferative diabetic retinopathy is not the primary pathogenic response to hyperglycemia but a compensatory response to retinal hypoxia. Diabetic retinopathy starts with the loss of two cell types of the retinal capillaries: the endothelial cells and the vessel supporting pericytes and the earliest pathologic signs are acellular, nonperfused capillary segments in the retina [45]. Pericyte loss may precede the endothelial damage in the retina and it is caused by angiotensin II overexpression induced by oxidative stress in diabetes. However, the increased number of migrating pericytes and loss of pericytes from the straight parts of capillaries may also occur as a result of hypoxia, and thus might be a consequence of prior endothelial damage. On the other hand, the loss of pericytes results in reduced proliferation of stalk endothelial cells leading to fewer phalanx cells and promotes hypoxia in the retina. Hypoxia is the main stimulus of uncontrolled proliferation in diabetic vessels and both angiotensin II and vascular endothelial growth factor (VEGF) are involved in the neovascularization. In the pathological angiogenesis not only the retinal endothelial cells take part but also the bone marrow derived progenitor cells that may explain how enhanced proliferation capacity replaces the cell loss at the later stage.

1.3. Triggers of endothelial dysfunction and damage

1.3.1 Hyperglycemia and ‘glucose memory’

Glucose-induced endothelial damage is not only caused by constantly high glucose concentration but by transiently elevated glucose levels. In experimental models, damage induced by intermittent high glucose is comparable or more severe than the injury induced by constantly high glucose concentration. Glucose levels studied in most experimental models are often much higher than the values that cause irreversible damage in humans on the long term and result in accelerated progression of diabetic complications.

Diagnostic criteria for diabetes are based on the relationship between plasma glucose values and the risk of diabetes-specific microvascular complications: blood glucose concentration that cause diabetic vascular damage has been empirically determined and diagnostic criteria were established. The World Health Organization (WHO) introduced new diagnostic criteria in 1980, which were globally accepted, but had to lower the cut-off values for diabetes in 1999 since growing body of evidence supported the development of complications at lower blood glucose levels [46, 47]. The updated threshold values has raised considerable dispute and are often criticized for not preventing complications but further lowering has not been achieved because of the risk of hypoglycemia. The definition of hyperglycemia is challenging, since blood glucose values show a physiological increase after a meal and this calls for separate normal values for fasting, postprandial and random blood glucose levels. Still, it is evident that “high” glucose levels that induce damage in endothelial cells in the long term are very close to the normal blood glucose values, less than a two-fold increase in the blood glucose level triggers injury in the cells. In the past, osmotic damage was presumed to play a pathogenic role in glucose-induced cellular injury but the minor changes in osmolality rule out this possibility. In healthy human subjects the rise in blood glucose levels after a meal typically reaches or goes beyond these values, making the definition of hyperglycemia rather confusing [48]. From the pathogenic viewpoint of hyperglycemia, absolute cut-off values cannot be established to separate normoglycemic and hyperglycemic concentration ranges.

While earlier studies confirmed that the risk of cardiovascular complications corresponds to the average increase in glucose level (measured as glycated hemoglobin, HbA1c), more recent studies also found independent associations with the postprandial peaks [49]. These results highly suggest the action of secondary mediators that are rather induced by the fluctuations in blood glucose (glycemic variability) than by an absolute increase. Experimental models confirmed that glycemic swings caused at least as severe tissue damage as constant hyperglycemia and persistence of high-glucose memory was postulated in cells and animals that were exposed to normoglycemic conditions following a hyperglycemic exposure [50-52]. Endothelial cells when returned to normal glucose concentration after exposure to high glucose showed increased ROS production and activation of poly(ADP-ribose) polymerase (PARP) even a week following the normalization of the glucose level and

in this respect they showed similar characteristics to cells maintained at high glucose [51]. The persistence of oxidative stress in endothelial cells *in vitro* confirms that ‘glucose memory’ is an inherent feature of these cells. It also means that once hyperglycemia activates the various ROS producing pathways they continue to produce oxidants for multiple days or weeks in endothelial cells even if the glucose level is fully normalized. Oxidative stress is the key feature of the changes induced by hyperglycemia and ‘metabolic memory’ is another term used that refers to the characteristic metabolic changes [50]. The length of high glucose memory is unknown in humans but it is suspected to last longer than *in vitro* because (1) inflammatory pathways are also involved and (2) the response is not limited by the life cycle of single cells but it is possibly carried over to multiple cell generations.

Blockade of the early changes has been confirmed to prevent or slow down the progression of complications but the reversal at a later phase may not be achieved by glycemic control [53]. Benefits of intensive glucose control can be detected after 3 years of treatment if no retinopathy or mild disease is present at the start of the treatment strategy in type 1 diabetes [54]. The importance of blocking the glucose-induced damage early on in type 2 diabetes has been confirmed by the results of the United Kingdom Prospective Diabetes Study (UKPDS) [40]. On the other hand, there is little benefit of strict glucose control if established cardiovascular disease is already present at the start of the treatment regimen [53]. Similarly, in diabetic rats a 6-month-long period of good glycemic control following 2 months of poor glycemic control results in significantly reduced progression whereas no benefit is observed on retinopathy if good glycemic control was started after 6 months of poor glycemic control: both nitrosative stress and tissue damage were similarly advanced as with 12 months of poor glycemic control [55, 56]. These suggest that the processes started by hyperglycemia may be partially reversed if normoglycemia follows a shorter period of high glucose exposure. It is still unclear whether the detrimental effects of transient hyperglycemia is buffered within the individual cells or it is the entire population of endothelial cells that compensate for the changes and the reason why progressive damage occurs following an extended hyperglycemic period is the loss of the renewal capacity of the cells.

1.3.2. Downstream molecules responsible for the injury

The mechanism of high glucose memory is still obscure and little is known about the pathways involved. Hyperglycemia modifies the metabolism of the cells and is suspected to induce various downstream pathways or molecules that are responsible for maintaining the tissue damaging actions. Oxidative stress pathways act as executors of tissue damage but the linkage between hyperglycemia and the sustained activation of oxidative pathways still remains rather elusive.

Alterations in the metabolome in diabetes are suspected to maintain the metabolic changes for extended periods even if there is little change in the expression profile of proteins [57]. Excess glucose load induces changes in a series of metabolite levels and the normalization of these levels may not occur as rapidly as glucose lowering. Apart from glucose the concentrations of glucose-1-phosphate, lactate, glucosamine, mannose, mannosamine, hydroxybutyrate and glyoxalate also elevate in the plasma in diabetes [58]. All of the above intermediates and the increased fatty acids increase the tricarboxylic acid (TCA) cycle flux in the cells. Perturbation of the TCA cycle flux is also supported by other metabolomics studies in diabetes [59]. Associations between diabetes risk and the plasma levels of branched chain (BCAA, isoleucine, leucine and valine) and aromatic (phenylalanine, tyrosine) amino acids have been found suggesting that the changes not only involve the carbohydrate and lipid metabolism but also the catabolism of proteins and amino acids [60]. Catabolism of BCAAs provides intermediates for the TCA cycle and potentially drive the TCA flux. Apart from the systemic changes that affect the milieu of the cells, specific changes of amino acid levels have been observed in endothelial cells: hyperglycemia increases the concentration of alanine, proline, glycine, serine and glutamine within the cells and induce elevation of the amino adipate, cystathionine and hypotaurine levels [61]. Whether these changes are only markers of hyperglycemia or they play a pathogenic role in oxidative stress induction is still undetermined.

1.4. Mechanisms of ROS production in hyperglycemia

1.4.1. Glucose-induced oxidative stress pathways

Changes in glucose metabolism are presumed to be directly responsible for provoking oxidant production in endothelial cells. Endothelial cells predominantly use glucose

as energy source and rely on glycolysis to generate ATP molecules [14]. Glycolytic flux exceeds the rate of oxidative phosphorylation (OXPHOS) by two orders of magnitude in endothelial cells *in vitro* and similar ratio is suspected *in vivo* [62, 63]. The contribution of fatty acid oxidation to energy production is thought to be negligible in capillary endothelial cells, though endothelial cells take up fatty acids and transport them to the neighboring cells, thus play important role in transendothelial fatty acid delivery [64]. Since the function of capillary endothelial cells is to deliver oxygen and fuel sources to other cells in tissues, they do not consume much oxygen or store energy but preserve them to other perivascular cells. Thus, excess glucose is not converted to glycogen for storage in endothelial cells, but is pushed toward glycolysis [65]. Glutamine is a further energy source in endothelial cells via glutaminolysis that directly produces one GTP molecule (that can be converted to ATP) and further 5 ATP molecules from NADH^+ and FADH_2 via OXPHOS. Glutamine is the most abundant amino acid in the plasma and glutaminolysis is a valuable energy source if glycolytic output is low since it feeds alpha-ketoglutarate to the TCA cycle and similarly produces lactate (or pyruvate). However, all the energy producing steps in glutaminolysis occur in the mitochondria via the TCA cycle and OXPHOS and mitochondrial impairment may affect the energy efficacy of glutaminolysis [66].

The metabolic balance between glycolysis and OXPHOS is controlled by nutrients (the ATP and NADH output) via Sirtuin 1 (SIRT1) and AMP-activated protein kinase (AMPK) in the cells. SIRT1 is a NAD^+ dependent histone deacetylase enzyme that regulates energy homeostasis via gene expression changes induced by deacetylating a variety of histone proteins, transcription factors and coregulators [67]. The activity of SIRT1 is primarily controlled by NAD^+ abundance and NAD^+/NADH ratio. AMPK is a master sensor of the energy level in the cells: it detects the cellular ATP concentration and is activated by a decrease in the ATP level. There is a complex interplay between AMPK and SIRT1: the two enzymes indirectly activate each other. SIRT1 activation deacetylates LKB1 (tumor suppressor liver kinase B1) that phosphorylates and activates AMPK [68, 69], while AMPK activates SIRT1 by increasing the NAD^+/NADH ratio either by inducing the NAD^+ biosynthesis enzyme NamPRT (nicotinamide phosphoribosyltransferase) or by a NamPRT-independent mechanism [70]. Thus, caloric restriction activates both AMPK and SIRT1, whereas

both enzymes are suppressed if energy sources are abundant like in hyperglycemia [71, 72]. In caloric restriction, SIRT1 deacetylates and activates peroxisome proliferation activating receptor- γ (PPAR- γ) coactivator 1- α (PGC-1) and forkhead-box O1 protein 1 (FOXO1) and leads to glucose sparing: suppressed glycolysis and increased mitochondrial activity and they also activate gluconeogenesis [73, 74]. On the other hand, in hyperglycemia the activity of AMPK and SIRT1 is suppressed and it results in enhanced glycolysis, inhibition of gluconeogenesis and decreased mitochondrial biogenesis and OXPHOS [74].

Overload of glycolysis and the pentose phosphate pathway are the initial steps that trigger alternate pathways of glucose metabolism (**Fig. 1**). Prior perturbation of mitochondrial metabolism (TCA cycle overload and impaired OXPHOS) is highly possible since inhibition of mitochondrial superoxide generation prevents the activation of the above pathways but the exact mechanism that initiates these events is unknown [26]. The high glycolytic input and low OXPHOS capacity may gradually block the main metabolic steps and shunt the metabolism to alternative pathways. These include the methylglyoxal, hexosamine and polyol pathways: dihydroxyacetone phosphate (DHAP) is diverted to the methylglyoxal pathway and leads to protein kinase C (PKC) activation, fructose-6-phosphate (F6P) increases the flux through the hexosamine pathway and excess glucose enters the polyol pathway when converted to sorbitol [75, 66]. Suppressed expression of the gluconeogenetic enzyme glucose-6-phosphate dehydrogenase (G6PDH) prevents shunting of glucose to the pentose phosphate pathway that further increases the glycolytic load [76, 77]. All these processes lead to ROS production and the generation of advanced glycation end products (AGEs), the products of nonenzymatic glycation and oxidation of proteins and lipids that accumulate in diabetes. AGEs signal through the receptor of AGE (RAGE), a cell surface receptor that is also activated by the damage-associated molecular patterns (DAMP) HMGB1 (high-mobility group box 1) and S100 proteins [78]. RAGE activates nuclear factor kappa B (NF- κ B) and controls several inflammatory genes, thus links hyperglycemia to inflammation. Since RAGE itself is upregulated by NF- κ B, inflammation is maintained by positive feedback in hyperglycemia as AGEs, the ligands are continuously produced.

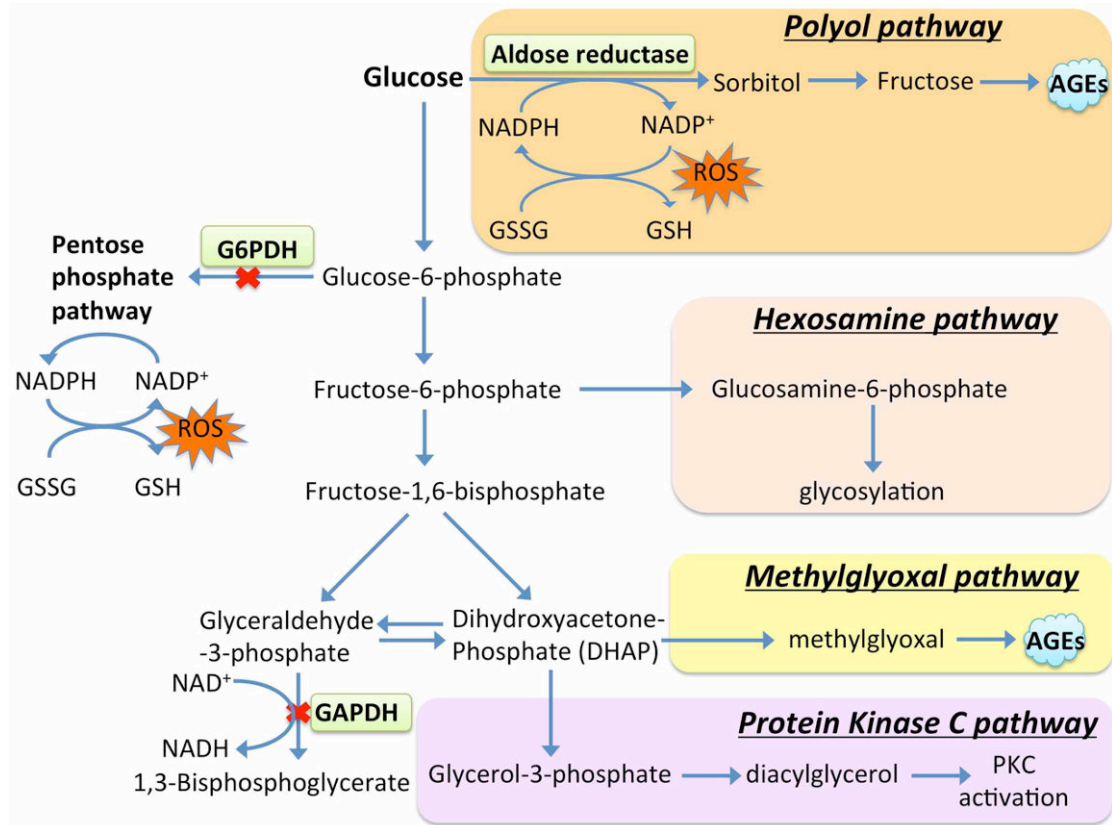


Fig. 1. Hyperglycemia-induced ROS-producing pathways in the cytoplasm.

AGEs: advanced glycation end-products; G6PDH: glucose-6-phosphate dehydrogenase; GAPDH: glyceraldehyde-3-phosphate dehydrogenase; GSH/GSSG: reduced/oxidized glutathione; NAD^+/NADH : Nicotinamide adenine dinucleotide; $\text{NADP}^+/\text{NADPH}$: Nicotinamide adenine dinucleotide phosphate; ROS: reactive oxygen species

Interestingly, hyperglycemia induces a long-lasting suppression in SIRT1 and AMPK activity in endothelial cells: the activity of both enzymes remains low weeks after the normalization of glucose level following a week long hyperglycemia [69]. Thus, SIRT1 and AMPK have been implicated in glucose memory since restoration of their activity reduces the ROS production and PARP activity in the cells.

One further molecule that possibly takes part in the maintenance of oxidative stress in hyperglycemic endothelial cells is p66SHC (66-kDa Src homology 2 domain-containing protein) [79]. p66SHC is induced by hyperglycemia and it contributes to oxidative stress and endothelial damage. Genetic ablation of p66SHC reduces the oxidative stress in diabetic animals, protects against vascular dysfunction and blocks the progression of nephropathy [79, 80]. p66SHC is a redox enzyme that associates with 70 kDa heat shock protein (Hsp70) and localizes within the intermembrane space

in the mitochondria. Upon oxidative stress p66SHC is released from the complex and transfers electrons from the electron transfer chain (from cytochrome c specifically) to oxygen and produces hydrogen peroxide (H₂O₂) [81]. Under basal conditions p66SHC is also present as an inactive enzyme in the cytoplasm where it becomes activated via phosphorylation in response to cellular stress and translocates to the mitochondria. The active p66SHC diverts a fraction of the mitochondrial electron flow between complexes III and IV to produce ROS instead of water and is involved in the opening of the permeability transition pore during apoptosis. In hyperglycemia p66SHC may function as a shunt pathway if complex IV activity is impaired. The activity of p66SHC is also regulated by acetylation: it is a direct target of SIRT1 and diminished SIRT1 activity increases the acetylation and activity of p66SHC in hyperglycemia [82]. Furthermore, acetylation of p66SHC promotes the phosphorylation-mediated activation of the protein and since the acetylation-resistant p66SHC isoform partially protects against the vascular impairment it may play a pathogenic role in diabetic vascular dysfunction. The linkage to SIRT1 and the protection associated with the loss of p66SHC suggest that p66SHC make a substantial contribution to oxidative stress in diabetes and it may represent the key target of SIRT1.

1.4.2. Unifying hypothesis: the role of mitochondrial oxidants

With the growth of our knowledge about glucose-induced cellular damage and the various molecules and pathways involved in the process, the pathomechanism of glucose-induced damage has become inexplicable. In an effort to explain the puzzling complexity of the cellular events Michael Brownlee introduced a unifying hypothesis in which he placed the events in an integrating linear model [26]. In the unifying mechanism mitochondrial superoxide generation is placed in center stage followed by all other ROS producing pathways as secondary events. As the contribution of mitochondrial energy production seems negligible in endothelial cells, this proposition was a striking novelty at first, but it renders the series of events logically based on a wealth of scientific results. First of all, the unifying framework assumes that the main ROS producing mechanisms implicated in hyperglycemic cellular damage are interrelated and a common pathway is responsible for their activation [75]. Secondly, the overload of glycolysis rather occurs as a single downstream

perturbation of metabolism that leaves behind glycolytic intermediates than by multiple blockades of glycolytic enzymes in response to excess glucose input. Thus, inhibition of a downstream step of glucose catabolism in the mitochondria might be responsible for the activation of the ROS-producing shunt pathways in the cytoplasm. The observation that prevention of mitochondrial superoxide generation inhibits the cytoplasmic ROS production pathways (PKC activation, sorbitol accumulation and AGE production) also supported the assumption that mitochondrial damage precedes the glycolytic impairment [83].

The exact nature of hyperglycemic perturbation of mitochondrial metabolism remains enigmatic and it is still debatable whether superoxide itself or the steps leading to its increased production is the triggering event of glucose-induced damage. High TCA flux and elevated glycolytic pyruvate input were detected in hyperglycemia and these may serve as inducers of mitochondrial ROS production but might also be the consequences of dysfunctional OXPHOS [83]. Various pharmacological interventions that reduce the mitochondrial ROS production effectively inhibit the hyperglycemic damage [75, 26, 38]. Higher flux through the electron transport chain is expected to reduce the accumulation of glycolytic intermediates and prevent the activation of oxidative stress pathways but only some of the interventions increased the electron transport (eg. uncoupling agents and proteins), while others (eg. antioxidants) did not change it or severely reduced it (complex II inhibition). Also, the increased electron flow may induce a proportional rise in superoxide generation by the electron transport chain if electron leakage is unaffected. Furthermore, endothelial cells, in which the mitochondrial DNA is selectively depleted (rho zero cells) and lack a functional electron transport chain, fail to activate PKC, the polyol and hexosamine pathways and they do not produce AGEs, though their mitochondrial metabolism is impaired and they are expected to accumulate glycolytic intermediates [26]. These observations led to the proposition that mitochondrial superoxide generated by the electron transport chain is responsible for the initiation of hyperglycemic endothelial damage [84, 83, 26].

1.4.3. The mechanism of glucose-induced mitochondrial superoxide generation

Mitochondria produce superoxide non-enzymatically via multiple respiratory complexes in the electron transport chain and enzymatically via the mitochondrial

xanthine oxidase [85-87]. The non-enzymatic production of superoxide occurs when a single electron is directly transferred to oxygen by prosthetic groups of the respiratory complexes or by reduced coenzymes that act as soluble electron carriers. The electron transport chain may leak electrons to oxygen and it is the main source of superoxide in hyperglycemia. Mitochondrial monoamine oxidase (MAO) and p66SHC also produce H_2O_2 within the mitochondria that may contribute to oxidative stress in hyperglycemia [88].

Molecular oxygen is bi-radical, it has two unpaired electrons in the outer orbitals, which makes it chemically reactive. In the ground state the unpaired electrons are arranged in the triplet state, and as a result of spin restrictions, molecular oxygen is not highly reactive: it can only react with one electron at a time. If one of the unpaired electrons is excited and changes its spin (oxygen goes from the triplet state to the short-lived singlet state), it will become a powerful oxidant that is highly reactive [85]. The reduction of oxygen by one electron at a time produces superoxide ($O_2^{\bullet-}$) anion that might be converted to hydrogen peroxide (either spontaneously or through a reaction catalyzed by superoxide dismutase) that may be fully reduced to water or partially reduced to hydroxyl radical (OH^{\bullet}). In addition, superoxide may react with other radicals including nitric oxide (NO^{\bullet}) and form peroxynitrite ($ONOO^{\bullet-}$), another very powerful oxidant. The respiratory components are thermodynamically capable of transferring one electron to oxygen and form superoxide in the highly reducing environment of the mitochondria, since the standard reduction potential of oxygen to superoxide is -0.160 V and the respiratory chain incorporates components with standard reduction potentials between -0.32 V (NAD(P)H) and $+0.39$ V (cytochrome a_3 in Complex IV) [85].

In the respiratory chain electrons move along the electron transport chain going from donor to acceptor molecules until they are transferred to molecular oxygen (the standard reduction potential of oxygen/ H_2O couple is $+0.82$ V) while the generated free energy is used to synthesize ATP from ADP and inorganic phosphate. Respiratory Complex I transfers electrons from NADH and Complex II from $FADH_2$ to coenzyme Q (CoQ, ubiquinone), which is the substrate of Complex III. Complex III transfers electrons from reduced CoQ to cytochrome C, which is used by Complex IV to reduce oxygen into water. The step-by-step transfer of electrons allows the free energy to be released in small increments. The energy released as electrons flow

through the respiratory chain is converted into a H^+ gradient through the inner mitochondrial membrane: protons are transported from the mitochondrial matrix to the intermembrane space (by Complexes I, III and IV) and a proton concentration gradient forms across the inner mitochondrial membrane [89]. Since the mitochondrial outer membrane is freely permeable to protons, the pH of the mitochondrial matrix is higher (the proton concentration is lower) than that of the intermembrane space and the cytosol. An electric potential (mitochondrial membrane potential) of 140-160 mV is formed across the inner membrane by pumping of positively charged protons outward from the matrix, which becomes negatively charged [90]. Thus free energy released during the oxidation of NADH or $FADH_2$ is converted to an electric potential and a proton concentration gradient — collectively, the proton-motive force — and this energy is used by ATP synthase (Complex V) for ATP generation via the chemiosmotic coupling [91]. While the majority of oxygen molecules are used for water formation during the above processes, superoxide is generated at an estimated rate of 0.1-2% of oxygen consumption under normal respiration (State 3) and physiological operation of the respiratory chain [87, 88].

The electron transport chain may produce superoxide by multiple mechanisms but electron leakage before Complex III is suspected to represent the main source of superoxide in hyperglycemic endothelial cells [83, 26]. Complexes I and III are the respiratory complexes that are capable to produce large amounts of superoxide under certain conditions (**Fig. 2**). Complex I may produce superoxide by two mechanisms: (1) the reduced flavin mononucleotide (FMN) center can transfer electrons to oxygen instead of CoQ when the NADH/ NAD^+ ratio is high (and the CoQ binding site is blocked or the CoQ pool is mostly reduced) or (2) by reverse electron transfer (RET) from the CoQ binding site if there is high electron supply from Complex II and the electrons are forced back to Complex I instead of proceeding to Complex III (by a reduced CoQ pool and high proton-motive force) [87, 92]. In Complex III superoxide is produced from the semiquinone anionic state of CoQ (semiubiquinone) by directly reacting with oxygen instead of completing the Q-cycle [87, 93]. Reduced CoQ diffuses through the bilipid layer of the membrane to its binding site in Complex III and transfers the electrons to the iron-sulfur protein (Rieske protein) in two steps that produce a semiquinone intermediate state of CoQ after the first electron transfer, which is the source of superoxide. In the presence of respiratory inhibitors Complex I

may produce the highest amount of superoxide, especially through RET, but the contribution of Complexes I and III to superoxide production is unknown in healthy mitochondria [85]. Superoxide is also produced in the matrix by other enzymes that interact with the NADH pool and by enzymes connected to the inner membrane CoQ pool. These include α -ketoglutarate dehydrogenase that may produce superoxide if its substrate (α -ketoglutarate) concentration and the NADH/NAD⁺ ratio increase in the matrix. In the membrane α -glycerophosphate dehydrogenase may produce superoxide partly via RET and Complex II, which transfers electrons from succinate to CoQ, is also suspected to generate some superoxide [87].

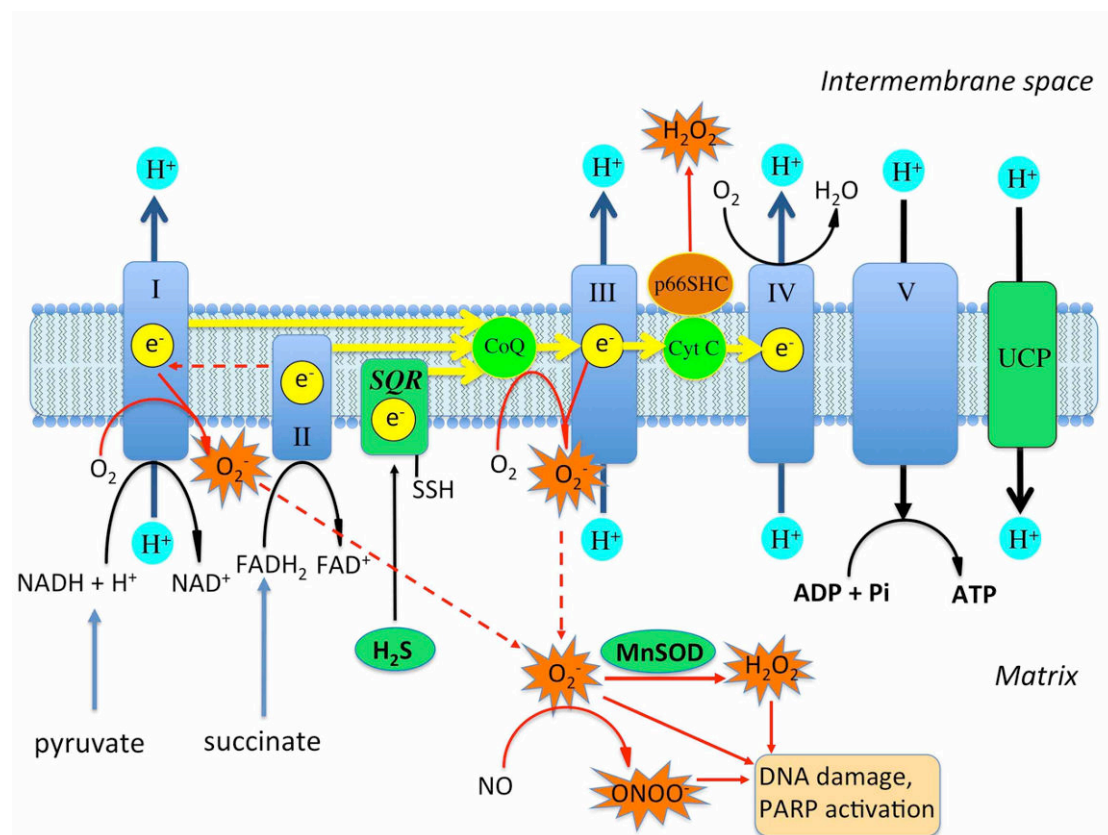


Fig. 2. Oxidant production by the mitochondrial electron transport chain.

CoQ: Coenzyme Q, ubiquinone; Cyt C: Cytochrome C; FAD⁺/FADH₂: flavin adenine dinucleotide; H₂O₂: hydrogen peroxide; MnSOD: manganese-dependent superoxide dismutase; NO•: nitric oxide; O₂•⁻: superoxide, ONOO•: peroxynitrite; PARP: poly(ADP-ribose) polymerase, p66SHC: 66-kDa Src homology 2 domain-containing protein; SQR: sulfide:quinone oxidoreductase; UCP: uncoupling protein

In hyperglycemic endothelial cells, the increased production of superoxide originates from the reduced CoQ pool before Complex III [83, 75]. The high electron donor input from glycolysis and the TCA cycle may increase the membrane potential and

inhibit the electron transfer at Complex III, thus increase the concentration of reduced and free-radical intermediates of CoQ. Superoxide generation may occur as direct 'leakage' of electrons to oxygen, as a result of the longer half-life of CoQ intermediates in the lipid bilayer and bound to Complex III or via RET through Complex I. Superoxide generation is also promoted by the increased membrane potential and proton concentration gradient through the inner membrane [31, 83, 94, 35]. Superoxide production was found to increase exponentially above 140 mV with the increase of the mitochondrial membrane potential [95]. Since with the generation of each superoxide molecule one electron is lost compared to the number of protons, superoxide production per se may increase the membrane potential and the proton gradient or might be responsible for the maintenance of the elevated membrane potential. Furthermore, the proton and charge transfer of Complexes III and IV are disproportional since Complex III picks up two protons from the matrix side of the inner membrane (the negatively charged N-face) and releases 4 protons to the intermembrane space side (positively charged P-face), whereas Complex IV abstracts 4 protons from the matrix and releases 2 protons to the intermembrane space per transfer of 2 electrons. Thus, Complex III transfers 4 protons but only 2 positive charges, while Complex IV transfers 2 protons and 4 positive charges [96, 89], which may lead to an increase in the membrane potential if there is a mismatch between the activity of the two complexes. Also, while it is possible to generate considerably higher membrane potential than the physiological value, since the proton motive force is sufficient to generate about 240 mV, the proton permeability of biological membranes increases above 130 mV, thus the higher values are associated with energy loss [95]. To optimize the energy efficiency, OXPHOS is tightly regulated by the ATP concentration (or ATP/ADP ratio) in the matrix: high ATP concentration in the matrix allosterically inhibits Complex IV of the respiratory chain and decreases the mitochondrial membrane potential [97]. Complex IV has a low reserve capacity and it may represent the major controlling site of respiration and mitochondrial ATP synthesis [95]. This immediate regulation is supplemented by the phosphorylation-mediated regulation of respiratory complexes, that transmit the extramitochondrial and extracellular stimuli to adapt OXPHOS to stress conditions [95]. Phosphorylation sites were detected in all respiratory complexes and there is a growing list of stress factors that may induce phosphorylation of the complexes or mitochondrial

hyperpolarization that might be associated with the adaptive process. This is how inflammatory cytokines may affect superoxide generation in diabetes.

Hyperglycemia-induced mitochondrial superoxide production is a functional change of the respiratory chain; no difference is detectable in the assembly or the relative amounts of the respiratory complexes in the early phases of the injury [26, 35]. At later stages, changes in the expression or assembly of some components of the respiratory chain may occur and these are typically associated with impaired functionality [98, 99]. The glucose-induced changes in the mitochondrial superoxide production are reversible: normalization of the membrane potential suppresses the ROS production in endothelial cells [83, 26, 94, 35, 100]. While elevated mitochondrial membrane potential is detectable in endothelial cells exposed to high glucose concentration, the overexpression of either uncoupling protein 1 (UCP1) or uncoupling protein 2 (UCP2) normalizes the membrane potential and reduces the ROS production [83, 26, 35]. The function of UCP2 is regulated by ROS itself: the proton conductance of the protein is controlled by glutathionylation and if ROS is present it increases the proton leakage, while in the absence of ROS the channel closes, thus this feedback may control the mitochondrial potential and the ROS production simultaneously [32, 33]. Furthermore, hydrogen sulfide donors that normalize the mitochondrial potential by electron supplementation via sulfide:quinone oxidoreductase (SQR) also inhibit the superoxide generation induced by hyperglycemia [94, 100].

The mitochondrial matrix possesses antioxidant enzymes to defend against oxidative damage. Manganese-dependent superoxide dismutase (MnSOD, also known as superoxide dismutase 2 (SOD2)) is the mitochondrial enzyme that neutralizes superoxide produced by the respiratory chain and converts it to H₂O₂. Since functional mitochondria constantly produce ROS, it is necessary to scavenge oxygen radicals. The importance of MnSOD is underlined by the fact that MnSOD deficient mice exhibit extensive mitochondrial injury and only survive for less than 3 weeks [101]. Mutations associated with reduced activity of MnSOD accelerate diabetic nephropathy and neuropathy [102-104]. On the other hand, overexpression of MnSOD prevents hyperglycemic injury in endothelial cells suggesting that the respiratory chain is the source of oxidants in hyperglycemia [83, 26]. The amount of superoxide produced by the respiratory chain may not be excessively higher in

hyperglycemia, since the overexpression of the MnSOD can efficiently scavenge the oxidants or low amounts of mitochondria-targeted antioxidants are able to neutralize ROS in hyperglycemia [83, 26, 38].

1.5. Mechanism of damage: Cell damaging responses to ROS production in hyperglycemia

In cells exposed to hyperglycemia, mitochondrial ROS production activates various mechanisms to reduce the oxidant production. This includes immediate responses that may control the mitochondrial potential in the short term and also longer-term responses that may protect against the increase of the mitochondrial potential but these mostly reduce the energy efficiency of OXPHOS. Hyperglycemia and ROS production activate the uncoupling proteins in the mitochondrial inner membrane that allow higher proton transfer from the intermembrane space to the matrix without coupled ATP production [32, 33]. This activity may reduce the mitochondrial membrane potential but also decreases the amount of ATP generated in the mitochondria.

Hyperglycemia also increases the consumption of hydrogen sulfide, an inorganic substrate of the mitochondria that can act as an endogenous electron donor [105-107]. Since H₂S oxidation may provide electrons to CoQ without the additional protons it can reduce the mitochondrial potential and promote ATP synthesis, thus H₂S may represent an alternative energy source that is used in small quantities or function as a buffer to control the mitochondrial potential. Hyperglycemia reduces the mitochondrial H₂S pool and the plasma concentration of H₂S and it may deplete the buffering capacity of H₂S in the mitochondria [108, 94, 109].

These immediate reactions are supplemented with the morphological changes of mitochondria. Mitochondria are dynamically changing organelles in the cells: they may form long tubes that cross the whole length of the cell or short rods that are as long as wide or any length in between. Mitochondria continuously change their shape by fusion (elongation) and fission (fragmentation) and they move along microtubular tracks within the cells. This process is believed to help maintain functional mitochondria, it allows rapid redistribution of mitochondrial proteins and may help the elimination of dysfunctional parts or proteins. Hyperglycemia stimulates the fission of mitochondria that can reduce the mitochondrial membrane potential but also

helps dissociate the respiratory complexes and decrease the chance of assembly of various proteins within a complex [110-114]. Altogether, it results in partly assembled respiratory complexes and higher superoxide production that will reduce the energy efficiency of mitochondria [98, 99]. Mitochondrial fission is a later process induced by high glucose exposure, it occurs only after the superoxide production is induced. Mitochondrial ROS production plays an active role in the initiation of fragmentation, since administration of a mitochondrial scavenger prevents the hyperglycemia-induced fission of mitochondria [111]. Blocking of mitochondrial fission will also restore the acetylcholine-mediated eNOS (endothelial nitric oxide synthase) phosphorylation and cGMP response in hyperglycemic endothelial cells suggesting that the vascular impairment is partly caused by mitochondrial fission itself [112].

Mitochondrial ROS production results in DNA damage in the mitochondria that activates the mitochondrial DNA repair enzymes [115]. Oxidative DNA damage activates poly(ADP-ribose) polymerase 1 (PARP1) in the mitochondria similar to the situation in the nucleus [116]. PARP1 poly(ADP-ribosylates (PARylates) the mitochondrial enzymes exo/endonuclease G (EXOG) and DNA polymerase gamma (Poly) involved in base excision repair (BER), a key repair process in the mitochondria [116]. Activation of mitochondrial PARP1, as opposed to nuclear PARP1, may decrease the DNA repair and slow down the mitochondrial biogenesis. Integrity of the mitochondrial DNA (mtDNA) also relies on mitochondrial transcription factor A (TFAM), a protein that may act as a physical shield of the mitochondrial DNA, since it forms histone-like structures with mtDNA and is present in large amounts in mitochondria (~900 molecules for each mtDNA). Apart from protecting the DNA from damaging agents, it tightly binds to heavily damaged DNA parts, blocks the transcription and may promote the repair of affected sites [115]. TFAM is also implicated in mitochondrial biogenesis and the maintenance of stable mtDNA copy number. In diabetic retinas, the level of TFAM is reduced and it decreases the mitochondrial biogenesis that can lead to fewer mitochondria and less efficient OXPHOS [117].

Oxidant production will also induce several changes in the function of proteins that may be associated with cellular injury and result in altered cell metabolism, senescence and vascular dysfunction. Oxidative stress leads to oxidative DNA damage and DNA strand breaks that activates the predominantly nuclear PARP1 and

may lead to ATP depletion and necrosis or apoptosis [118]. However, the level of PARP activation is mostly lower than to induce cell death, it results in higher NAD⁺ consumption and changes in the PARylation pattern of proteins [52]. The higher NAD⁺ utilization and decreased mitochondrial output may decrease the nuclear and cytoplasmic NAD⁺ concentrations and by reducing the amount of substrate for SIRT1, another NAD⁺-dependent enzyme, will block the deacetylation of proteins [67, 69, 82]. A third posttranslational modification that changes in hyperglycemia is protein S-sulfhydration (or persulfidation), a reaction between H₂S and reactive cysteine residues [119]. Protein S-sulfhydration is a highly prevalent modification that typically increases the activity of target proteins. The antioxidant master regulator Nrf2 (nuclear factor E2-related factor 2) transcription factor is also activated by H₂S via sulfhydration of its key controller, Kelch-like erythroid cell-derived protein with Cap 'n' collar (CNC) homology (ECH)-associated protein 1 (Keap1) [120, 121]. A further target is ATP synthase in the respiratory chain: H₂S increases cellular bioenergetics via S-sulfhydration of Complex V [122]. Since hyperglycemia reduces the H₂S level in the cells and plasma, it will also decrease the protein S-sulfhydration and results in lower Nrf2 activity and OXPHOS efficiency [108, 109]. All these changes contribute to the dysfunction of proteins in hyperglycemia and promote cellular dysfunction.

There are further changes in the cellular metabolism that reduce the ATP output, which include diminished glucose uptake, blockage of anaerobic metabolism and inappropriate assembly of mitochondrial respiratory complexes. High extracellular glucose immediately stimulates glucose uptake, but decreases the glucose transport over longer term in endothelial cells [123, 124]. Down-regulation of GLUT1 glucose transporter is responsible for the diminished glucose uptake and it may contribute to the low ATP output. Hyperglycemia reduces the activity of the glycolytic enzyme glyceraldehyde-3-phosphate dehydrogenase (GAPDH) via PARylation and reduces the anaerobic glucose metabolism [125]. Aerobic metabolism is also decreased by mitochondrial fragmentation and disassembly of mitochondrial respiratory complexes that develop over longer exposure to hyperglycemia [99, 111, 93]. Altogether these changes reduce the ATP generation in the cells and block the anaerobic compensation for the diminished mitochondrial activity.

Oxidative stress will induce DNA strand breaks in the mitochondria and promote mutations and senescence of endothelial cells. Accelerated aging of endothelial cells and the lack of endothelial progenitor cells decrease the functional endothelial cell pool in hyperglycemia [126]. The number of bone marrow-derived progenitor cells is lower in the circulation in diabetes and the progenitor cells possess diminished proliferation capacity [127, 24]. It will reduce the resupply of endothelial cells and may place extra workload on the preexisting vascular endothelium extending the exposure to glucose, inflammatory mediators and oxidants.

Vascular dysfunction is characterized by inappropriate relaxation in response to acetylcholine, which is mediated by endothelial nitric oxide (NO) [128-131]. NO is synthesized from the guanidinium group of L-arginine by eNOS via a NADPH-dependent reaction. Mitochondrial superoxide may interact with NO, which leads to a loss of bioavailable NO, and form peroxynitrite (ONOO⁻), a very reactive radical that activates PARP1 [132-134]. Furthermore, tetrahydrobiopterin (the pteridine cofactor of eNOS) is an essential regulator of the enzyme: when tetrahydrobiopterin availability is inadequate, it becomes ‘uncoupled’ and produces superoxide, using molecular oxygen as substrate, instead of NO [135]. Tetrahydrobiopterin levels are lower in animal models of diabetes and tetrahydrobiopterin supplementation restores the vascular relaxation in these models suggesting a pathogenic role in diabetes [136, 137]. Another key element of vascular dysfunction is the reduced H₂S bioavailability in diabetes. H₂S and NO interact at multiple levels: H₂S stimulates eNOS expression and activity, promotes the action of NO by maintaining a reduced soluble guanylate cyclase (sGC) and by inhibition of the vascular cGMP phosphodiesterase (PDE5), it prolongs the half-life of cGMP [138-140]. Increased mitochondrial H₂S consumption and its diminished concentration in hyperglycemic endothelial cells inhibit the NO-dependent vasodilation and contribute to vascular damage in diabetes.

2. Aims

Endothelial dysfunction plays a fundamental role in the development of diabetic micro- and macrovascular complications. The glucose-induced cell damage is mediated by oxidative stress in endothelial cells, and according to the unifying hypothesis [26, 141] mitochondrial reactive oxygen species (ROS) production acts as an upstream player in this process. Reactive oxygen species are produced by the respiratory chain (complexes I and III) in the mitochondria [142] via directly transferring electrons to oxygen leaving behind extra protons in the intermembrane space.

To find potential inhibitors of hyperglycemic endothelial damage we pursued the following **Specific Aims**:

1. Establish a cell culture model of hyperglycemia-induced endothelial injury that is characterized by mitochondrial overproduction of ROS and is applicable for medium throughput cell-based drug screening
2. Screen the currently available clinical drugs and similar biologically active compounds to identify inhibitors of the glucose-induced mitochondrial ROS production in endothelial cells
3. Determine the mechanism of action of selected hit compounds against hyperglycemic mitochondrial ROS production.

A. Significance

1. This approach directly targets the complications and it can serve as a supportive therapy to glycemic control. There is no specific therapy against the complications, and glycemic control by itself may not be sufficient to reduce the prevalence of diabetic complications.
2. The drug repurposing approach allows rapid clinical translation, since evidence for the drug safety is readily available.
3. This is a low-cost therapeutic approach: drug re-purposing may not require a novel drug synthesis pathway, formulation or extensive toxicology studies.

B. Innovation

1. We use a phenotypic assay-based drug discovery approach to find compounds that reduce the glucose-induced ROS production in endothelial cells [38, 143]. This approach relies on the overall effect of the compounds on whole cells, thus it eliminates the drug delivery and toxicity-related issues commonly associated with target-based drug discovery.
2. This approach targets the mitochondrial ROS production that may function as an upstream element in the glucose-induced ROS [26]. While the significance of mitochondrial ROS was recognized, there are no currently available treatment modalities that specifically address the mitochondrial ROS production without blocking the respiration.
3. The conditions we chose in our screen mostly excluded the inhibitors of oxidative phosphorylation (OXPHOS) to focus on drugs that rather promote OXPHOS and have greater potential for therapeutic use.

3. Materials and methods

3.1. Compound libraries and commercially available drugs

A comprehensive screening set of 6,766 compounds was gathered from vendors listed in table 1 that includes clinical compounds and drug-like molecules. The compounds were dissolved at 10 mM in dimethyl-sulfoxide (DMSO) (apart from the Natural Products that were provided at 2 mg/ml) and dilutions were made either in DMSO or in phosphate-buffered saline (PBS, pH 7.4) to obtain 0.5% final DMSO concentration. Amitriptyline hydrochloride, antimycin A, carbonyl cyanide *p*-trifluoromethoxyphenylhydrazone (FCCP), citalopram hydrobromide, desipramine hydrochloride, escitalopram oxalate, fluoxetine hydrochloride, imipramine hydrochloride, 3,4-(methylenedioxy)phenol (sesamol), nefazodone hydrochloride, nortriptyline hydrochloride, oligomycin, paroxetine hydrochloride, sertraline hydrochloride, venlafaxine hydrochloride were purchased from Sigma-Aldrich (St Louis, MO) and trans-4-(4'-Fluorophenyl)3-hydroxymethyl-piperidine was from Oakwood Products (West Columbia, SC).

3.2. Synthesis of mitochondrial H₂S donors (10-(4-Carbamothioylphenoxy)-10-oxodecyl) triphenylphosphonium bromide (AP123) and (10-Oxo-10-(4-(3-thioxo-3H-1,2-dithiol-5-yl)phenoxy) decyl)triphenylphosphonium bromide (AP39) .

The mitochondrial H₂S donor compounds AP123 and AP39 were synthesized in house using chemicals supplied by Sigma-Aldrich Ltd. (Gillingham, Dorset, UK). AP123 was synthesised using the following procedure: acetonitrile (8 cm³) was added to 10-bromodecanoic acid (400 mg, 1.59 mmol) and triphenylphosphine (418 mg, 1.59 mmol) and the resulting mixture was stirred and heated under reflux for 48 h [144]. The acetonitrile was evaporated *in vacuo* and the colourless, oily residue was triturated with toluene (3 x 10 cm³) before thorough drying on a rotary evaporator and dissolution in dichloromethane (15 cm³). At room temperature, 4-hydroxythiobenzamide (244 mg, 1.59 mmol) was added to the stirred solution, followed by a solution of *N,N*-dicyclohexylcarbodiimide (330 mg, 1.60 mmol) in dichloromethane (8 cm³) and 4-dimethylaminopyridine (10 mg, 0.08 mmol). After stirring for 22 h, the reaction mixture was filtered through a cotton wool plug and

after removal of the solvent *in vacuo*, the crude product was applied as a dichloromethane solution onto a silica gel flash chromatography column (*ca* 120 cm³ silica gel, 3 cm diameter column). After flushing the silica gel with ethyl acetate (200 cm³), the product was eluted with methanol (200 cm³) and after evaporation of the solvent *in vacuo*, the product was re-dissolved in dichloromethane (20 cm³) and the resulting solution was dried (magnesium sulfate), filtered and evaporated *in vacuo* to generate AP123 (516 mg, 50%) as a crisp, yellow foam (found [M-Br]⁺ (ES⁺) 568.2429, C₃₅H₃₉NO₂PS requires 568.2434); n_{\max} (KBr disc)/cm⁻¹ 3415 (m), 3055 (m), 2925 (s), 2853 (s), 1752 (s) (C=O), 1619 (s), 1599 (s), 1587 (m), 1504 (m), 1483 (m), 1464 (w), 1438 (s), 1384 (m), 1311 (m), 1264 (m), 1205 (s), 1167 (s), 1112 (s), 1014 (m), 995 (m), 892 (m) and 851 (w); ¹H NMR (300 MHz, CDCl₃) 9.26 (1H, br s, NH), 8.20 (2 H, part of AA'BB', *J* = 8.5 Hz, aryl CH), 7.89-7.62 (16H, complex, phenyl CH and NH), 7.02 (2H, part of AA'BB', *J* = 8.5 Hz, aryl CH), 3.50 (2H, m, CH₂P⁺), 2.52, (2H, t, *J* = 7 Hz, CH₂C(O)), 1.72-1.55 and 1.42-1.13 (6H and 8H, 2 x broad m, (CH₂)₇C(O)); ³¹P NMR (121 MHz, CDCl₃) 24.0 (P⁺); ¹³C NMR (100 MHz, CDCl₃) 200.0 (C=S), 171.8 (C=O), 153.5 (aryl C-O), 135.6 (aryl C-C(S)), 135.2 (d, *J* = 3 Hz, phenyl C-H), 133.5 (d, *J* = 10 Hz, 2 x phenyl C-H), 130.5 (d, *J* = 13 Hz, 2 x phenyl C-H), 129.7 (aryl C-H), 121.0 (aryl C-H), 118.1 (d, *J* = 86 Hz, phenyl C-P⁺), 34.2 (CH₂C(O)), 30.3 (CH₂), 30.1 (CH₂), 28.9 (CH₂), 28.8 (CH₂), 28.6 (CH₂), 28.5 (CH₂), 24.5 (CH₂), 22.9 (CH₂) and 22.4 (d, *J* = 18 Hz, CH₂P⁺), extinction coefficient in DMSO ($\epsilon_{308\text{nm}} = 5275 \text{ M}^{-1} \text{ cm}^{-1}$; ($\epsilon_{262\text{nm}} = 8108 \text{ M}^{-1} \text{ cm}^{-1}$). AP39 was synthesised as previously described by us [145], extinction coefficient in DMSO ($\epsilon_{400\text{nm}} = 6162 \text{ M}^{-1} \text{ cm}^{-1}$; ($\epsilon_{327\text{nm}} = 12000 \text{ M}^{-1} \text{ cm}^{-1}$).

AP39 was synthesised according the following procedure: a solution of 10-bromodecanoic acid (500 mg, 1.99 mmol) in acetonitrile (5 cm³) was added to a stirred solution of triphenylphosphine (522 mg, 1.99 mmol) in acetonitrile (5 cm³) and the resulting mixture was heated at reflux for 70 h. After cooling to room temperature and evaporation of the solvent *in vacuo*, the residue was triturated with toluene (2 x 10 cm³) and dissolved in dichloromethane (30 cm³). 5-(4-Hydroxyphenyl)-3H-1,2-dithiole-3-thione (456 mg, 2.02 mmol), N,N-dicyclohexylcarbodiimide (431 mg, 2.09 mmol) and 4-dimethylaminopyridine (12 mg, 0.10 mmol) were added and the resulting solution was stirred at room temperature for 22 h before filtering through a cotton wool plug and evaporation of the filtrate *in vacuo*. A dichloromethane solution

of the residue was loaded onto a silica gel flash chromatography column, which was subsequently eluted with ethyl acetate, followed by methanol. The methanol fractions were combined and evaporated *in vacuo* and a dichloromethane solution of the residue was filtered through a filter paper to remove residual silica gel before evaporation *in vacuo* to produce AP39 (1.05 g, 73%) as a crisp, orange foam (found $[M - Br]^+$ (ES⁺) 641.1766, C₃₇H₃₈O₂PS₃ requires 641.1766); n_{\max} (KBr disc)/cm⁻¹ 2925 (m), 2852 (m), 1754 (m) (C=O), 1599 (w), 1521 (w), 1485 (s), 1437 (s), 1410 (m), 1317 (m), 1278 (m), 1185 (s), 1168 (s), 1112 (s), 1026 (s), 996 (m), 896 (w), 839 (w), 747 (m), 722 (m), 690 (m), 535 (m) and 508 (m); ¹H NMR (300 MHz, CDCl₃) 7.95–7.65 (17H, m, aryl C(2)H, aryl C(6)H and phenyl CH), 7.42 (1H, s, CHC=S), 7.23 (2H, part of AA'BB', $J = 8.5$ Hz, aryl C(3)H and C(5)H), 3.85 (2H, m, CH₂P⁺), 2.58 (2H, t, $J = 7.5$ Hz, CH₂C=O), 1.80–1.55 (6H, m, 3 x CH₂) and 1.42–1.19 (8H, m, 4 x CH₂); ³¹P NMR (121 MHz, CDCl₃) 25.7 (P⁺); ¹³C NMR (75 MHz, CDCl₃) 214.9 (C=S), 183.7 (CH=C-S), 171.7 (C=O), 153.6 (arylC-O), 135.8 (arylC-C=CH), 134.9 (phenylC-H), 133.6 (d, $J = 9$ Hz, phenylC-H), 130.4 (d, $J = 13$ Hz, phenylC-H), 128.9 (C=CH-C(S)), 128.1 (arylC-H), 122.9 (arylC-H), 118.3 (d, $J = 83$ Hz, phenylC-P+), 34.2 (CH₂C(O)), 30.3 (d, $J = 13$ Hz, CH₂), 29.0 (CH₂), 28.9 (2 x CH₂), 28.8 (CH₂), 24.6 (CH₂), 23.0 (CH₂) and 22.5 (d, $J = 18$ Hz, CH₂P⁺).

3.3. H₂S release detection in solution and *in situ* in endothelial cells

H₂S donors were dissolved and diluted in DMSO. Compounds or vehicle were added in 1/10 volume and mixed with DMEM supplemented with 10% FBS and 0.5 mg/ml MTT. Free H₂S as strong reducing agent reacts with the tetrazolium dye MTT and forms purple colour formazan. Changes in absorbance were recorded every 24 hours on a microplate reader (Molecular Devices Spectramax M2e, Sunnyvale, CA) at 570 nm with background measurement at 690nm. The reaction was carried out in a humidified incubator at 37 °C with 5% CO₂ atmosphere to closely mimic the cell culture conditions and minimise evaporation. H₂S calibration curve was created by preparing serial dilutions of freshly dissolved Na₂S (Alpha Aesar, Haverhill, MA) and by measuring the reducing capacity. The slow release H₂S donors liberate H₂S over several days and the low background of MTT reduction allows H₂S detection up to 2 weeks. The H₂S generation is shown as the cumulative increase or daily change in absorbance with respective H₂S values.

The toxic concentration of H₂S donors was determined in b.End3 endothelial cells. Cells (20 000/well) were seeded in 96 well plates and cultured in DMEM containing 1 g/l glucose supplemented with 10% FBS, 1% non-essential amino acids and antibiotics at 37 °C in 5% CO₂ atmosphere for 5 days. H₂S donors were diluted in PBS containing 10% DMSO and added in 1/20 volume, then cells were incubated at 37 °C for 24 hours. Non-mitochondrial H₂S donors were added in the concentration range of 100nM to 1mM and mitochondrial H₂S donors in the range of 10nM to 100µM. After 24 hours, the supernatant was saved to detect LDH release and fresh culture medium supplemented with 0.5 mg/ml MTT was added to the cells. MTT and LDH assays were performed as detailed below. The cellular viability values and percent cell lysis values were plotted and the 50% toxic concentration was calculated using Prism 6 analysis software (GraphPad Software, Inc., La Jolla, CA)

b.End3 cells (2×10^5 /well) were seeded on 4-well Nunc Lab-Tek chambered coverglass (Nalge Nunc, Rochester, NY) and cultured overnight. H₂S donor compounds were diluted in PBS and DMSO and were added at 30 µM final concentration in 1/20 culture volume. The cells were treated with the compounds at 37 °C for 2 hours, followed by loading with fluorescent H₂S sensor 7-azido-4-methylcoumarin (AzMc) (40nM, Sigma-Aldrich, St. Louis, MO) and Mitotracker Green FM (200 µM, Life Technologies, Carlsbad, CA) mitochondrial stain at 37 °C for 1 hour to detect H₂S release simultaneously with the endogenous H₂S production. AzMc fluorescence and the MitoTracker signal were detected on a Nikon TE2000 inverted microscope (Nikon UK Limited, Surrey, UK) using a Hamamatsu ORCA-ER monochrome camera (Hamamatsu Photonics UK Ltd., Hertfordshire). The H₂S signal is shown in green and the MitoTracker signal in red.

3.4. Cell culture and cell-based screening for inhibitors of hyperglycemia induced mitochondrial ROS production

bEND.3 murine and EA.hy926 human endothelial cells were obtained from the American Type Culture Collection (ATCC, Manassas, VA) and maintained in Dulbecco's modified Eagle's medium (DMEM) (Hyclone, Logan, UT) containing 1g/l glucose supplemented with 10% fetal bovine serum (FBS, Hyclone, Logan, UT), 1% non-essential amino acids, 100 IU/ml penicillin and 100 µg/ml streptomycin (Invitrogen, Carlsbad, CA) at 37 °C in 10% CO₂ atmosphere.

b.End3 cells (20 000/well) were plated into 96-well tissue culture plates and were cultured for 24 hours. Hyperglycemia (40 mM glucose) was initiated by replacing the culture medium with fresh DMEM containing 7.2 g/l glucose supplemented with 10% FBS, 1% non-essential amino acids, 100 IU/ml penicillin and 100 µg/ml streptomycin and were cultured for 10 days before measuring the oxidant production. The culture medium was supplemented with pyruvate (10 mM) as fresh source of energy after 4 days of exposure. Test compounds were tested at 3 µM final concentration (0.5% DMSO) in the culture medium. The Natural Products Library was screened at 1 µg/ml final concentration. Compounds were administered in 1/20 volume on the 7th day of exposure and control cells were treated with vehicle.

EA.hy926 cells were used in similar manner but were exposed to hyperglycemia in medium 199 supplemented with 15% FBS, 4 mM glutamine, 7.5 U/ml heparin, 2.5 µg/ml human endothelial cell growth factor, 2 ng/ml human epidermal growth factor, 100 IU/ml penicillin and 100 µg/ml streptomycin.

After 10 days of exposure the cells were loaded with mitochondrial superoxide sensor MitoSOXTM Red (2.5 µM) and DNA stain Hoechst 33342 (10 µM) for 25 min. Reading medium (PBS supplemented with 1 g/l glucose and 10% bovine growth serum) was added to the cells and the oxidation of MitoSOXTM Red was recorded kinetically (Ex/Em: 530/590 nm) on Synergy 2 (BioTek, Winooski, VT) at 37°C for 35 min as previously described (9). Vmax values were used as a measure of mitochondrial reactive oxygen species (ROS) production rate. The fluorescence of Hoechst 33342 (Ex/Em: 360/460 nm) was used to calculate the viability of the cells using a calibration curve created by serial dilution of b.End3 cells. In select experiments test compounds were administered in 1/20 volume 3 hours prior to the MitoSOXTM Red loading or immediately thereafter. ROS scores (ROS score of 1 was defined as 25% decrease of the average mitochondrial ROS production of hyperglycemic cells on test plate) and viability scores (viability score of 1 as the standard deviation of the hyperglycemic cells on each test plate) were calculated to minimize inter-plate variability and to identify active compounds.

3.5. Measurement of cytoplasmic ROS generation

Following the hyperglycemic exposure the cells were loaded with cell-permeable ROS indicator 5-(and-6)-chloromethyl-2',7'-dichlorodihydrofluorescein diacetate

(CM-H₂DCFDA, 10 μ M) and DNA stain Hoechst 33342 (10 μ M) for 25min. Reading medium (PBS supplemented with 1 g/l glucose and 10% bovine growth serum) was added to the cells and the oxidation of CM-H₂DCFDA was measured kinetically (Ex/Em: 485/528nm) on Synergy2 plate reader (BioTek) at 37°C for 35 min. ROS production are shown as V_{max} values or percent values of V_{max} values of control cells. The fluorescence of Hoechst 33342 (Ex/Em: 360/460nm) was used to calculate the viability of the cells using a calibration curve created by serial dilution of b.End3 cells.

3.6. *In situ* detection of ROS generation

Cells were plated (50,000/well) into Lab-Tek™ II 8-well chamber slides (Nalge Nunc, Rochester, NY) and were treated with hyperglycemia and compounds as described earlier. Following the hyperglycemic exposure the cells were washed with PBS and the cells were loaded with MitoSOX™ Red and Hoechst 33342 for 25 min. The cells were incubated in reading medium for two hours and then images were taken on an Eclipse 80i fluorescent microscope (Nikon Instruments, Melville, NY) with Coolsnap *HQ*² CCD camera (Photometrics, Tucson, AZ).

3.7. Mitochondrial ROS measurement in isolated mitochondria

Mitochondria were isolated from male Sprague-Dawley rats (225-250 g, Harlan Laboratories, Houston, TX). Fresh liver tissue was rinsed 3 times in ice-cold mitochondria isolation buffer (MSHE: 70 mM sucrose, 210 mM mannitol, 5 mM HEPES, 1 mM EGTA, 0.5% (w/v) fatty acid-free BSA, pH 7.2), then 400-600 mg liver was minced and homogenized with teflon/glass homogenizer in 10 volumes of mitochondrial isolation buffer. The homogenate was centrifuged at 600 g for 10 min at 4°C. Lipids were carefully aspirated, and the supernatant was decanted through 2 layers of cheesecloth and centrifuged at 10,000 g for 10 min at 4°C. After removal of the light mitochondrial layer, the pellet was resuspended in MSHE, and the centrifugation was repeated at 10,000 g for 10 min at 4°C. The final pellet was resuspended in 5 ml mitochondria assay solution (MAS: 10 mM KH₂PO₄, 5 mM MgCl₂, 2 mM HEPES, 1 mM EGTA and 0.2% (w/v) fatty acid-free BSA, pH 7.2 at 37 °C). The protein concentration was determined using the BCA Protein Assay (Pierce, Rockford, IL) and mitochondria (10 μ g protein/well) were plated into 96-well

plates in 50 μ l/well volume. Mitochondria were centrifuged at 2,000 g for 20 min at 4°C, then 50 μ l/well assay solution supplemented with succinate, rotenone, ADP and MitoSOX™ Red (final concentrations 10mM, 2 μ M, 4mM and 1.25 μ M respectively) and the test compounds (10 μ l/well) were added. The oxidation of MitoSOX was recorded kinetically (Ex/Em: 530/590nm) on Synergy 2 plate reader (BioTek, Winooski, VT) at 37°C for 35 min. Vmax values were used as a measure of mitochondrial reactive oxygen species (ROS) production rate. The functional integrity of the isolated mitochondria was simultaneously confirmed on a Seahorse metabolic analyzer.

3.8. Xanthine-oxidase assays

Superoxide was generated by bovine xanthine oxidase (0.25mU/ml, Sigma-Aldrich, St. Louis, MO) in 50mM potassium phosphate buffer (pH 7.5) containing 50 μ M xanthine and 50 μ M diethylenetriaminepentaacetic acid (DETAPAC, Sigma-Aldrich, St. Louis, MO). The superoxide generation was measured kinetically at 37°C for 35 min on Synergy 2 plate reader (BioTek, Winooski, VT) either by colorimetric detection (490nm) using 40 μ M nitrotriazolium blue (NBT) or by a fluorescent method using MitoSOX™ Red (1.25 μ M, Ex/Em: 530/590nm) and 1 μ g/ml Hind III digest of λ DNA to increase the signal intensity. Test compounds were added in 1/20 volume and were diluted in 50mM potassium phosphate buffer (pH 7.5).

3.9. Viability assays: MTT and LDH assays, ATP measurement

The MTT assay and LDH activity measurements were performed as previously described [146, 147]. Briefly, the cells were incubated in medium containing 0.5 mg/mL 3-(4,5-dimethyl-2-thiazolyl)-2,5-diphenyl-2H-tetrazolium bromide (MTT, Calbiochem, EMD BioSciences, San Diego, CA) for 1 hour at 37°C at 10% CO₂ atmosphere. The converted formazan dye was dissolved in isopropanol and the absorbance was measured at 570 nm. Serial dilution of the cells was used to fit a curve on the absorbance values. MTT conversion rate values are shown as percent values relative to normoglycemic controls.

Total LDH content of the cells was measured by lysing the cells in 0.15 M saline containing 1% Triton-X-100 (30 μ l/well) and measuring the LDH activity by adding

100 μ L LDH assay reagent containing 110 mM lactic acid, 1350 mM nicotinamide adenine dinucleotide (NAD^+), 290 mM *N*-methylphenazonium methyl sulfate (PMS), 685 mM 2-(4-Iodophenyl)-3-(4-nitrophenyl)-5-phenyl-2*H*-tetrazolium chloride (INT) and 200 mM Tris (pH 8.2). The changes in absorbance were read kinetically at 492 nm for 15 min (kinetic LDH assay). LDH activity values are shown as percent values relative to cells maintained under normoglycemia.

ATP concentration was determined by the commercially available CellTiter-Glo® Luminescent Cell Viability Assay (Promega, Madison, WI). The cells were lysed in 100 μ L of CellTiter-Glo reagent according to the manufacturer's recommendations and the luminescent signal was recorded for 1 s on a high sensitivity luminometer (Synergy Mx, Biotek, Winooski, VT, USA). The assay is based on ATP requiring luciferin-oxyluciferin conversion mediated by a thermostable luciferase that generates a stable "glow-type" luminescent signal. ATP standard (dilution series) was used to calculate the cellular ATP amount and the ATP values are shown as percent values of the normoglycemic controls.

3.10. Mitochondrial membrane potential measurement

The mitochondrial potential was measured with JC-1 (Sigma-Aldrich, St. Louis, MO) fluorescent probe as previously described [148]. The cells were loaded with the dye by exposing them to JC-1 stain solution containing 10 μ M JC-1 and 0.6 mM β -cyclodextrin (Sigma-Aldrich, St. Louis, MO) in OptiMEM I medium at 37 °C for 30 min. Subsequently, the cells were washed in phosphate buffered saline (PBS) and the red (Ex/Em: 485/528nm) and green (Ex/Em: 530/590nm) fluorescence was measured on a microplate reader (Synergy 2, Biotek, Winooski, VT, USA). The mitochondrial potential is reported as percent values of the ratio of the mitochondrial J-aggregates (red fluorescence) and the cytoplasmic monomer form of the dyes (green fluorescence) compared to vehicle-treated normoglycemic control cells.

Changes in the mitochondrial potential were also investigated by measuring the uptake of Mitotracker Green FM (Life Technologies, Carlsbad, CA). The uptake of the Mitotracker Green FM is potential-sensitive but it is less sensitive for rapid changes than JC-1 [149]. The cells were loaded with Mitotracker Green FM (0.5 μ M) and Hoechst 33342 (10 μ M) in PBS at 37 °C for 30 min, then the cells were washed

twice and the fluorescence of Mitotracker Green (Ex/Em: 485/528 nm) and Hoechst 33342 (Ex/Em: 360/460 nm) was recorded on Synergy 2 reader (BioTek, Winooski).

3.11. Gene expression array

Total RNA was isolated from bEND.3 cells exposed to hyperglycemia or normoglycemia for 7 days using TRIzol® reagent according to the protocol provided by the manufacturer. 2 µg RNA was treated with DNase (Epicentre, Madison, WI) and reverse transcription was carried out using High Capacity cDNA Archive kit (Applied Biosystems, Foster City, CA) following the manufacturer's instructions. 1 µg RNA was used according to the manufacturer's protocol for gene expression measurements using the mouse mitochondrial energy real-time PCR array (SABiosciences, Frederick, MD) on CFX96 thermocycler (Biorad, Hercules, CA).

3.12. siRNA mediated gene silencing and real-time PCR measurements

Gene silencing and RNA level gene expression measurements were performed as previously described [147]. b.End3 cells (20,000/well) were plated on 96-well plates, the following day the cells were transfected with uncoupling protein 2 (UCP2) siRNA (1 pmol/well, Silencer Select, assay ID: s75721, Life Technologies, Carlsbad, CA) using Lipofectamine 2000 transfection reagent. Control cells were transfected with Silencer Select negative control #1 siRNA (ID: 4390844, Life Technologies, Carlsbad, CA). The knockdown efficiency was evaluated by real time PCR to confirm that the silencing lasts for 10 days.

Total RNA was isolated using a commercial RNA purification kit (SV total RNA isolation kit, Promega, Madison, WI). 2 µg RNA was reverse transcribed using the High Capacity cDNA Archive kit (Applied Biosystems, Foster City, CA) as previously described [147, 38, 150]. UCP2 expression was measured using species-specific UCP2 Taqman assays (murine assay ID: Mm00627598_m1, human assay ID: Hs01075227_m1, Life Technologies, Carlsbad, CA) and VIC-labeled 18S rRNA control reagents (Cat# 4308329 for murine and Cat# 4310893E for human samples, Life Technologies, Carlsbad, CA) for normalization on a CFX96 thermocycler (BioRad, Hercules, CA). The expression of uncoupling protein 3 (UCP3) was measured by the following Taqman assay: assay ID: Mm01163394_m1 (Life Technologies, Carlsbad, CA).

In a separate set of experiments the expression of the nuclear encoded glucocorticoid receptor (GR), sirtuin 1 (SIRT) and cytochrome C (Cyt C) and the two mitochondrial encoded genes: the cytochrome c oxidase III (COX3) and 16S ribosomal RNA (16S RNA) was measured in cells exposed to hyperglycemia and dexamethasone. b.End3 cells were exposed to hyperglycemia or maintained at normoglycemia for 7 days and treated with dexamethasone (3 μ M) for 3 days. RNA was isolated and reverse transcribed as described above. The gene expression was measured in PCR reactions utilizing the SYBR Green method using the primers at 0.4 μ M (16S RNA forw. 5'-AAACAGCTTTTAACCATTGTAGGC-3', 16S RNA rev. 5'-TTGAGCTTGAA GCTTTCTTTA-3', COX3 forw. 5'-AGACGTAATTCGTGAAGGAACC-3', COX3 rev. 5'-CCGAGACGATGAATAGAATTA TACC-3', Cyt C forw. 5'-AAATCTCCACGGTCTGTTCG-3', Cyt C rev. 5'-CCAGGTGATGCCTTTGTTCT-3', GR forw. 5'-TTACCCCTACCCTGGTGTCA-3', GR rev. 5'-AAGGGTCATTTGGTCATCCA-3', SIRT forw. 5'-AAAAGATAATAGTTCTG ACTGGAGCTG-3', SIRT rev. 5'-GGCGAGCATAGATACCGTCT-3') on a CFX96 thermocycler (Bio-Rad, Hercules, CA). Expression values were normalized to the amount of 18S rRNA (Life Technologies, Carlsbad, CA).

3.13. Mitochondria isolation and western blotting

Endothelial cells were exposed to hyperglycemia or maintained under normoglycemic conditions for 10 days and the mitochondria were isolated using the Mouse Mitochondria Isolation Kit (Miltenyi Biotec Inc., Auburn, CA). The cells were washed in PBS, scraped in separation buffer and lysed using a Dounce homogenizer. The lysates were incubated with anti-TOM22 microbeads (1:200) at 4 °C for 1 hour to magnetically label the mitochondria. Then the labeled mitochondria were captured on a MACS separation column and washed with separation buffer. Finally, mitochondria were eluted by flushing the column with 1.5 ml buffer, pelleted and resuspended in 100 μ l storage buffer. Mitochondria samples (10 μ g protein) were heated to 37°C for 5 min. and resolved on 4-12% NuPage Bis-Tris acrylamide gels (Invitrogen, Carlsbad, CA) then transferred to nitrocellulose. Membranes were blocked in 10% non-fat dried milk and probed overnight with MitoProfile Total OXPHOS Rodent WB Antibody Cocktail (1:500, MitoSciences/Abcam, Cambridge, MA). The Antibody Cocktail contains antibodies against the following proteins in the respective

respiratory complexes: NADH dehydrogenase (Ubiquinone) 1 beta subcomplex 8 (NDUFB8, Complex I), Succinate dehydrogenase [ubiquinone] iron-sulfur subunit (SDHB, Complex II), Ubiquinol-Cytochrome c reductase Core Protein II (UQCRC2, Complex III), Cytochrome c oxidase subunit I (MTCO1, Complex IV), ATP synthase subunit alpha (ATP5A1, Complex V). The antibodies in the cocktail detect subunits that are labile when the complexes are not assembled.

Cell samples were lysed in denaturing loading buffer (20 mM Tris, 2% SDS, 10% glycerol, 6 M urea, 100 µg/ml bromophenol blue, 200 mM β-mercaptoethanol) [147, 150]. Lysates were sonicated, boiled and resolved on 4-12% NuPage Bis-Tris acrylamide gels (Invitrogen, Carlsbad, CA), then transferred to nitrocellulose. Membranes were blocked in 10% non-fat dried milk and probed overnight with UCP-2 antibody (1:100, Santa Cruz Biotechnology Inc., Dallas, TX). After incubation with peroxidase conjugates (Cell Signaling, Danvers, MA) the blots were detected on a CCD-camera based detection system (GBox, Syngene USA, Frederick, MD) with enhanced chemiluminescent substrate. To normalize the signals, membranes were reprobed with horseradish peroxidase labeled actin antibody (1:3000, Santa Cruz Biotechnology Inc., Dallas, TX). The signals were quantitated using Genetools analysis software (Syngene USA, Frederick, MD).

3.14. Detection of oxidative nucleic acid and protein damage

DNA strand breaks in bEND.3 cells exposed to hyperglycemia were detected with a single-cell gel electrophoresis using a commercially available Comet assay system (Trevigen, Gaithersburg, MD) as previously described [94]. Micrographs were transformed to binary images at a fixed intensity scale to measure the tail length.

In a separate series of experiments, cells were plated (50,000/well) into Lab-Tek™ II 8-well chamber slides (Nalge Nunc, Rochester, NY) and were exposed to hyperglycemia and treated with compounds as described above. Then the cells were fixed in 4% buffered formalin and were probed with an antibody against 8-hydroxyguanosine (1:200, Pierce, Rockford, IL) overnight, followed by incubation with Alexa-546 labeled anti-mouse antibody (Invitrogen, Carlsbad, CA) and subsequent staining with nuclear stain Hoechst 33342 and Alexa-488-phalloidin conjugate. Oxidative damage of nucleic acids was visualized on a Nikon Eclipse 80i microscope and images were taken as above described. The red fluorescence (sum of intensity of

every pixel) of individual cells was analyzed using NIS Elements Basic Research software package and shown as relative fluorescence (RFU/cell).

Protein oxidation was measured in crude mitochondrial fraction prepared by lysing bEND.3 cells exposed to hyperglycemia in lysis buffer comprising 50mM Tris-HCl, pH 7.4, 50mM sodium fluoride, 5mM sodium pyrophosphate, 1mM EDTA, 250mM mannitol, 1% Triton X-100 supplemented with protease inhibitors (Complete mini, Roche Applied Science, Indianapolis, IN). Nuclei were removed by centrifuging the samples at 300 x g and mitochondrial fraction was prepared from the supernatant by centrifuging at 12 000 x g. The pellet was dissolved in RIPA buffer (Cell Signaling, Danvers, MA) and protein concentration was measured by DC protein assay (Bio-Rad, Hercules, CA). 2.5ug protein was processed using the Oxyblot Protein Oxidation detection kit (Millipore, Billerica, MA). Samples were resolved on 4-12% Nupage Bis-Tris gel (Invitrogen, Carlsbad, CA) and blotted to nitrocellulose. Pierce enhanced chemiluminescent substrate (Pierce ECL, Thermo Fisher Scientific Inc., USA) was used to detect the chemiluminescent signal in a CCD-camera based detection system (GBox, Syngene USA, Frederick, MD).

3.15. Detection of oxidative damage of the mitochondrial DNA (mtDNA)

b.End3 cells were exposed to hyperglycemia and were treated with paroxetine (10 μ M) for 3 days. The cells were lysed in 0.8% sarcosine, 20mM EDTA, 100mM Tris pH 8.0 and treated with RNase A and Proteinase K. Phenol-chloroform extracted DNA samples (200ng) were subjected to 8-oxoguanine DNA glycosylase (hOGG1, 2U) digestion at 37 °C for 1 hour, followed by heat inactivation (65°C, 15min). Equal amount of DNA was incubated simultaneously in the same buffer without the enzyme. The amplifiable amount of mtDNA was measured by real-time PCR using primers targeting the mitochondrial Tyr-tRNA coding region (forward primer: 5'-CACCTTAAGACCTCTGGTAAAAAGA-3', reverse primer: 5'-TGAGAATAATCAACGATTAATGAACA-3') and the difference was calculated between the hOGG1-treated and non-treated samples.

3.16. Respiratory complex II/ III activity assay

Complex II+III activity was measured by the MitoTox Complex II+III OXPHOS Activity Microplate assay (Abcam, Cambridge, UK). Respiratory complex II

(succinate-ubiquinone oxidoreductase) transfers electrons from succinate to Complex III (ubiquinolcytochrome c oxidoreductase) *via* mobile electron shuttle ubiquinone. Complex III transfers electrons to Complex IV (cytochrome c oxidase) *via* mobile electron carrier cytochrome *c*. The assay measures cytochrome *c* reduction using succinate as substrate (Complex II+III activity).

Bovine heart mitochondria were used as source of respiratory complexes. Complex I was inhibited by rotenone (10 μ M) to block electron transfer from NADH to ubiquinone and Complex IV by potassium cyanide (2 mM) to avoid to reoxidation of cytochrome *c*. H₂S donor compounds (10 nM to 10 μ M) were mixed with mitochondria (30 μ g/ml) in the presence of succinate and oxidised cytochrome *c*. Cytochrome *c* reduction was monitored kinetically on a microplate reader (Molecular Devices Spectramax M2e, Sunnyvale, CA) at 550 nm. Mitochondrial complex II/III activity is shown as the maximum velocity of cytochrome *c* reduction in mOD/min.

3.17. Extracellular Flux Analysis

An XF24 Analyzer (Seahorse Biosciences, Billerica, MA) was used to measure metabolic changes in b.End3 cells as previously described [151]. The XF24 creates a transient 7 μ l chamber in specialized microplates that allows real-time measurement of oxygen and proton concentration changes via specific fluorescent dyes and calculates OCR (oxygen consumption rate) and ECAR (extracellular acidification rate), measures of mitochondrial respiration and glycolytic activity. The proton production rate is similarly denotes the cellular acid production but in pMol/min, while ECAR is expressed in pH/min. The OCR and ECAR values represent the metabolism of cells, but may also reflect the number of viable cells. After determining the basal OCR and ECAR values, oligomycin, FCCP and antimycin A were injected through the ports of the Seahorse Flux Pak cartridge to reach final concentrations of 1 μ g/ml, 0.3 μ M and 2 μ g/ml, respectively, to determine the amount of oxygen consumption linked to ATP production, the level of non-ATP-linked oxygen consumption (proton leak) as well as the maximal respiration capacity and the non-mitochondrial oxygen consumption. Following the metabolic measurements, the cells were lysed in M-PER mammalian protein extraction reagent (Pierce, Rockford, IL) and the protein content was determined using the bicinchoninic acid (BCA)

method (Pierce, Rockford, IL). OCR and ECAR values were normalized to protein content and are shown as OCR or ECAR/protein.

3.18. Vascular studies of *in vitro* hyperglycemia

Thoracic aortic rings from Sprague-Dawley rats were incubated for 48 h under normoglycemic (5 mM) or hyperglycemic (30 mM) conditions in DMEM in the presence or absence of 10 μ M paroxetine, followed by the determination of acetylcholine-induced relaxations as previously described [94].

3.19. Vascular studies of streptozotocin-induced diabetes

Diabetes in male Sprague-Dawley rats was induced with a single streptozotocin injection of 60 mg/kg body wt i.p. prepared in citrate buffer (pH=4.5). On Day 14, animals were implanted with osmotic pump (Alzet, Cupertino, CA) filled with paroxetine (releasing a dose of 10 mg/kg/day) or vehicle. Rats were divided into groups as follows: control group (CTL/V, $n=10$) (non-diabetic rats treated with vehicle), control with paroxetine (CTL/P, $n=10$) (non-diabetic rats treated with paroxetine), STZ induced diabetes group (STZ/V, $n=10$) (diabetic rats treated with vehicle), and STZ induced diabetes group treated with paroxetine (STZ/P, $n=10$). Minipumps were replaced at 2 weeks. Paroxetine or vehicle treatment lasted for 28 days, at which point thoracic aortae were obtained and acetylcholine-induced relaxations were measured as described [94].

3.20. Statistical analysis

Data are shown as mean \pm SEM values. One-way analysis of variance (ANOVA) was used to detect differences between groups. Post hoc comparisons were made using Tukey's test. A value of $p < 0.05$ was considered statistically significant. All statistical calculations were performed using GraphPad Prism 6 (La Jolla, CA, USA) software.

4. Results

4.1. Characterization of the hyperglycemic endothelial cell injury model

We exposed b.End3 microvascular endothelial cells to high glucose for several days to enhance the mitochondrial reactive oxygen species (ROS) production. Extended hyperglycemic exposure significantly stimulated the ROS production after a couple of days and induced a progressive increase until the 10th to 14th days of hyperglycemia (**Fig. 3A-D**). The enhanced ROS production was not associated with marked alterations in the expression level of genes related to the mitochondrial respiration and ATP production (**Fig. 3E, Suppl. Tables 1-2**).

The glucose-induced ROS production was associated with metabolic changes in the b.End3 cells, though. When exposed to hyperglycemia, the cells showed a progressive increase in the mitochondrial MTT conversion but no change was detectable in the lactate dehydrogenase (LDH) activity in the cells (**Fig. 4A, B**). MTT is presumed to be reduced predominantly by the enzyme mitochondrial succinate dehydrogenase (respiratory complex II) [152], thus the MTT assay may indirectly measure the aerobic metabolism and the oxidative phosphorylation (OXPHOS) in the cells, whereas the anaerobic metabolism is represented by the LDH activity, a key enzyme in anaerobic respiration. Similar to the changes in the MTT reduction, the mitochondrial membrane potential showed a progressive increase in the cells with significantly elevated values after 5 days of exposure (**Fig. 4C**). These changes had no effect on the cellular ATP content. The cells maintained a stable energy level until the 10th day of exposure and started to show a decline in the ATP level afterwards (**Fig. 4D**). While the cellular LDH content (anaerobic metabolism) increased at that time (**Fig. 4B**), it was not sufficient to reinstate the cellular energy level (**Fig. 4D**).

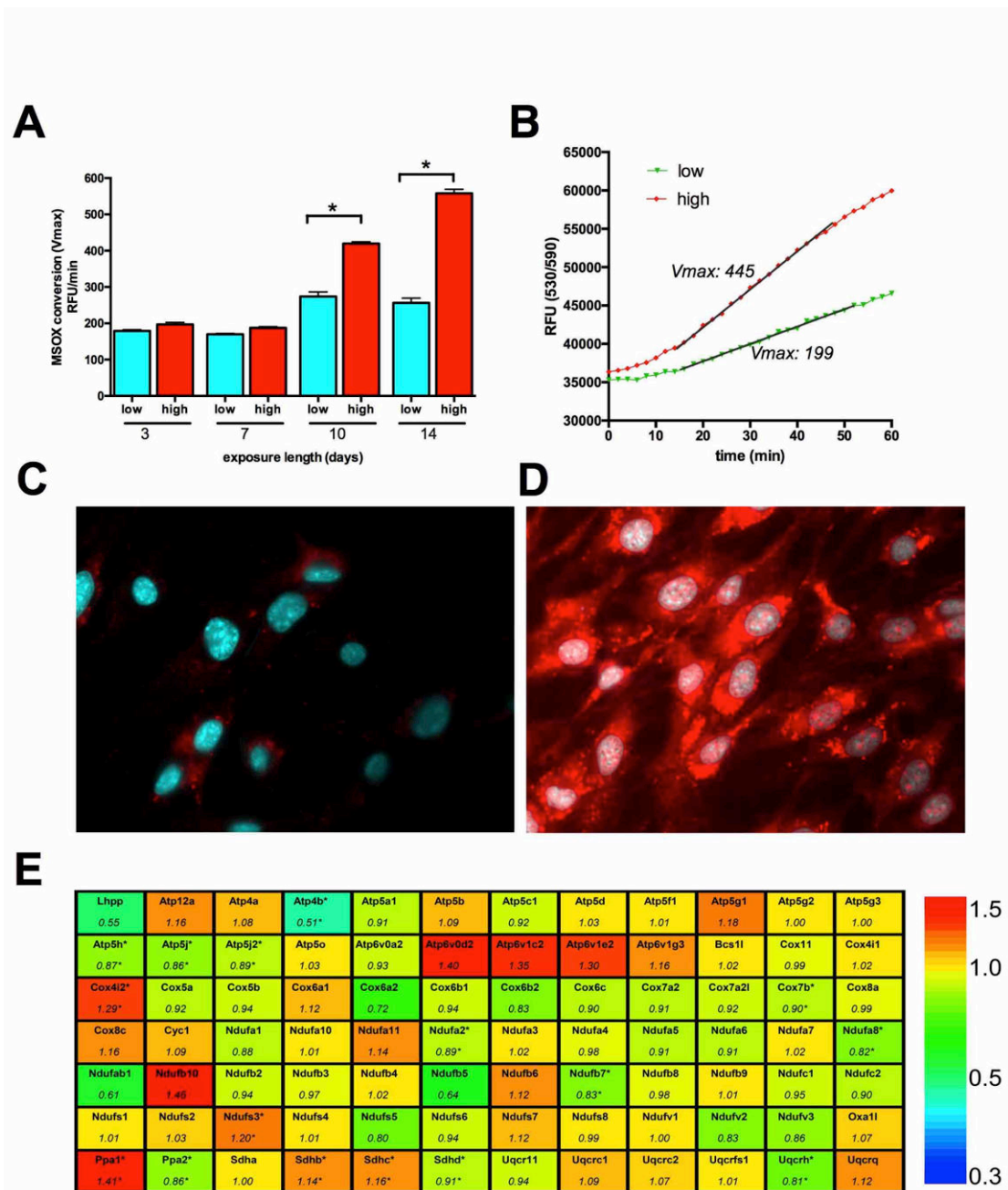


Fig. 3. Long-term hyperglycemia induces mitochondrial oxidant production in endothelial cells. *A-D*: *b.End3* cells were exposed to hyperglycemia (high) or maintained in 5mM glucose (low) containing medium for 10 days or for the indicated time period, then the cells were loaded with superoxide sensor MitoSOX Red and Hoechst 33342. The oxidation of MitoSOX was recorded on kinetic reader, the maximum reaction rates (V_{max}) (**A**) and typical kinetic curves are shown (**B**). Micrographs of cells maintained in normoglycemic (**C**) or hyperglycemic (**D**) medium were taken 2 hours following the superoxide sensor loading. **E**: Gene expression changes in *b.End* cells exposed to hyperglycemia for 7 days were analyzed with mitochondrial energy array. The gene symbols and relative expression (fold change) in hyperglycemic cells are shown compared to normoglycemic cells. (* $p < 0.05$)

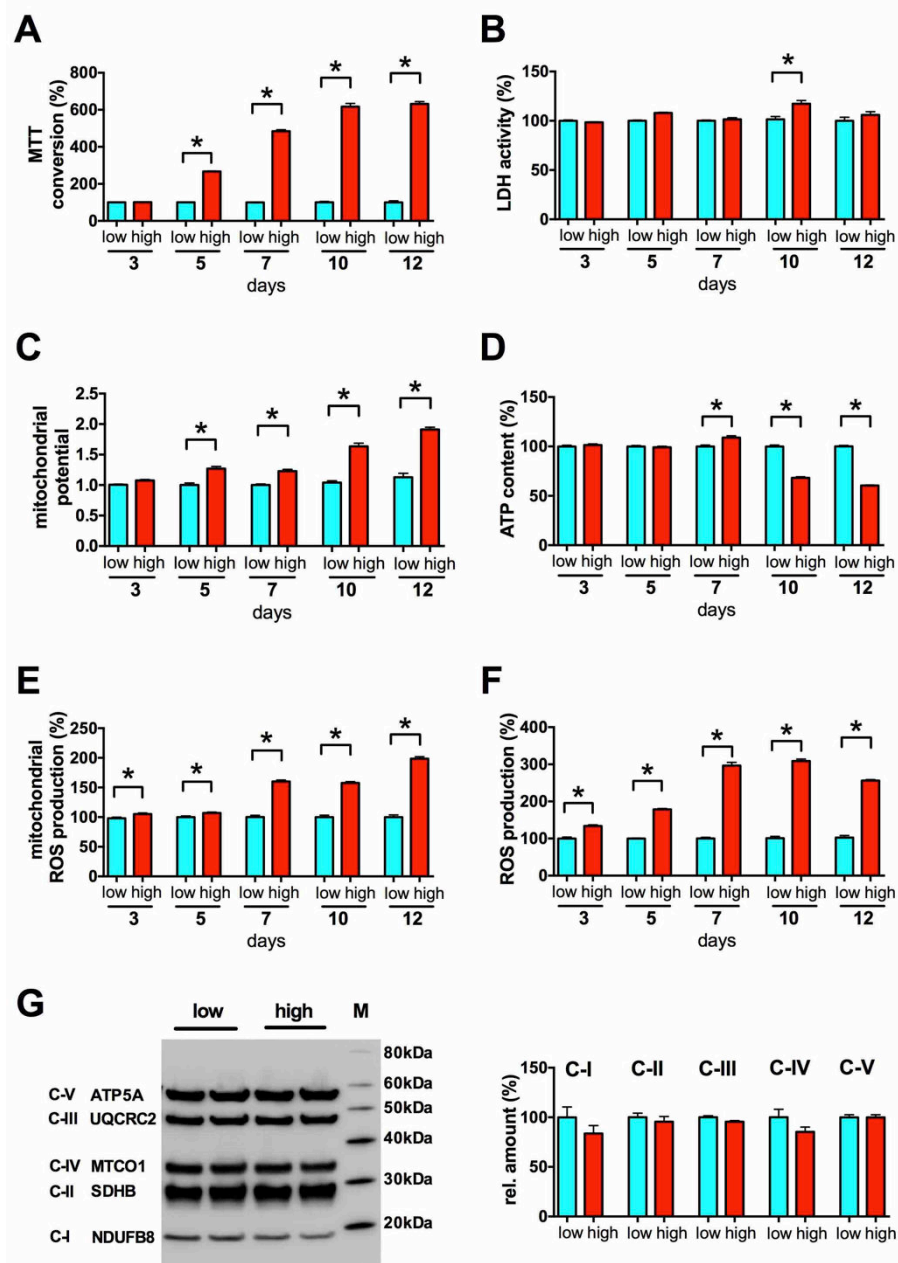


Fig. 4. High glucose exposure induces mitochondrial hyperpolarization and oxidant production in b.End3 microvascular endothelial cells. A-F: Confluent b.End3 endothelial cells were maintained in low or high-glucose containing medium for 3-12 days and metabolic indices and ROS production were determined. **A:** The mitochondrial citric acid cycle activity was determined by measuring the MTT converting capacity of the cells. **B:** The anaerobic metabolic capacity of the cells was determined by measuring the LDH activity of the cells. **C:** The mitochondrial membrane potential was determined by JC-1 dye. **D:** The cellular ATP content was measured. **E, F:** The cellular ROS production was determined by **(E)** measuring the mitochondrial superoxide generation and **(F)** the cellular H_2O_2 production. **G:** Respective levels of the mitochondrial respiratory complexes were determined by MitoProfile total OXPHOS antibody cocktail. Representative blot image and densitometric analysis results are shown. (* $p < 0.05$ high-glucose exposure induced significant changes compared to cells maintained in low glucose containing medium.)

Hyperglycemia increased both the mitochondrial and the cytoplasmic ROS production in the cells, as measured by the mitochondrial superoxide-sensitive MitoSOX Red probe and the H₂O₂-sensitive 5-(and-6)-chloromethyl-2',7'-dichlorodihydrofluorescein diacetate, acetyl ester (CM-H₂DCFDA) (**Fig. 4E, F**). Significantly increased ROS production was detectable already on the 3rd day of the hyperglycemic exposure, and on the subsequent days a progressive increase was observed similar to the increase in the mitochondrial membrane potential. We tested, whether there was any change in the assembly of the mitochondrial respiratory complexes (**Fig. 4G**), but we found no alteration in them. While there was no detectable change in the respiratory complex assembly, there seemed to be a functional deficit in the mitochondrial electron transfer or in the chemiosmotic coupling, since the mitochondria failed to use the elevated membrane potential to produce more ATP or even to maintain the basal cellular energy level after prolonged exposure to high glucose. Thus, the increased glucose load led to mitochondrial hyperpolarization that might have been responsible for the increased ROS generation in the b.End3 cells.

4.2. Cell-based screening for inhibitors of hyperglycemia-induced mitochondrial ROS production in endothelial cells

We conducted a phenotypic screen to identify compounds that inhibit the mitochondrial ROS production induced by elevated extracellular glucose by measuring the oxidation of MitoSOX in cultured b.End3 endothelial cells. We tested a focused library consisting of 6,766 compounds, which included clinical-stage drugs, biologically active compounds with defined pharmacological activity and natural compounds. (The compound libraries tested in the primary screen are listed in **Table 1**.)

Table 1. Bioactive compound libraries. Source libraries of the compounds used in cell-based screening.

Library	Supplier	Description	Code	Number of compounds
NIH Clinical Collection	BioFocus, South San Francisco, CA	phase I-III trial compounds	B	446
FDA Approved Library	Enzo Life Sciences, Farmingdale, NY	FDA approved bioactive compounds	F	640
Prestwick Chemical	Prestwick Chemical, Washington, DC	marketed drugs in Europe	P	1200
US Drug Collection	MicroSource	clinical trial stage USP drugs	U	1040
International Drug Collection	Discovery Systems, Gaylordsville, CT	compounds marketed in Europe or Asia but not in the US	I	240
Killer Plates		toxic substances	K	160
LOPAC1280	Sigma-Aldrich, Saint Louis, MO	various biologically active compounds	L	1280
TocriScreen	Tocris BioScience, Ellisville, MI		T	1120
Natural Products	TimTec LLC, Newark, DE	natural compounds and derivatives	N	640

We decided to test the compounds on cells showing a pre-existing (but potentially reversible) damage, thus compounds (3 μ M) were administered on day 7 of hyperglycemia and the effect on ROS production was evaluated after a 3-day long exposure. The measurement of mitochondrial ROS production was combined with simultaneous assessment of the cellular viability (measured in the same wells) (**Fig. 5**).

Both the cellular ROS production and the viability showed a Gaussian distribution, and the majority of the compounds did not affect mitochondrial ROS generation. (Detailed results of the primary screen are provided in the supplementary data of reference [38]). Compounds that decreased the mitochondrial ROS production (ROS score > 1) fell into two categories: they either reduced the viability (viability score < -1) or did not affect it. Cytotoxic compounds (i.e. compounds that simultaneously decreased both the ROS production and cell viability) were excluded from further analysis. The non-toxic compounds that inhibited hyperglycemia-induced ROS production at 3 μ M by more than 25% in the primary screen were re-tested in replicates at 10 μ M using the same assay. Results of the hit confirmation assay are summarized in **Suppl. Table 3**. Compounds whose activity on ROS production was confirmed in the secondary assay are listed in the **Table 2**.

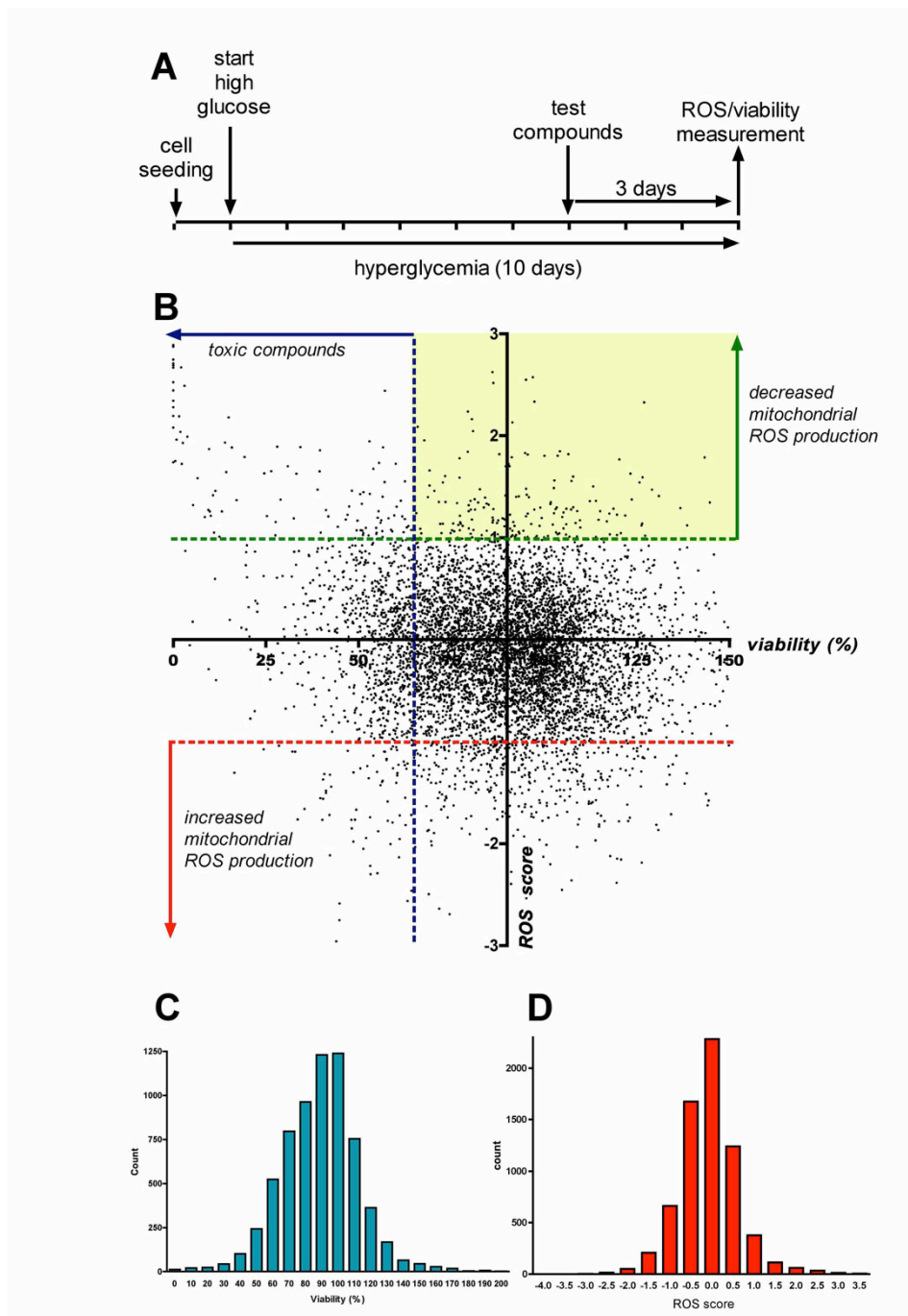


Fig. 5. Cell-based screening for compounds that decrease the mitochondrial ROS production in endothelial cells. *A:* Timeline of the cell-based screening; *b.* End3 cells were exposed to hyperglycemia for 10 days with 3-day-long compound treatment (3 μ M). Mitochondrial ROS production was measured with the superoxide MitoSOX Red with simultaneous assessment of viability. **B:** Dot graph showing the individual ROS/viability results of the tested 6766 compounds. Oxidant production data are shown as ROS score (1 ROS score=25% decrease in ROS production compared to hyperglycemic average value) and viability values are plotted as percent values. The yellow area denotes the compounds that decreased the ROS production without marked reduction of cellular viability. **C-D:** Distribution of viability (**C**) and ROS (**D**) data (SD of viability=24.69%, SD of ROS score=0.717 or SD of ROS production=17.93%).

Table 2. Confirmed inhibitors of the hyperglycemia-induced mitochondrial ROS production. Hit compounds of the primary screening were re-tested in replicates at 10 μ M final concentration in *b.End3* cells using the same assay. Compounds that decreased the mitochondrial ROS production (by at least 10%) without affecting the cellular viability (induced less than 10% decrease in viability) are listed categorized according to their known biological activity. The change in ROS production is shown as percent value of total mitochondrial oxidant production of hyperglycemic cells. (Data are shown as mean \pm SEM.) (Abbreviation: PKC: protein kinase C)

Compound Name	CAS registry number	Biological Activity	Compound Source Library	Change in mitochondrial ROS production (%)
paroxetine	61869-08-7	selective serotonin reuptake inhibitor	F, U, P,L,B	-50 \pm 4
sirolimus	53123-88-9	immunosuppressant, uncoupler	U	-61 \pm 4
rothlerin	82-08-6	uncoupling agent, PKC inhibitor	N	-35 \pm 3
nocodazole	31430-18-9	microtubule polymerization	T	-35 \pm 3
colchicine	64-86-8	inhibitors	K, U	-30 \pm 5
glimepiride	93479-97-1	sulfonylurea anti-diabetic drug	F	-33 \pm 2
flunarizine	52468-60-7	calcium channel blocker	U	-31 \pm 6
thioguanosine	85-31-4	antimetabolite	P	-28 \pm 0
tretinoin	302-79-4	retinoid, used in acute leukemia	U	-29 \pm 2
flunisolide	3385-03-3		U	-25 \pm 6
budesonide	51333-22-3		U,P,L	-23 \pm 4
flurandrenolide	1524-88-5	glucocorticoids	U	-19 \pm 4
methylprednisolone	83-43-2		P	-17 \pm 1
dexamethasone	50-02-2		U	-16 \pm 5
betamethasone	378-44-9		L	-15 \pm 6
AP39	1429173-57-8	mitochondrial H ₂ S donors		-22 \pm 4
AP123				-20 \pm 3

Hit molecules included steroids, non-steroidal anti-inflammatory agents, antioxidants, mitochondrial uncouplers and antimetabolites. Statins, which have previously been shown to suppress hyperglycemic ROS production in endothelial cells [153, 154] also inhibited ROS production in our experimental conditions; these effects, however, were also associated with a suppression of cellular viability (Fig. 6).

From the multiple classes of pharmacologically active compounds identified in the screen, we have focused our subsequent studies on paroxetine (a clinically used antidepressant compound), glucocorticoid steroids and the novel mitochondrial H₂S donor compounds AP39 and AP123.

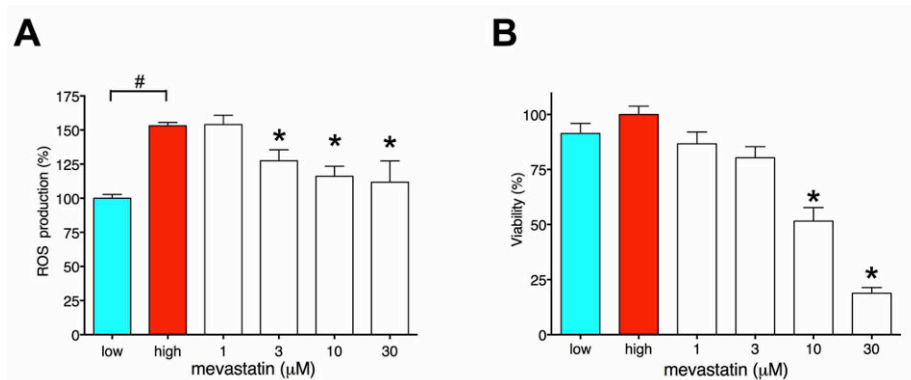


Fig. 6. Effect of mevastatin on mitochondrial ROS production and viability in endothelial cells. In the primary screens mevastatin proved to be the least toxic statin in bEND.3 cells. bEND.3 endothelial cells were exposed to hyperglycemia for 10 days with 3 -day-long mevastatin treatment at the indicated concentrations. Mitochondrial ROS production and viability was measured with MitoSOX Red and Hoechst 33342, and are expressed as percent values compared to normoglycemic control cells (low). Mevastatin decreased the mitochondrial ROS generation with simultaneous viability reduction. (# $p < 0.05$ compared to normoglycemic control, * $p < 0.05$ compared to hyperglycemic cells)

4.3. Characterization of the mode of action of hit compounds

4.3.1. The mechanism of action of paroxetine: mitochondrial superoxide scavenging in hyperglycemic endothelial cells

Paroxetine (both its hydrochloride and maleate salts, as present in different compound libraries) consistently reduced the mitochondrial ROS production in the screens and showed preference to inhibit mitochondrial ROS production, as opposed to total cellular ROS generation (as measured by the DCFDA assay) (Fig. 7). Paroxetine remained effective against the hyperglycemia-induced mitochondrial ROS generation in cultured human endothelial cells (Fig. 7). Furthermore, the effect of paroxetine depended on an immediate mode of action, because it remained effective in shorter treatment schedules (Fig. 7), and did not affect the expression of any of the mitochondrial genes studied during hyperglycemia (Fig. 8, Suppl. Table 4).

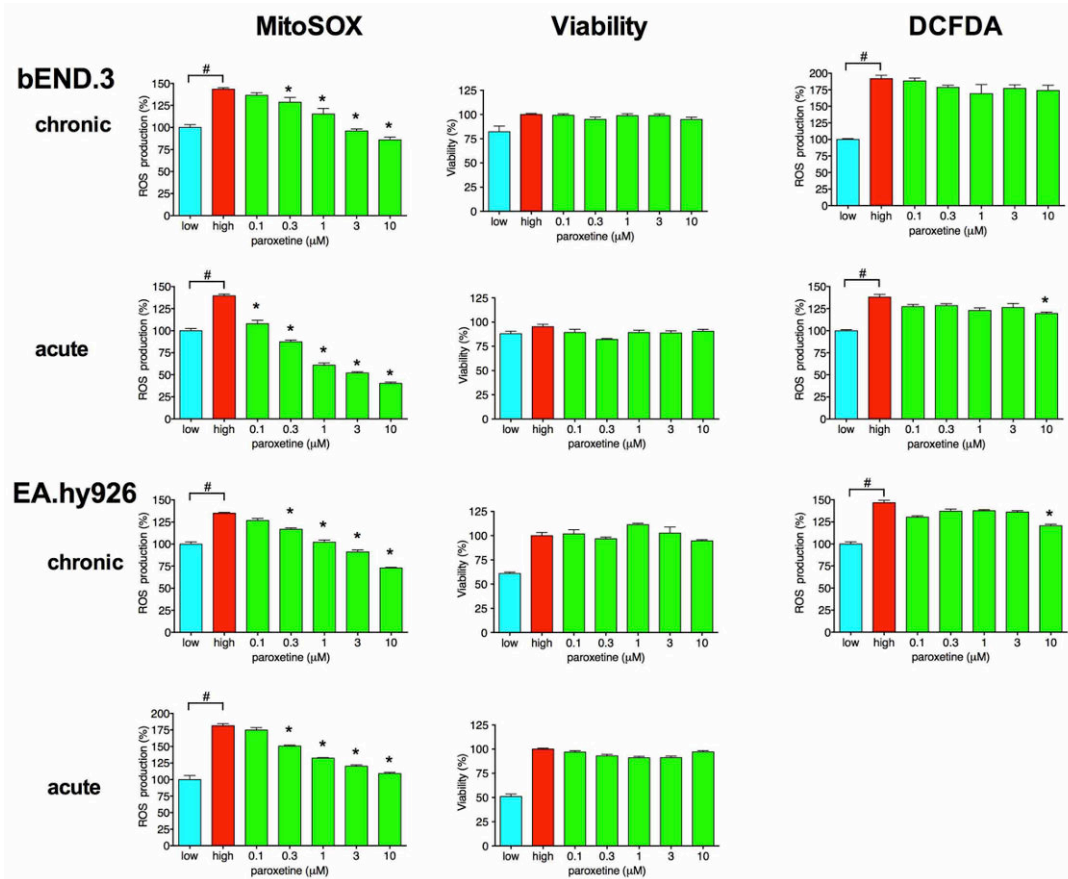


Fig. 7. Paroxetine inhibits the mitochondrial oxidant production in endothelial cells. *b.End3* murine (top panels) and *EA.hy926* human endothelial cells (bottom panels) were exposed to hyperglycemia for 10 days with 3-day-long (chronic) paroxetine treatment at the indicated concentration or immediately prior to the ROS measurement (acute). Mitochondrial ROS, viability and cytoplasmic ROS production was measured with MitoSOX Red, Hoechst 33342 and CM- H_2 DCFDA (DCFDA), respectively, and are expressed as percent values compared to normoglycemic control cells (low). (# $p < 0.05$ compared to normoglycemic control, * $p < 0.05$ compared to hyperglycemic cells)

Lhpp	Atp12a	Atp4a	Atp4b	Atp5a1	Atp5b	Atp5c1	Atp5d	Atp5f1	Atp5g1	Atp5g2	Atp5g3
1.49	1.30	1.06	1.01	1.04	1.02	1.13	1.06	1.01	0.84	1.07	0.93
Atp5h	Atp5j	Atp5j2	Atp5o	Atp6v0a2	Atp6v0d2	Atp6v1c2	Atp6v1e2	Atp6v1g3	Bcs1l	Cox11	Cox4i1
1.15	1.12	1.12	1.08	1.06	0.86	1.04	1.04	1.30	1.01	0.96	1.13
Cox4i2	Cox5a	Cox5b	Cox6a1	Cox6a2	Cox6b1	Cox6b2	Cox6c	Cox7a2	Cox7a2l	Cox7b	Cox8a
1.07	1.08	1.07	0.87	2.61	1.11	1.30	1.13	1.19	1.01	1.13	1.15
Cox8c	Cyc1	Ndufa1	Ndufa10	Ndufa11	Ndufa2	Ndufa3	Ndufa4	Ndufa5	Ndufa6	Ndufa7	Ndufa8
1.30	0.94	1.19	1.08	0.82	1.08	1.08	1.04	1.02	1.23	1.04	0.96
Ndufab1	Ndufb10	Ndufb2	Ndufb3	Ndufb4	Ndufb5	Ndufb6	Ndufb7	Ndufb8	Ndufb9	Ndufc1	Ndufc2
1.35	0.91	1.04	0.96	1.04	1.07	1.04	1.16	1.03	1.01	1.09	0.97
Ndufs1	Ndufs2	Ndufs3	Ndufs4	Ndufs5	Ndufs6	Ndufs7	Ndufs8	Ndufv1	Ndufv2	Ndufv3	Oxa1l
1.10	1.01	1.03	0.99	1.07	1.14	1.03	0.88	1.05	1.11	1.23	1.15
Ppa1	Ppa2	Sdha	Sdhb	Sdhc	Sdhd	Uqcrc1	Uqcrc2	Uqcrc2	Uqcrcs1	Uqcrcs1	Uqcrcs1
0.95	1.19	1.02	1.00	1.11	1.03	1.10	0.99	1.01	1.11	1.11	1.09

Fig 8. Mitochondrial energy production-related gene expression changes induced by paroxetine. Gene expression changes were analyzed with mitochondrial energy array in *bEND.3* cells exposed to hyperglycemia for 7 days and treated with paroxetine (10 μ M) or vehicle for 3 days. The gene symbols and relative expression (fold change) in paroxetine treated cells compared to vehicle-treated cells are shown. Background color represents the relative expression level on a color scale (shown on the right). The list of full gene names, Genbank accession number and statistical analysis results can be found in **Suppl. Tables 1 and 2.**

To test whether the paroxetine-mediated decrease in hyperglycemic ROS production is a result of inhibition of the mitochondrial respiration and oxidative phosphorylation, we have characterized the metabolic profile of b.End3 cells exposed to hyperglycemia in the presence or absence of paroxetine using extracellular flux analysis. Elevated extracellular glucose increased the cellular oxygen consumption (an indicator of aerobic metabolism) with no change in the degree of acid production (Fig. 9). Elevated glucose caused an increase in the mitochondrial potential (total respiratory capacity, measured in response to the uncoupling agent FCCP) in the absence of any detectable anaerobic compensation (Fig. 9B). Paroxetine did not affect the cellular ATP content or the oxygen consumption of the cells (Fig. 9D), while it decreased mitochondrial superoxide generation (Fig. 9E).

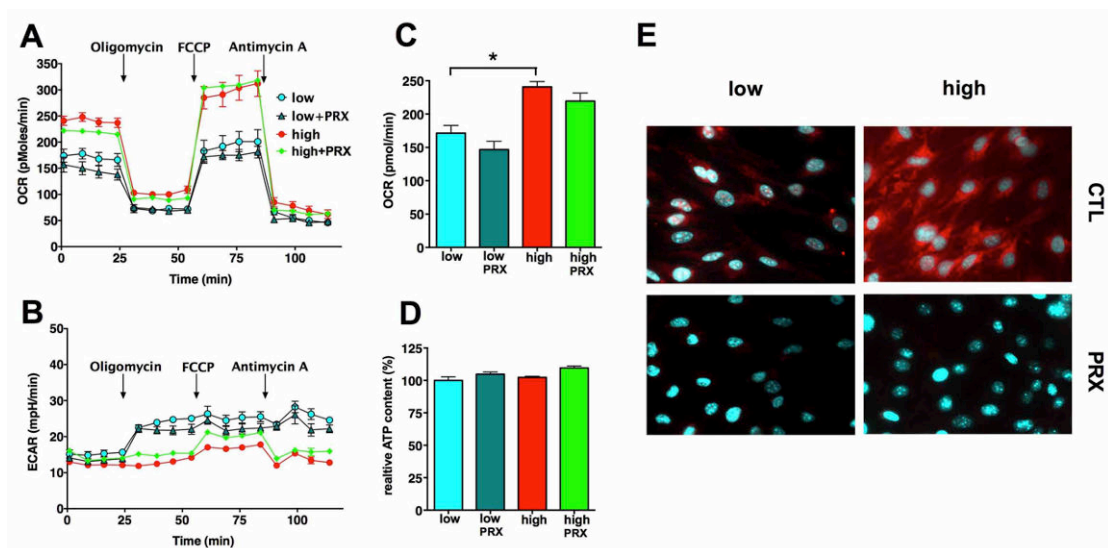


Fig. 9. The paroxetine-mediated mitochondrial antioxidant effect is not associated with perturbed cellular respiration. b.End3 cells were exposed to hyperglycemia (high) with or without paroxetine (PRX, 3 μM for 3 days) treatment, control cells were maintained in medium containing 5mM glucose (low). A-C: Cellular metabolism was measured with the Seahorse metabolic analyzer. ATP-production linked oxygen consumption rate (OCR) (A) and extracellular acidification rate (ECAR) (B) were measured, followed by determination of the non-ATP-linked oxygen consumption (proton leak), maximal respiration capacity and the non-mitochondrial oxygen consumption by adding oligomycin, FCCP and antimycin A, respectively. The ATP production linked (basal) OCR values (C) and cellular ATP levels (D) are shown. (* $p < 0.05$) E: Representative micrographs of b.END3 cells treated with paroxetine (PRX, 3 μM) and loaded with MitoSOX Red.

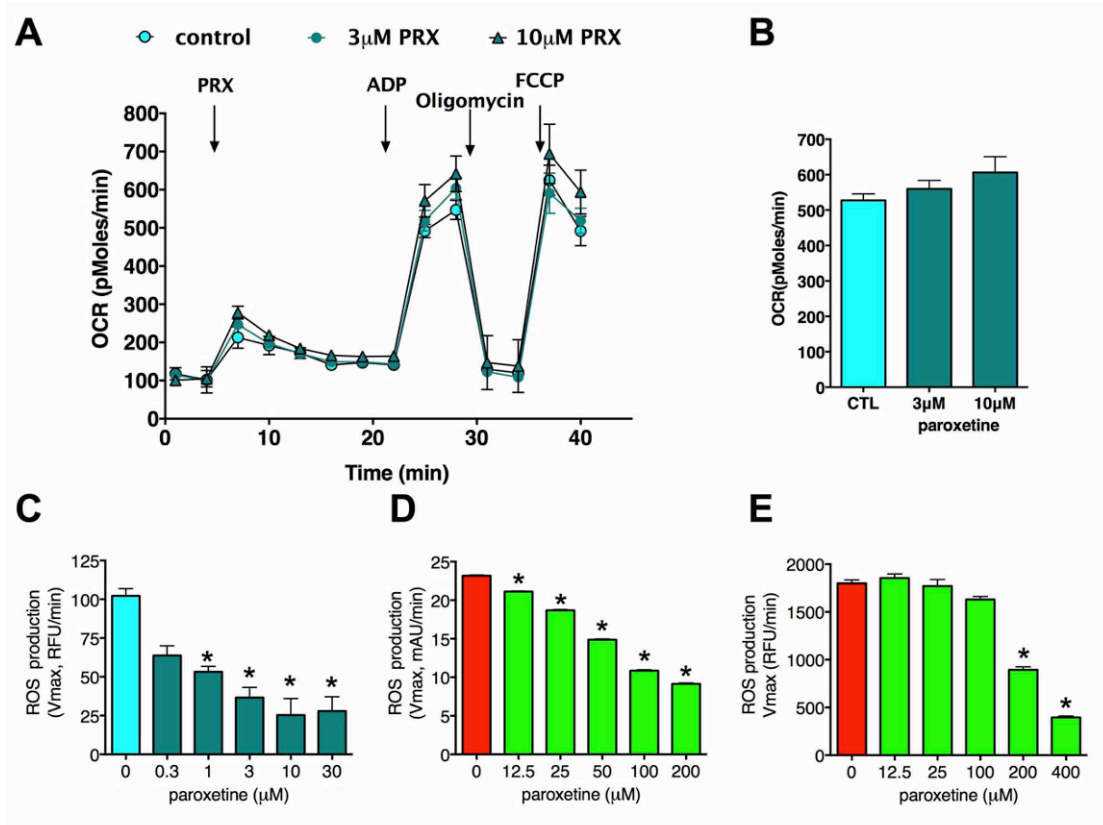


Fig. 10. Effect of paroxetine on mitochondrial function in isolated hepatic mitochondria. Rat liver mitochondria were isolated as described in the methods section. Mitochondria were resuspended in mitochondrial assay solution (MAS, 1X) that comprises 70 mM sucrose, 220 mM mannitol, 10 mM KH₂PO₄, 5 mM MgCl₂, 2 mM HEPES, 1 mM EGTA and 0.2% (w/v) fatty acid-free BSA, pH 7.2 at 37 °C. Mitochondria (10 μg protein/well) were placed on Seahorse assay plates, centrifuged to let them attach to the bottom and substrate (succinate) was added. **A:** Paroxetine (PRX, 3 or 10 μM) or vehicle was injected and basal respiration was measured. Phosphorylating respiration was measured following the addition of ADP (4 mM). ATP synthesis-linked oxygen consumption was blocked with oligomycin (2.5 μg/ml) and maximal uncoupler-stimulated respiration was measured following the injection of FCCP (4 μM). **B:** The ATP synthesis-linked oxygen consumption rates were measured in the presence of ADP and substrate. No significant differences were found. Paroxetine does not inhibit mitochondrial ATP generation in the tested concentrations. **C:** ROS production of isolated mitochondria was measured by the superoxide sensor MitoSOX Red in the presence of paroxetine at the indicated concentrations. **D-E:** Superoxide was generated by xanthine oxidase and detected by nitroblue tetrazolium (NBT) (**D**) or MitoSOX Red (**E**) in the presence of paroxetine at the indicated concentrations. (**p*<0.05 compared to vehicle)

Since the action of paroxetine was rapid-onset, and did not involve changes in gene expression, we next tested the activity of paroxetine on ROS production in isolated mitochondria. Paroxetine had no effect on the oxygen consumption rate in isolated mitochondria (**Fig. 10A,B**), but significantly reduced the detectable superoxide

generation in the low micromolar range (**Fig. 10C**). Next, we generated superoxide using the enzyme xanthine oxidase to test whether paroxetine directly interacts with superoxide. We used MitoSOX Red and nitroblue tetrazolium to measure the superoxide generation. Paroxetine reduced the superoxide signal in a dose-dependent manner in these cell-free systems (**Fig. 10D,E**).

To further elucidate whether the inhibitory function of paroxetine on the mitochondrial ROS generation depends on its antioxidant properties, we compared the effect of several selective serotonin reuptake inhibitors (SSRIs) and substructures of paroxetine on hyperglycemic mitochondrial ROS production in b.End3 cells. None of the other SSRI compounds (or norepinephrine reuptake inhibitors) tested affected the mitochondrial ROS production either in pre-treatment or when acutely added to the cells (**Fig. 11A,B**).

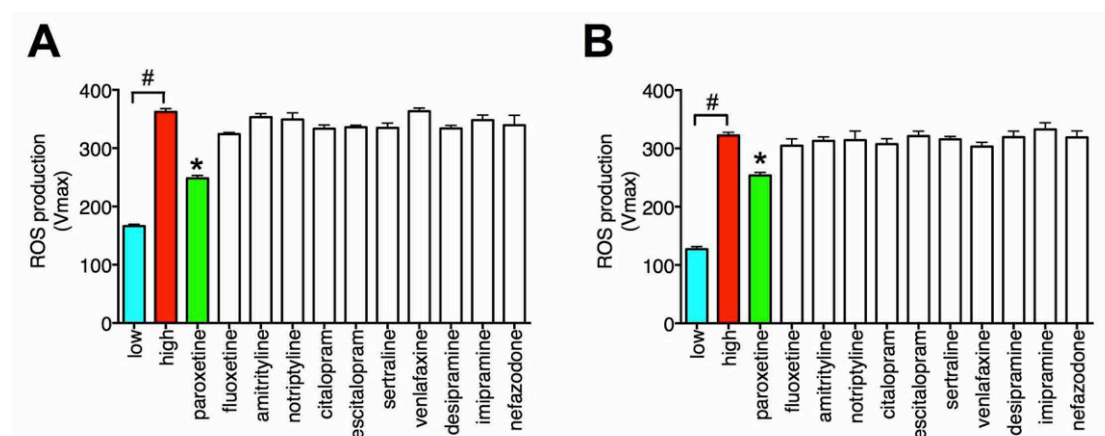


Fig. 11. The mitochondrial antioxidant property of paroxetine-related SSRI compounds. A-B: The indicated serotonin or norepinephrine reuptake inhibitors were added to the cells 3 h prior to MitoSOX loading at 10 μ M (A) or immediately prior to the ROS measurement at 1 μ M (B). Mitochondrial ROS production is shown as Vmax value of MitoSOX oxidation. (# p <0.05 compared to normoglycemic cells (low), * p <0.05 compared to hyperglycemic cells).

Paroxetine is reported to decompose under certain conditions to trans-4-(4'-fluorophenyl)3-hydroxymethyl)-piperidine which involves the cleavage of the sesamol part [155]. Both trans-4-(4'-fluorophenyl)3-hydroxymethyl)-piperidine and sesamol decreased the mitochondrial ROS production by themselves, but sesamol was more potent than the piperidine compound. Sesamol significantly decreased the hyperglycemia-induced mitochondrial ROS generation at 1 μ M, and the combination of trans-4-(4'-fluorophenyl)3-hydroxymethyl)-piperidine potentiated the antioxidant activity of sesamol (**Fig. 12A-D**).

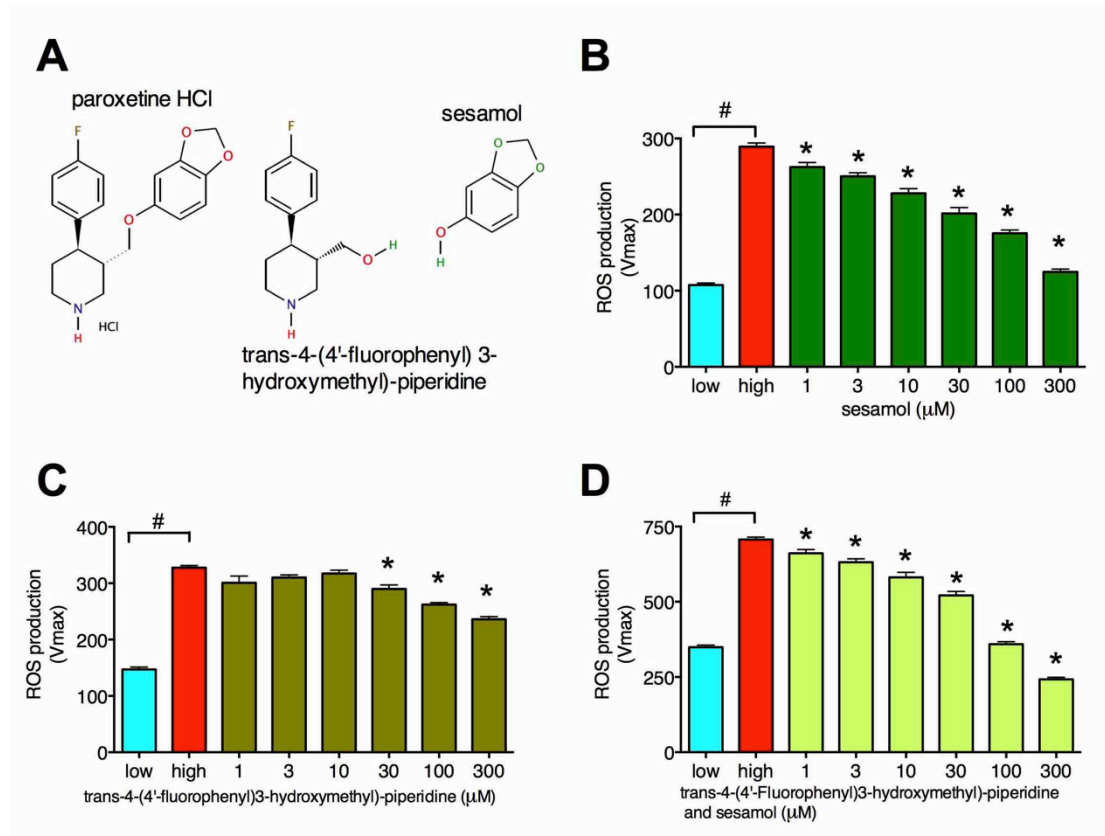


Fig. 12. The mitochondrial antioxidant property of paroxetine “building blocks”. *A:* Structure of paroxetine, trans-4-(4'-fluorophenyl)3-hydroxymethyl-piperidine and sesamol. *B-D:* b.End3 cells were exposed to hyperglycemia (high) for 10 days and loaded with MitoSOX Red. Paroxetine building blocks sesamol, trans-4-(4'-fluorophenyl)3-hydroxymethyl-piperidine or their combination was added to the cells at the indicated concentrations immediately before the ROS measurement.

Further decomposition of paroxetine can be attained by photolysis that includes the cyclization of the piperidine compound [155]. We degraded paroxetine by UV irradiation in aqueous solution and found that the partially degraded paroxetine retained its activity to a certain extent, but the end products of the complete photolysis no longer showed an inhibitory effect on ROS production (**Fig. 13**).

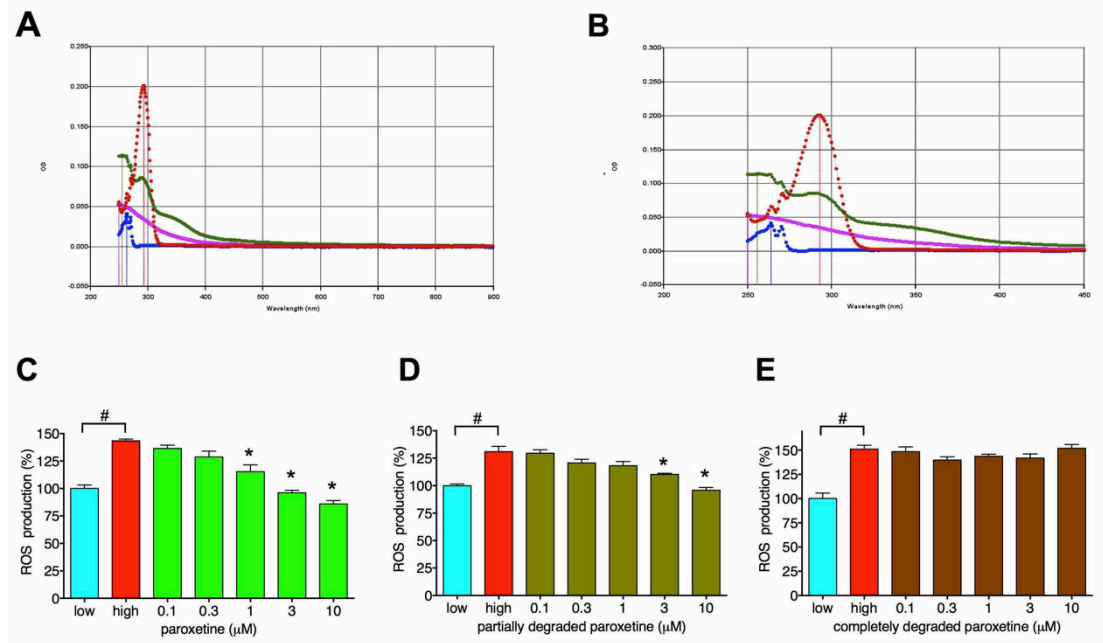


Fig. 13. Effect of partial and complete degradation of paroxetine by UV light on its ability to attenuate ROS production in hyperglycemic endothelial cells. A-B. 1mM aqueous solution of paroxetine was exposed to UV light (254nm) for 12 hours in either a UV-transparent or partially UV-blocking container. Paroxetine degradation was monitored with spectrophotometric analysis of the solution. The UV-VIS absorbance spectra were measured of the 100uM solution (10x dilution) of intact paroxetine (red), UV-exposed paroxetine (pink) or partially-protected paroxetine (green) and trans-4-(4'-Fluorophenyl)3-hydroxymethyl-piperidine (blue) A: The spectrum from 250-900nm and B: from 250 to 400nm. The peaks at 264 and 273nm are associated with the trans-4-(4'-Fluorophenyl)3-hydroxymethyl-piperidine part of paroxetine while the 290nm peak comes from the sesamol part. (Sesamol has a single peak at 290nm, not shown here.) C-E: The mitochondrial ROS production inhibitory potential of intact paroxetine (C), partially (~50% degraded, D) and completely decomposed paroxetine (E) was tested in bEnd.3 cells. Endothelial cells were exposed to hyperglycemia for 10 days with 3-day-long compound treatment at the indicated concentration. Mitochondrial ROS production and viability was measured with MitoSOX Red and Hoechst 33342, and are expressed as percent values compared to normoglycemic control cells (low). (# $p < 0.05$ compared to normoglycemic control, * $p < 0.05$ compared to hyperglycemic cells)

4.3.2. Paroxetine protects against oxidative damage: prevents the hyperglycemia- and diabetes-induced endothelial dysfunction in vascular rings

To test that the superoxide scavenger function of paroxetine is translated into measurable benefits in hyperglycemia we determined the oxidative damage at DNA, RNA and protein levels. b.End3 cells were exposed to hyperglycemia with paroxetine treatment (10 μ M for days 7-10 of the experiment) and the oxidative damage of the nuclear DNA was studied using the Comet assay. Hyperglycemia-mediated DNA fragmentation was attenuated by paroxetine, indicative of the ability of paroxetine to reduce the downstream consequences of mitochondrial ROS production (**Fig. 14A,B**). High glucose exposure also suppressed the relative amount (amplifiable) of mitochondrial DNA but it was maintained at higher levels in the presence of paroxetine (**Fig. 14C**). The formation of 8-hydroxy-guanosine (an indicator of oxidative damage to the RNA) was also detected in hyperglycemic cells, and paroxetine markedly reduced the 8-hydroxyguanosine signal in the hyperglycemic endothelial cells (**Fig. 14D,E**). Oxidative damage of mitochondrial proteins was also detectable in hyperglycemic cells by the oxyblot technique, as evidenced by a 1.5-fold increase in the level of oxidized proteins in the 20-45 kDa molecular weight range; this effect was also attenuated by paroxetine (**Fig. 14F,G**).

We tested whether paroxetine prevents the hyperglycemia- and diabetes-induced endothelial dysfunction in vascular rings. Isolated rat aortic rings exposed to hyperglycemia *ex vivo* developed endothelial dysfunction, as evidenced by an impaired relaxation in response to acetylcholine (**Fig. 15A**). Paroxetine maintained normal endothelium-dependent relaxant responsiveness of the hyperglycemic vessels. Next we tested the ability of paroxetine to affect the development of endothelial dysfunction in streptozotocin-diabetic rats. Paroxetine did not affect body weight and did not influence the degree of hyperglycemia in the diabetic animals (**Fig. 15B, D**). However, the diabetes-induced impairment of the endothelium-dependent relaxations *ex vivo* was prevented by paroxetine treatment (**Fig. 15C**).

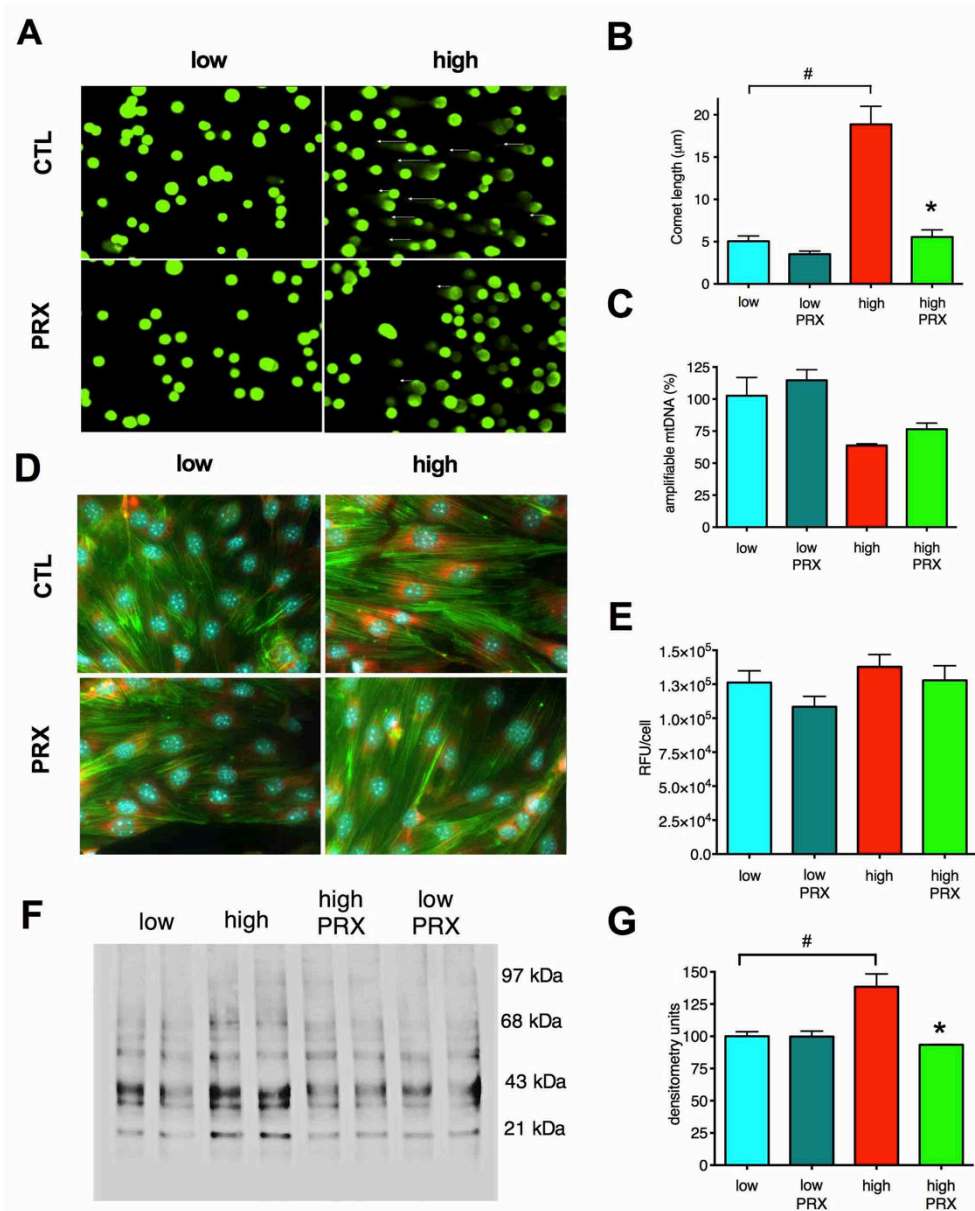


Fig. 14. Paroxetine reduces the hyperglycemia-induced oxidative damage in endothelial cells. *bEnd.3* cells were exposed to hyperglycemia (high) or maintained in medium containing normal glucose (low) for 10 days and treated with paroxetine (10 µM, PRX) or vehicle (CTL) for 3 days. Representative micrographs and respective bar graphs of the Comet assay (A,B), 8-hydroxyguanosine (red) immunostaining with simultaneous Hoechst 33342 (blue) nuclear and phalloidin (green) actin staining (D,E) are shown. C: Cellular DNA was exposed to 8-oxoguanine glycosylase to excise oxidized bases and the amount of amplifiable mitochondrial DNA was measured by real-time PCR. The ratio of the measured DNA amount in the hOGG1-treated and non-treated samples is shown. F,G: Crude mitochondrial fractions were prepared and processed with Oxyblot protein oxidation detection kit. Representative blot image of oxidized proteins (F) and densitometric analysis (G) are shown. (# $p < 0.05$ compared to normoglycemic cells; * $p < 0.05$ compared to hyperglycemic cells).

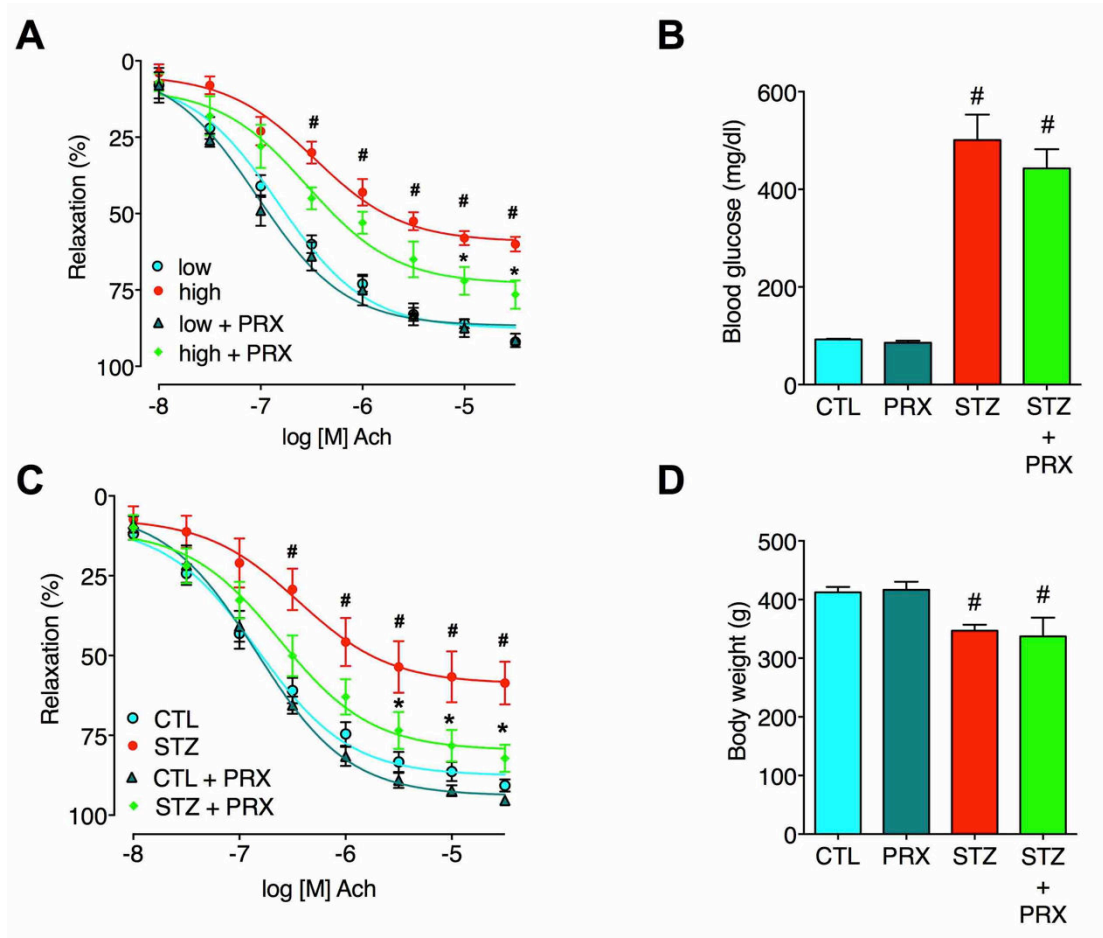


Fig. 15. The protective effect of paroxetine in ex vivo vessels and in vivo. **A:** Rat thoracic aortic rings were exposed to 30 mM hyperglycemia (high) for 48 hours or incubated in culture medium containing 5 mM glucose (low) and were treated with paroxetine (PRX, 10 μ M) or vehicle. Endothelium-mediated relaxation to acetylcholine was measured at the indicated concentrations of acetylcholine and expressed as percent of precontraction. **B, D:** Paroxetine treatment of streptozotocin-diabetic rats failed to affect hyperglycemia or body weight loss. **C:** Rat thoracic aortic rings prepared from streptozotocin-diabetic (STZ) or control non-diabetic (CTL) rats treated with vehicle or paroxetine (PRX, 10 mg/kg/day). Endothelium-mediated relaxation to acetylcholine was measured at the indicated concentrations of acetylcholine and expressed as percent of precontraction. # $p < 0.05$ hyperglycemia/diabetes compared to normoglycemic samples (low), * $p < 0.05$ paroxetine treatment compared to hyperglycemia/diabetes.

4.3.3. Glucocorticoids inhibit the mitochondrial ROS production in microvascular endothelial cells

Glucocorticoid steroids inhibited the glucose-induced mitochondrial ROS production and emerged as hit compounds in our screen. This unprecedented anti-ROS action of glucocorticoids was clearly shared by the whole class of glucocorticoids tested. Flunisolide reduced the mitochondrial ROS production by 25%, budesonide by 23%, flurandrenolide by 19%, methylprednisolone by 17%, dexamethasone by 16% and betamethasone by 15% in our previous screen [38]. We found that dexamethasone reduced the high glucose-induced mitochondrial ROS production both in the Sv129-derived b.End3 and the BalbC-derived bEnd.3 microvascular endothelial cells in a concentration-dependent manner (**Fig. 16A, C**) without affecting the cellular viability (**Fig. 16B, D**). Dexamethasone reached its maximum effect in the nanomolar concentration range in microvascular endothelial cells, but it had no effect on the hyperglycemia-induced mitochondrial ROS production in the EA.hy926 venous endothelial cell line (**Fig. 16E, F**). Next we tested the effect of the partial glucocorticoid receptor (GR) antagonist mifepristone on the ROS production inhibitory effect of dexamethasone in b.End3 cells. Unexpectedly, mifepristone did not block the effect of dexamethasone, but further reduced the mitochondrial ROS production in endothelial cells (**Fig. 17A, B**). We found that mifepristone by itself decreased the hyperglycemia-induced ROS production in both microvascular endothelial cell lines (**Fig. 17C-F**), and at low micromolar concentrations it was more effective than dexamethasone. Interestingly, the antifungal ketoconazole and miconazole, that also show glucocorticoid receptor antagonist activity, similarly reduced the mitochondrial ROS production (by 9.6 and 18.7% respectively) in our previous screen [38].

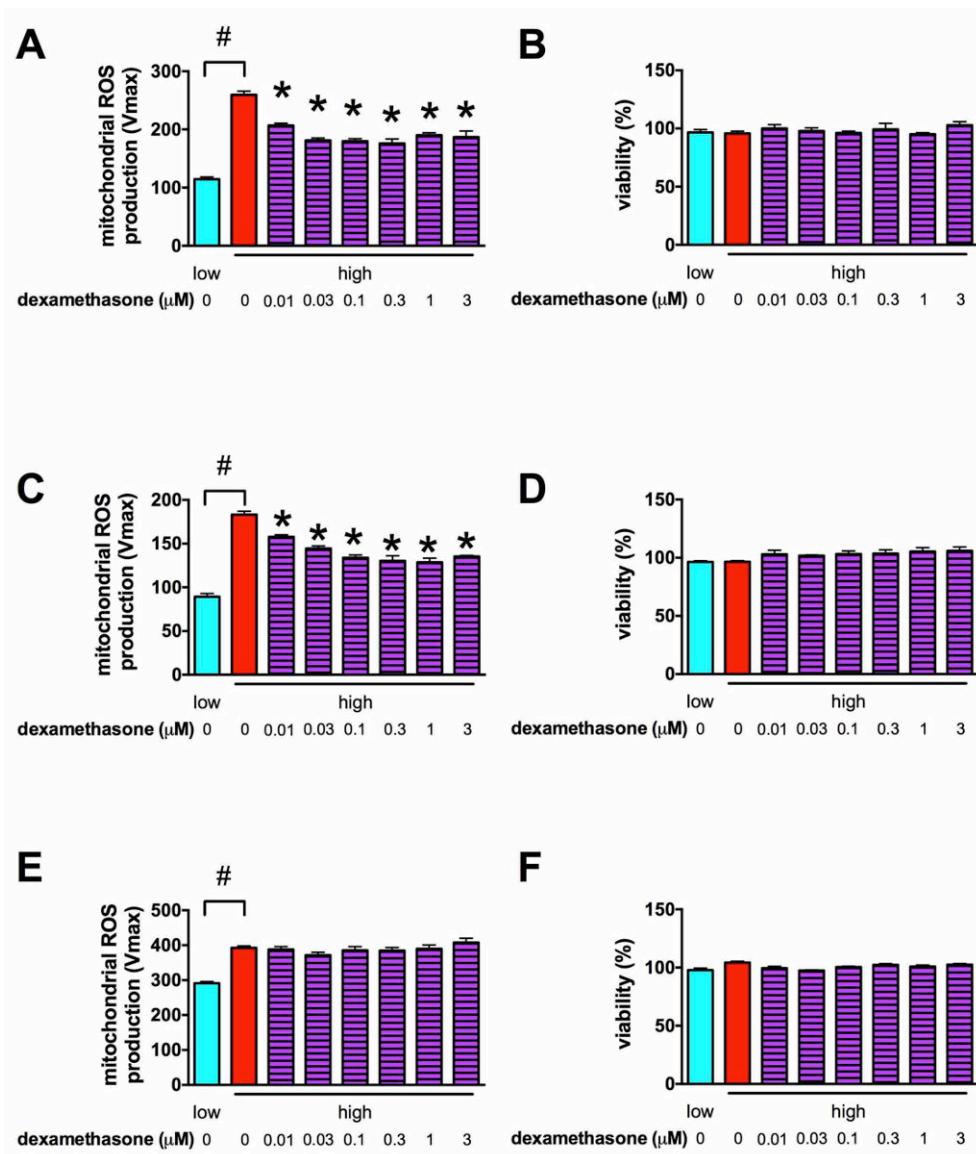


Fig. 16. Glucocorticoids decrease the glucose-induced mitochondrial ROS production in microvascular endothelial cells. **A, B:** *b.End3* microvascular endothelial cells were exposed to high glucose for 7 days and were treated with dexamethasone at the indicated concentrations for 3 days. **A:** ROS production was measured with the mitochondrial superoxide specific MitoSOX Red and **(B)** the viability was determined by measuring the Hoechst 33342 DNA dye uptake. **C, D:** *b.End3* cells were exposed to high glucose for 7 days and were treated with mifepristone at the indicated concentrations for 3 days. **C:** ROS production was measured with the mitochondrial superoxide specific MitoSOX Red and **(D)** viability was determined by measuring the Hoechst 33342 DNA dye uptake. **E, F:** EA.hy926 human venous endothelial cells were exposed to high glucose for 7 days and treated with dexamethasone at the indicated concentrations for 3 days. **E:** The mitochondrial superoxide production was determined by MitoSOX Red stain and **F:** the viability by Hoechst 33342 DNA dye uptake. (# $p < 0.05$ high-glucose exposure induced significant changes compared to cells maintained in low glucose containing medium, * $p < 0.05$ glucocorticoid treatment significantly reduced the ROS production)

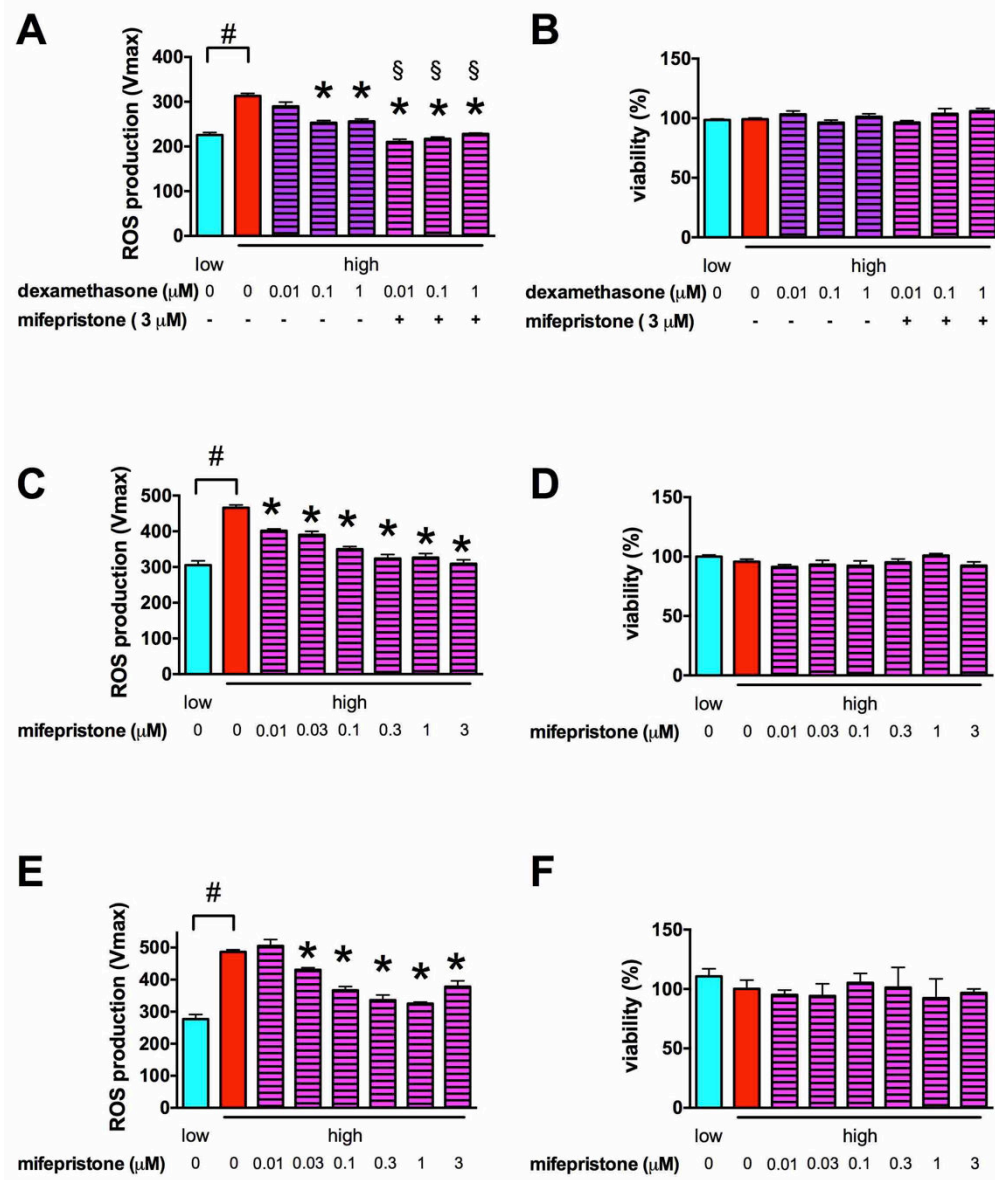


Fig. 17. Mifepristone inhibits the glucose-induced mitochondrial ROS production in microvascular endothelial cells. *A-D*: *b.End3* microvascular endothelial cells were exposed to high glucose for 7 days and were treated with dexamethasone and mifepristone (*A, B*) or with mifepristone alone (*C, D*) at the indicated concentrations for 3 days. *A, C*: The ROS production was measured with the mitochondrial superoxide specific MitoSOX Red *B, D*: The viability was determined by measuring the Hoechst 33342 DNA dye uptake. *E, F*: *bEnd.3* BALB/c murine microvascular endothelial cells were exposed to high glucose for 7 days and were treated with mifepristone for 3 days at the indicated concentrations. *E*: The mitochondrial ROS production was measured by MitoSOX Red and *F*: the viability was determined by the Hoechst 33342 uptake. (# $p < 0.05$ high-glucose exposure induced significant changes compared to cells maintained in low glucose containing medium, * $p < 0.05$ glucocorticoid treatment significantly reduced the ROS production, § $p < 0.05$ mifepristone induced significant reduction in the ROS generation compared to dexamethasone alone.)

4.3.4. The mode of action of glucocorticoids: restoration of the mitochondrial potential via UCP2 induction

We found that hyperglycemia induced an increase in the mitochondrial potential, thus we tested whether the mitochondrial potential is affected by the anti-ROS activity of glucocorticoids. Both dexamethasone and mifepristone normalized the mitochondrial potential in b.End3 cells (**Fig. 18A, B**), while no decrease but an increase was detectable in the EA.hy926 venous endothelial cells in which dexamethasone did not reduce the mitochondrial ROS production (**Fig. 18C**). Next, we measured the expression of uncoupling proteins to test the involvement of uncoupling protein 2 (UCP2) and/or 3 (UCP3) in the steroid-induced decrease in the mitochondrial potential. Both dexamethasone and mifepristone induced a ~10-fold increase in the expression of UCP2 at the mRNA level in b.End3 microvascular endothelial cells (**Fig. 18D, E**). On the other hand, in the EA.hy926 venous endothelial cells, hyperglycemia by itself induced a ~1.5 fold increase in UCP2 expression and dexamethasone significantly reduced the expression of UCP2 both at the mRNA (**Fig. 18F**) and at the protein level (**Fig. 18G, H**). While glucocorticoids were found to induce the expression of UCP3 in muscle cells [156] we found that the expression of UCP3 was very low in the endothelial cells (threshold cycle values over 35 were measured) and remained unchanged in response to steroids suggesting a predominant role for UCP2 in the endothelial cells.

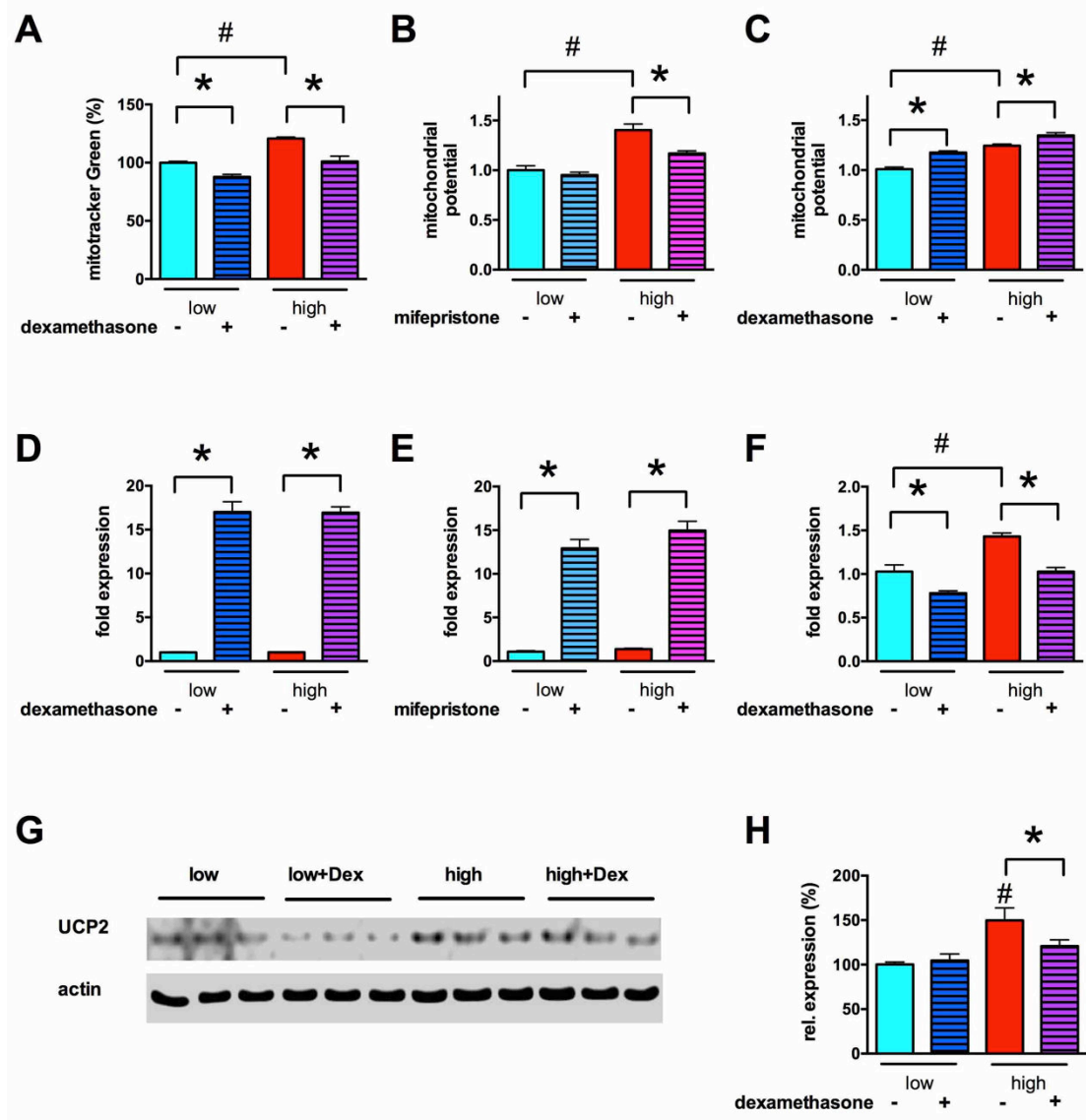


Fig. 18. Glucocorticoid steroids block the glucose-induced mitochondrial hyperpolarization and induce UCP2 expression. **A, B, D, E:** b.End3 endothelial cells were exposed to high glucose for 7 days and treated with the dexamethasone (1 μ M) or mifepristone (3 μ M) for 3 days. **A, B:** Changes in the mitochondrial potential were determined by measuring the MitoTracker Green uptake (**A**) or the ratio of the mitochondrial J-aggregate and the free cytoplasmic form of JC-1 (**B**). **C, F, G, H:** EA.hy926 human venous cells were exposed to high glucose for 7 days and treated with dexamethasone (1 μ M) for 3 days. **C:** The mitochondrial membrane potential was measured by JC-1 dye. **D, E, F:** UCP2 expression was determined by realtime PCR using Taqman assays. **G, H:** UCP2 expression was determined by Western blotting. Representative blot image (**G**) and densitometric analysis results (**H**) are shown. (# p <0.05 high-glucose exposure induced significant changes compared to cells maintained in low glucose containing medium, * p <0.05 glucocorticoid treatment induced significant changes.)

Next we investigated the time course of UCP2 induction by glucocorticoid steroids in b.End3 cells. We found that both dexamethasone and mifepristone induced UCP2 expression in a time-dependent fashion: the level of UCP2 mRNA doubled every two hours in the first 8 hours of steroid exposure with further increase measurable after 24 hours (**Fig. 19A, B**). Similar changes were measured at the protein level in the first 8 hours, but no further increase was detectable at 24 hours (**Fig. 19C, D**). Glucocorticoids steroids affected the UCP2 expression in microvascular endothelial cells at a concentration that is close to the circulatory levels of cortisol, so we tested whether they affect the expression of UCP2 in hepatocytes, the major site of energy metabolism. No change was detectable in UCP2 expression following dexamethasone treatment in HepG2 cells (**Fig. 19D**), only a slight reduction was measurable in response to mifepristone (**Fig. 19E**) suggesting that the glucocorticoid-induced UCP2 expression is not a universal phenomenon, but this effect is restricted to certain cell types including the microvascular endothelial cells.

UCP2 expression is regulated by glutamine availability at the translational level [157], thus we tested whether the expression level of UCP2 or the mitochondrial ROS production were affected by its concentration in endothelial cells. Restricting the glutamine amount or supplementing the culture medium with additional glutamine had little effect on the mitochondrial ROS production in the absence of glucocorticoids (**Fig. 20A, B**), but it had a marked effect in combination with dexamethasone if the ROS production was measured after a longer treatment period. The complete removal of glutamine blocked the ROS inhibitory effect of dexamethasone and the extra glutamine potentiated the effect of dexamethasone (**Fig. 20A, B**). As expected, the amount of UCP2 protein increased after the combined dexamethasone and glutamine treatment in the cells (**Fig. 20C, D**).

Previous reports found that glucocorticoids may control the mitochondrial oxidative phosphorylation by multiple mechanisms: 1) by inducing the expression of nuclear-encoded OXPHOS genes, including cytochrome c [158] and cytochrome c oxidases 1-4 [159-162], 2) by directly controlling the mitochondrial gene expression [163], 3) by affecting the mitochondrial DNA replication [164, 165] and 4) by regulating the expression of UCP3 via a sirtuin 1 (SIRT)-mediated mechanism [156]. To test the possible contribution of the above actions of glucocorticoid steroids to the inhibitory

effect on mitochondrial ROS generation, we measured the mitochondrial DNA (mtDNA) content of endothelial cells and the expression of previously identified target genes. We found that the hyperglycemic exposure reduced the mtDNA content of the cells and dexamethasone induced a significant reduction in the mtDNA content (Fig. 21A).

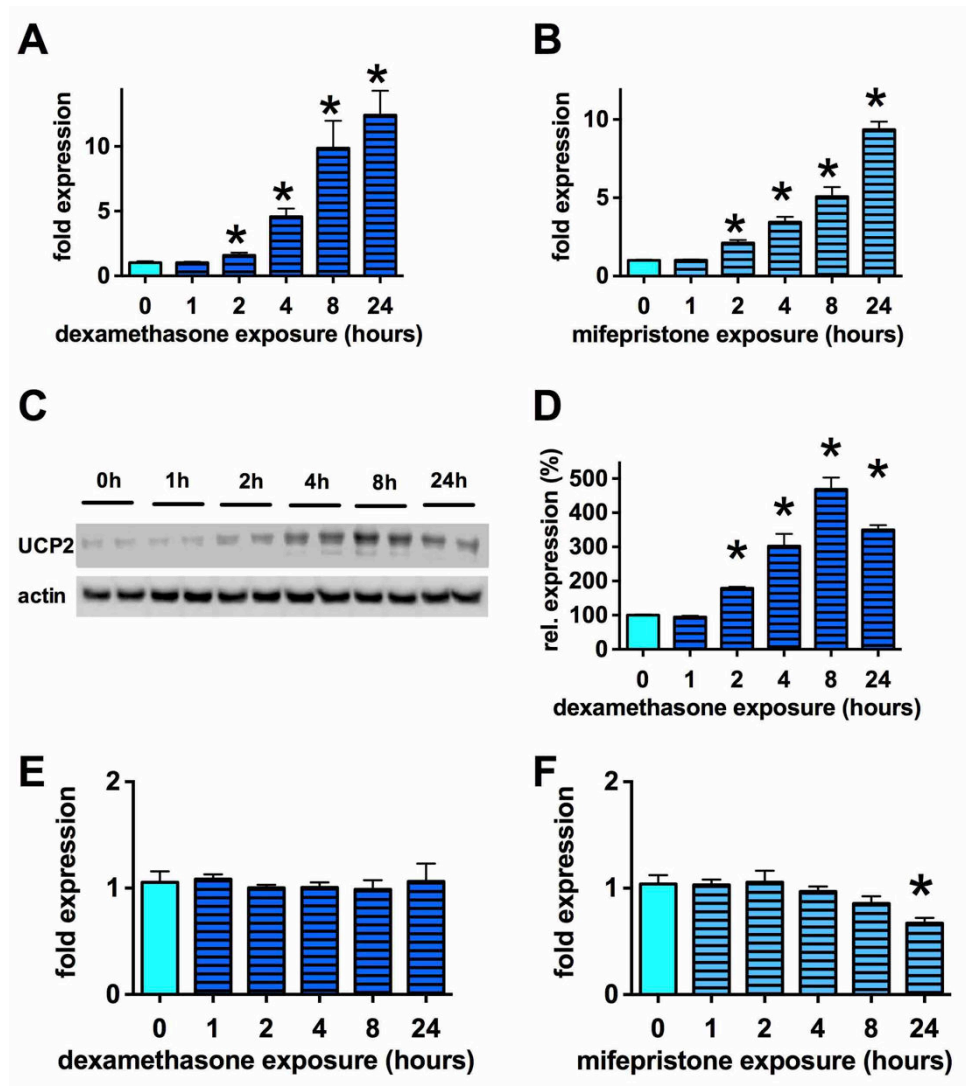


Fig. 19. Time course of steroid induced UCP2 expression. A-D: Confluent b.End3 endothelial cells were exposed to A, C, D: dexamethasone (1 μM) or B: mifepristone (3 μM) for the indicated time period. A, B: UCP2 mRNA expression was measured by UCP2 Taqman assay using rRNA normalization. C, D: UCP2 protein expression was measured by Western blotting. Representative blot image (C) and densitometry results (D) are shown. E, F: HepG2 human liver cells were treated with dexamethasone (1 μM, E) or mifepristone (3 μM, F) for the indicated time periods and UCP2 expression was determined by Taqman assay. (* $p < 0.05$ glucocorticoid treatment induced significant changes in the UCP2 expression)

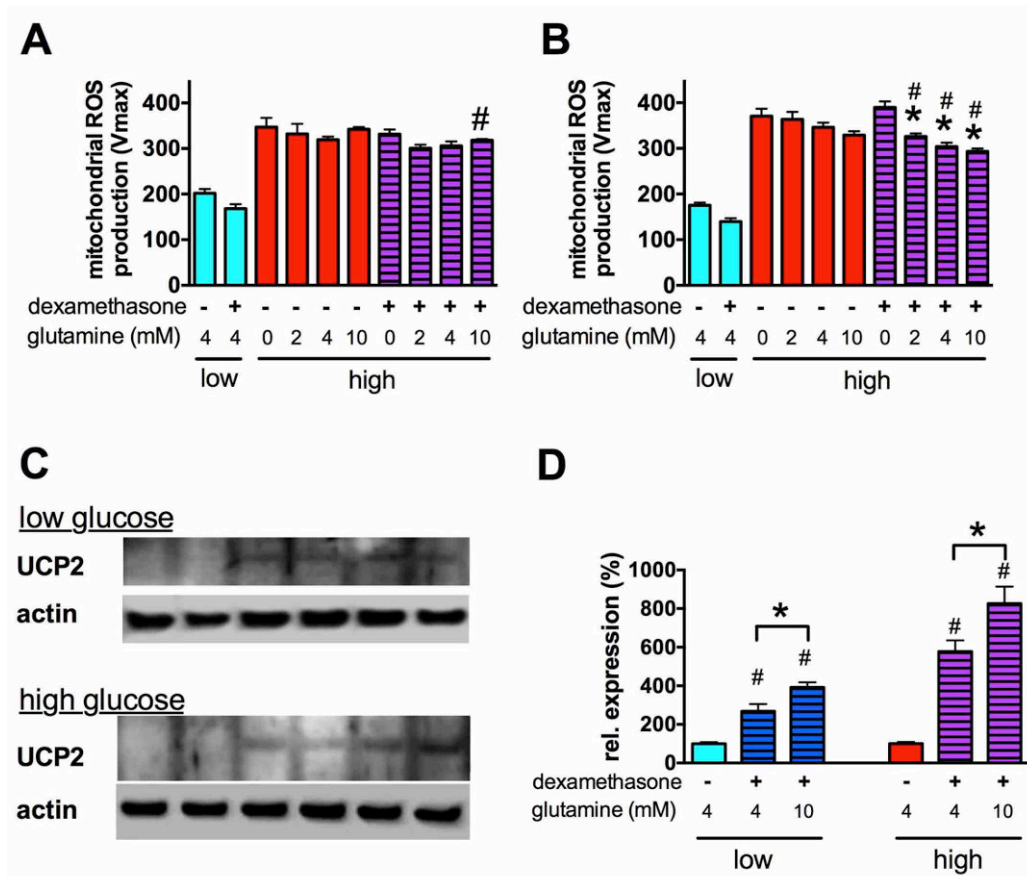


Fig. 20. Glutamine potentiates the dexamethasone-mediated UCP2 induction and inhibition of ROS production. *A-D*: b.End3 cells were exposed to hyperglycemia for 7 days and were treated subsequently with dexamethasone (1 μ M) and the indicated amount of glutamine for 6 hours (*A*) or 3 days (*B-D*). *C*: The mitochondrial superoxide production was measured by MitoSOX Red. *C-D*: UCP2 protein expression was measured by Western blotting. Representative blot image (*C*) and densitometric analysis results (*D*) are shown. (High-glucose exposure induced significant increase in the mitochondrial ROS production. # $p < 0.05$ dexamethasone significantly decreased the ROS production compared to the high glucose group, * $p < 0.05$ glutamine treatment resulted in a significant decrease in ROS production.)

The expression of glucocorticoid receptor (GR) was suppressed in cells treated with dexamethasone confirming a negative feedback regulation (**Fig. 21B**), but no reduction were measured in the expression of SIRT (**Fig. 21C**), nor in the expression of the mitochondria-encoded 16S RNA or COX3 genes (**Fig. 21D, F**). While the complete depletion of the mtDNA may have an effect on the mitochondrial OXPHOS in the cells [166, 167], we found that the expression of the mitochondria-encoded genes (COX3, 16S RNA) remained unchanged, thus the reduction of the mtDNA content may not have a significant impact on the mitochondrial respiration and ROS production in b.End3 cells. The expression of the nuclear encoded electron carrier cytochrome c (Cyt C) was suppressed in dexamethasone-treated endothelial cells

(**Fig. 21E**). While the complete lack of cytochrome c causes deficiency in the respiration and leads to embryonic lethality in mice [168, 169], the reduced expression may not be responsible for the reduced mitochondrial ROS production in the b.End3 cells, since the mitochondrial respiration is not blocked and there is no change in the cellular ATP content.

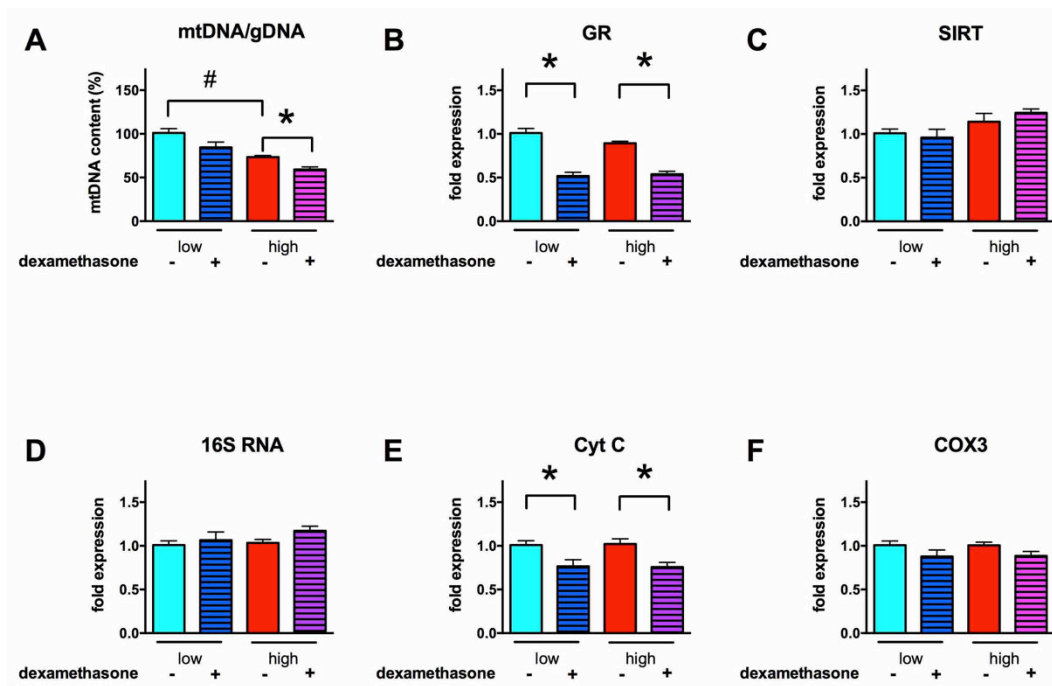


Fig. 21. Dexamethasone induced changes in gene expression and mitochondrial DNA content. *b.End3* cells were exposed to high glucose for 7 days and treated subsequently with dexamethasone (1 μ M) for 3 days. **A**: DNA was isolated from the cells and relative amount of mitochondrial and genomic DNA was determined by Taqman assay. **B-F**: Relative gene expression was determined by realtime PCR and normalized to 18S rRNA levels. The expression of **B**: the glucocorticoid receptor (GR), **C**: sirtuin 1 (SIRT), **D**: the mitochondrial 16S rRNA (16S RNA), **E**: cytochrome C (Cyt C) and **F**: the cytochrome C oxidase subunit 3 (COX3) were determined. (# p <0.05 high-glucose exposure induced significant changes compared to cells maintained in low glucose containing medium, * p <0.05 dexamethasone significantly reduced the mitochondrial DNA content and induced significant changes in gene expression.)

Since the above results suggested that the induction of UCP2 expression may be responsible for the glucocorticoid steroid-mediated anti-ROS effect in microvascular endothelial cells, we used siRNA-mediated gene silencing to study the role of UCP2 in the mitochondrial potential and superoxide generation in hyperglycemic endothelial cells. UCP2 silencing significantly reduced the expression of UCP2 and its effect lasted for 10 days both in normo- and hyperglycemic *b.End3* cells (**Fig. 22A**). siRNA

mediated silencing partially blocked the response to steroids (**Fig. 22B**) and also suppressed the ROS-inhibitory effect of mifepristone and caused an increase in the mitochondrial superoxide generation by itself (**Fig. 22C**). Interestingly, it coincided with a decrease in the cytoplasmic ROS generation as measured with the H₂O₂-sensitive CM-H₂DCFDA probe (**Fig. 22D**). The reduced level of UCP2 led to an increase in the mitochondrial potential and partially blocked the membrane potential normalizing effect of mifepristone as detectable with the JC-1 staining (**Fig. 22E**) or the MitoTracker Green FM uptake (**Fig. 22F**). No change was measured in the cell viability (**Fig. 22G**) but the cellular ATP content showed an increasing tendency with the reduced UCP2 level (**Fig. 22G**). Overall, these results suggest that UCP2 regulates the physiological mitochondrial membrane potential in microvascular endothelial cells and UCP2 expression is responsible for the decrease induced by glucocorticoid steroids in the hyperglycemic endothelial cells.

Finally, we tested whether the glucocorticoid mediated UCP2 induction affects the cellular metabolism in microvascular endothelial cells. UCP2 was found to regulate the energy metabolism in stem cells [170] and the induction of UCP2 expression was shown to reduce the mitochondrial membrane potential and ROS production in A549 lung adenocarcinoma cells in which it also induced a shift in the cellular metabolism [171]. To test the effect of glucocorticoid steroids on endothelial cell metabolism, we exposed b.End3 microvascular cells to hyperglycemia and measured the oxygen consumption and acid production in response to mifepristone. Mifepristone increased the oxygen consumption of the cells (**Fig. 23A, C**) and slightly reduced the acid production (**Fig. 23B, D**) resulting in an aerobic shift in the metabolism with a comparable time course to UCP2 induction. Following the steroid-mediated UCP2 induction, higher proton leak was measurable in the hyperglycemic cells (**Fig. 23E, G, J**). UCP2 silencing partially blocked the increase of oxygen consumption and diminished the increase in the proton leak (**Fig. 23E, G, I, J**). While no change was detectable in the basal oxygen consumption of the cells, the hyperglycemic cells showed higher increase in the anaerobic compensation following the inhibition of the mitochondrial respiration (**Fig. 23F, H**). This effect may not be accounted to the increase in the proton leak, since in this respect the UCP2 silenced cells showed similar changes. Altogether, these results suggest that pharmacological induction of UCP2 expression can be achieved in select cell populations and in microvascular endothelial cells it causes distinct changes in the cellular metabolism.

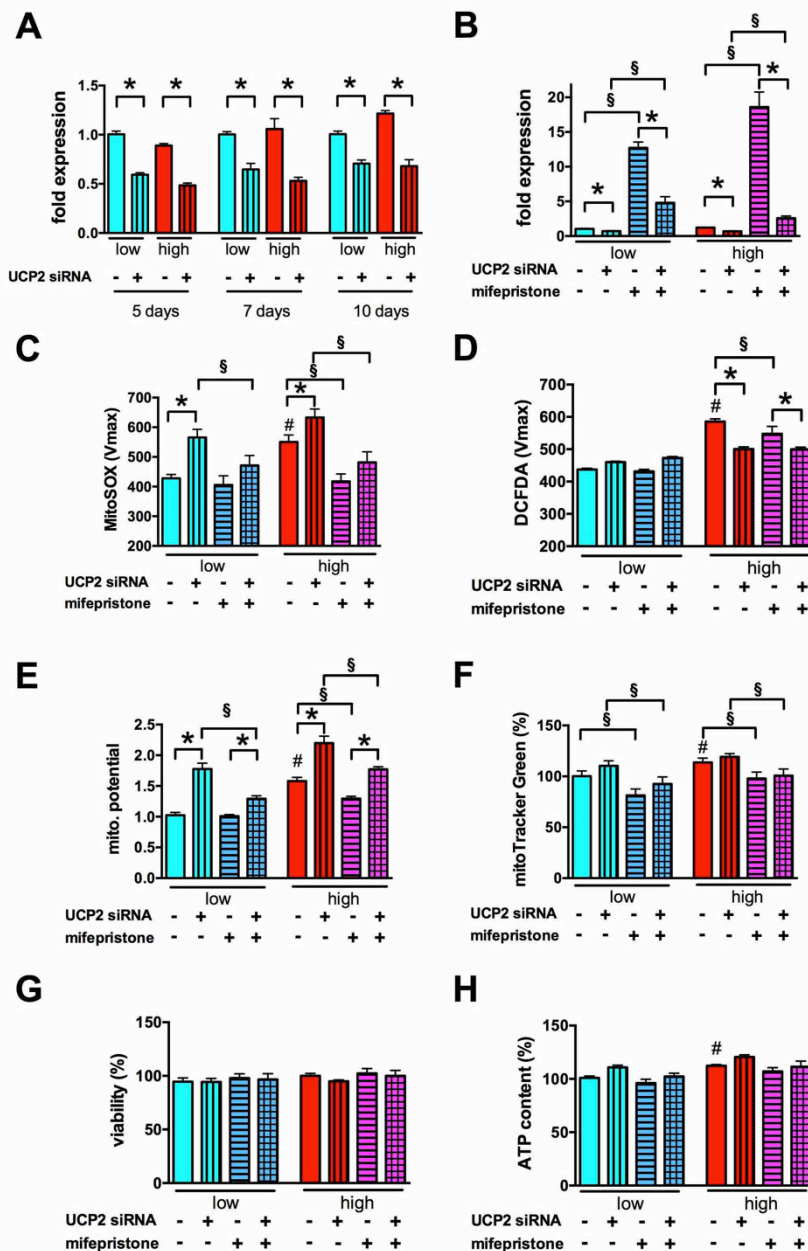


Fig. 22. UCP2 silencing blocks the mifepristone-mediated UCP2 induction and antioxidant effects. **A-H:** *b.End3* microvascular endothelial cells were transfected with UCP2 siRNA or negative control siRNA and exposed to high glucose for 5 days. Subsequently the cells were treated with mifepristone (3 μ M) for 1 day. **A:** The mitochondrial superoxide production was measured by MitoSOX Red. **B:** The cellular H_2O_2 production was measured by CM- H_2 DCFDA. **C, D:** The mitochondrial membrane potential was measured by JC-1 (**C**) and also by the uptake of MitoTracker Green (**D**). **E:** The cellular viability was determined by measuring the Hoechst 33342 DNA dye uptake. **F:** The cellular ATP content was measured. **G:** The viability was determined by measuring the Hoechst 33342 DNA dye uptake. **H:** Cellular ATP content was determined. (# $p < 0.05$ high-glucose exposure induced significant changes compared to cells maintained in low glucose containing medium, * $p < 0.05$ UCP2 silencing induced significant changes in ROS production and in the mitochondrial potential, $\$ p < 0.05$ mifepristone significantly reduced the ROS production and the mitochondrial potential.)

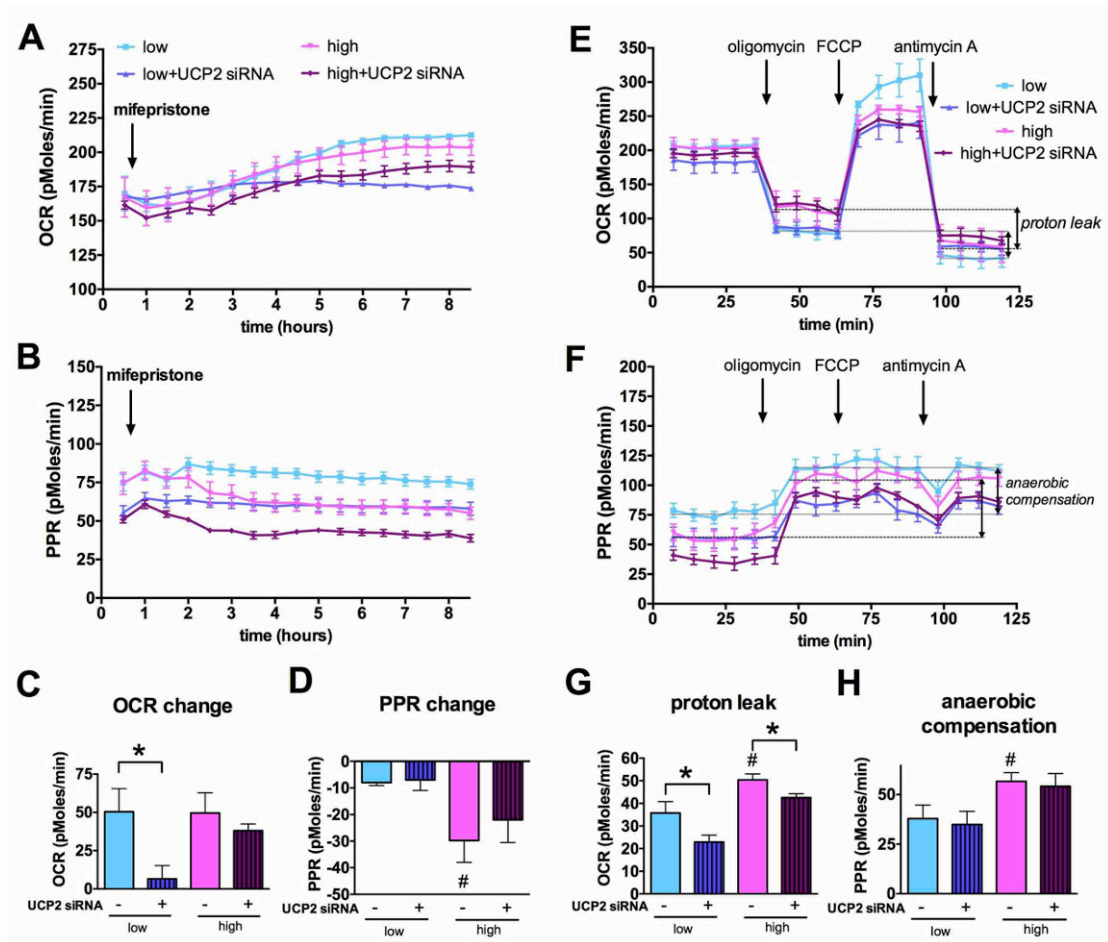


Fig. 23. UCP2 silencing blocks the metabolic changes induced by mifepristone. *A-H*: *b.End3* microvascular endothelial cells were transfected with UCP2 siRNA or negative control siRNA and exposed to high glucose for 5 days. *A-D*: The cells were treated with mifepristone (3 μ M) and *A*: the cellular oxygen consumption rate (OCR) and *B*: proton production rate (PPR) was monitored in real time by the Seahorse XF24 Extracellular Flux Analysis system for 8 hours. *C*, *D*: The increase in the OCR values (*C*) induced by mifepristone and the decrease in PPR values (*D*) are shown. *E-H*: Subsequently, metabolic profiling of the cells was carried out by adding oligomycin, FCCP and antimycin A, respectively, with monitoring the changes in the OCR (*E*) and PPR (*F*) values. *G*, *H*: The non-ATP-linked oxygen consumption (proton leak) rate (*G*) and the anaerobic compensation (*H*) are shown. *I*, *J*: Proton link/basal respiration rate and proton link/maximal respiration rate values are shown. (# $p < 0.05$ high-glucose exposure induced significant changes compared to cells maintained in low glucose containing medium, * $p < 0.05$ UCP2 silencing significantly reduced the OCR increase and the proton leak)

4.3.5. The mode of action of mitochondria-targeted H₂S-donor compounds against mitochondrial ROS production in hyperglycemic endothelial cells

The third group of compounds we studied in detail consisted of mitochondrial H₂S donors. We have previously found that H₂S provided protection against diabetic endothelial damage but at higher concentrations than the target range in our screen [94]. However, we found that novel slow-release H₂S donors AP39 and AP123 were effective against glucose-induced mitochondrial ROS production in the low micromolar and submicromolar concentration range (Table 2). The need for slow-release H₂S donor compounds was recognised since higher concentrations of the gas are toxic, the half-life of H₂S is very short and simple salts like sodium hydrosulfide (NaSH) and sodium sulfide (Na₂S) can only provide instantaneous H₂S generation [172-174]. Anethole dithiolethione (ADT-OH) and 4-hydroxythiobenzamide (HTB) represent two simple moieties that release H₂S slowly. Mitochondrial H₂S donors (AP39 and AP123) were generated by linking ADT-OH and HTB to a triphenylphosphonium mitochondrial targeting motif *via* a 10-carbon linker region (Fig. 24A, B). This targeting group may result in a 500-fold accumulation of the drug in the mitochondria [175]. Both mitochondrial H₂S donors and their non-mitochondrial counterparts provide gradual H₂S production lasting for 7-10 days in cell culture medium (Fig. 24C, D). The mitochondrial targeting group in AP39 does not change the time course of H₂S release by ADT-OH, but slightly slows down the H₂S liberation from HTB moiety in AP123 although the mechanism for this is not clear. HTB and AP123 contain a single sulfur atom, thus they can release one H₂S molecule per donor compound. The expected molar amounts of H₂S are produced over a 7-day-long period. AP39 and ADT-OH contain 3 sulfur atoms and are possibly capable of higher H₂S release over 10 days of follow-up. With the shorter period of H₂S release, a steeper decrease is detectable in H₂S production for AP123 and HTB than for AP39 and ADT-OH (Fig. 24E, F). While the kinetics are different, the total amount of H₂S production is comparable during a 3-day long treatment period: approx. 0.6 moles of H₂S are produced by a mole the H₂S donors (Fig. 24G, H).

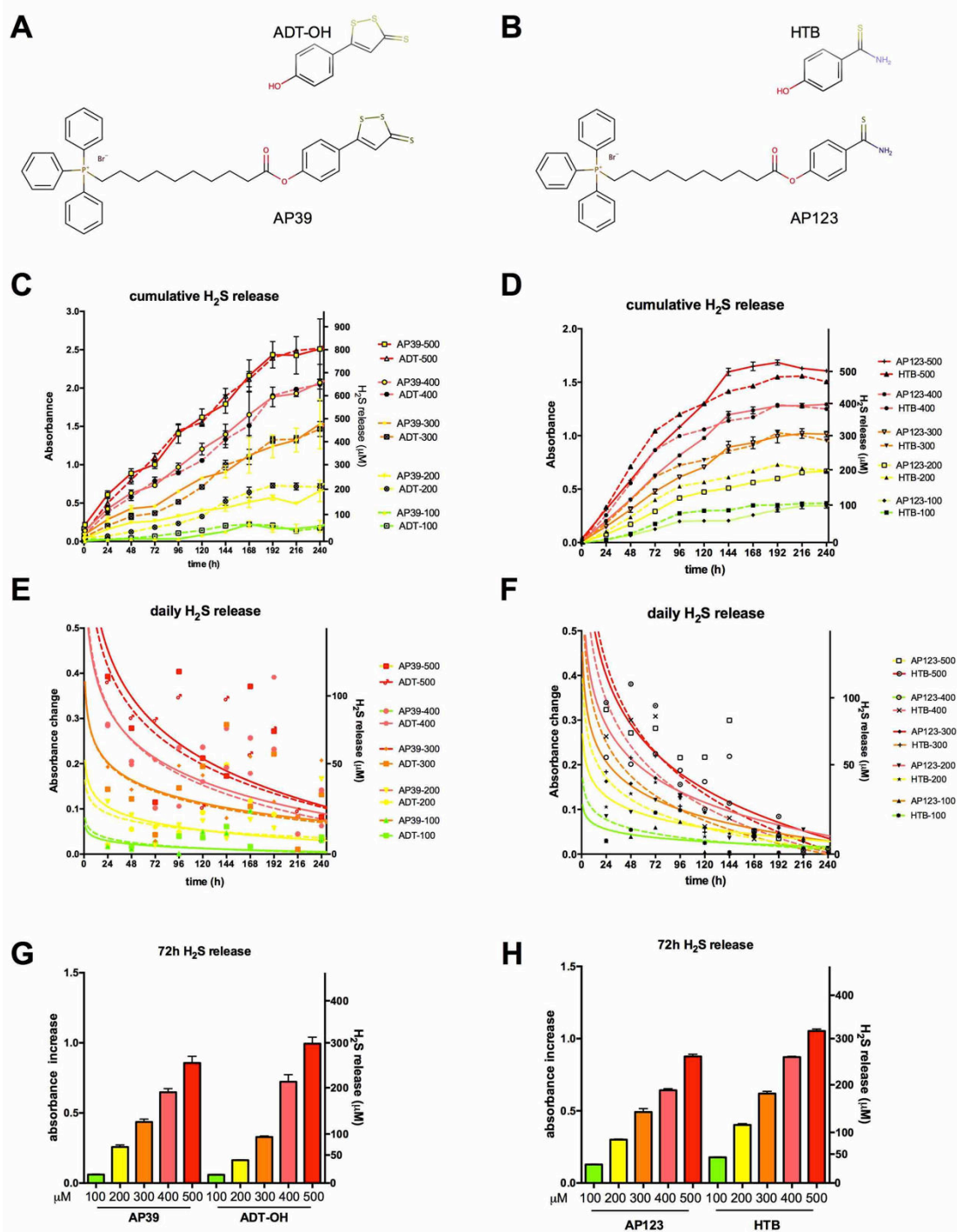


Fig. 24. H_2S release by mitochondrial H_2S donors. *A-B:* The chemical structure of mitochondrial H_2S donors: the H_2S releasing groups anethole dithiolethione (ADT-OH) in AP39 (**A**) and 4-hydroxythiobenzamide (HTB) in AP123 (**B**) are bound by ester linkage to 10-carbon alkyl linker region and the triphenyl phosphonium mitochondrial targeting group. *C-D:* The total amount of H_2S released from non-mitochondrial (ADT-OH, HTB) and mitochondrial (AP39, AP123) H_2S donors (100-500 μM) was detected in cell culture medium (DMEM supplemented with 10% FBS) for 10 days. *E-F:* Daily H_2S release values are plotted with curves fitting results to highlight the donor compound decomposition. *G-H:* The total amount of H_2S liberated from mitochondrial and respective non-mitochondrial H_2S donors over the first 3-day long period is shown.

Mitochondria-targeted compounds were selected since the glucose-induced ROS production primarily affects the mitochondria. We investigated the cellular localisation of H₂S production following the H₂S donor administration to confirm that the presence of the mitochondrial targeting group increases the mitochondrial H₂S release. Endothelial cells treated with the H₂S donor compounds were loaded with fluorescent H₂S sensor 7-azido-4-methylcoumarin (AzMc) [27] and the H₂S production was detected by fluorescence microscopy (**Fig. 25**). Cells treated with the mitochondrial donor compounds showed predominant mitochondrial H₂S production. While mitochondrial H₂S generation was evident in all cells, those treated with non-mitochondrial H₂S donors showed higher presence of extra-mitochondrial H₂S than those treated with the mitochondrial donors. The ester linkage between the mitochondrial targeting moiety and the H₂S donor group could be cleaved by cellular esterases increasing the non-mitochondrial H₂S production in cells treated with the triphenylphosphonium-based mitochondrial donor compounds [100]. However, mitochondrial but not cytoplasmic H₂S was rapidly detected with each compound suggesting esterase cleavage was minimal.

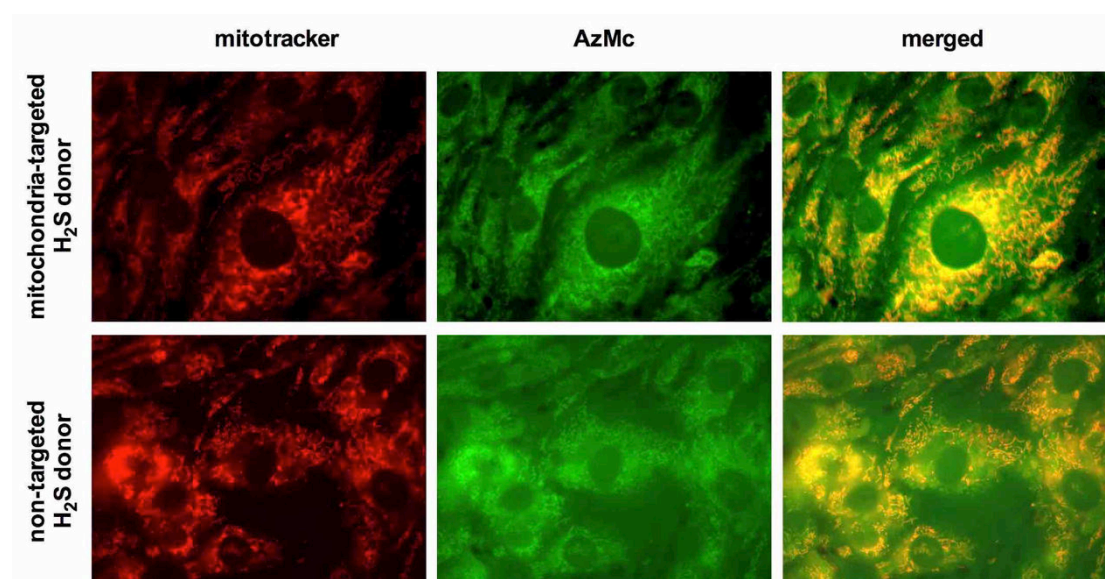


Fig. 25. Localization of H₂S release. *b.End3 microvascular endothelial cells were pre-treated with mitochondria-targeted and respective non-targeted H₂S donor compound (10 μM), then loaded with fluorescent H₂S sensor AzMc and mitotracker stain. The mitochondria (mitotracker signal) are shown in red and the H₂S production (AzMc signal) in the cells is shown in green. The H₂S signal completely overlaps with the mitochondrial signal in mitochondrial H₂S donor treated cells (as displayed in the merged channels), while in the non-mitochondrial H₂S donor-treated cells higher non-mitochondrial H₂S signal is detectable.*

It is well established that H₂S causes toxicity at high concentrations by blocking the mitochondrial respiration. This effect is believed to occur *via* inhibition of complex IV (cytochrome c oxidase) [176-178], but blockage of the mitochondrial respiration may also occur as a consequence of H₂S-mediated electron donation and reduction of the mitochondrial membrane potential. To test the tolerability of H₂S donor compounds, we exposed b.End3 endothelial cells to H₂S donors in a wide concentration range (1 nM-10 mM) and measured the cell survival after 24 hours (Fig. 26). All compounds were well tolerated at lower concentrations and induced cell death in a narrow concentration range. Sodium sulfide was tolerated by endothelial cells up to 300 μM but induced cell death above that (TC₅₀=318.9 μM). The tolerance of HTB was comparable to Na₂S (TC₅₀=165.5 μM) while ADT-OH had a lower TC₅₀ value (TC₅₀=69.5 μM) probably due to its higher H₂S producing capacity. (It has more sulfurs than the other compounds and could release more than one H₂S per drug molecule). The mitochondria-targeted H₂S donors caused no toxicity up to 1 μM in endothelial cells and the tolerable concentration was only one order of magnitude lower than their non-mitochondrial counterparts (AP123: TC₅₀=16.7 μM, AP39: TC₅₀=7.7 μM). In summary, mitochondrial H₂S donors are safe to use at sub-micromolar concentrations in endothelial cells.

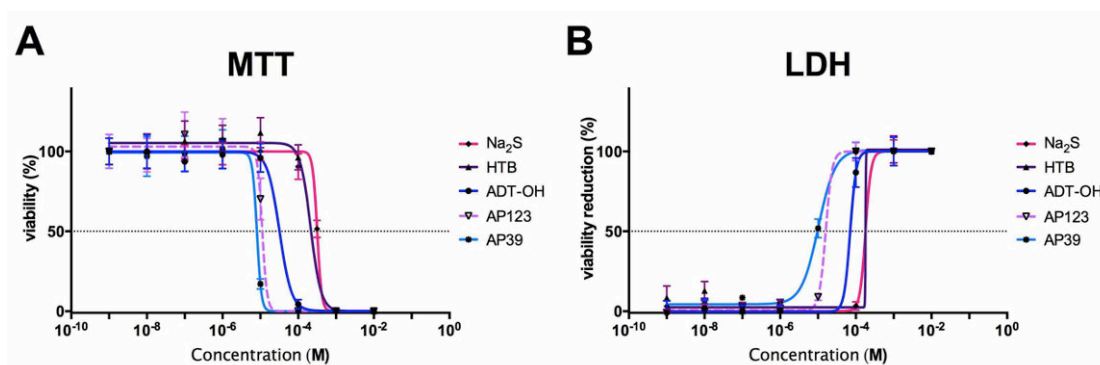


Fig. 26. Tolerability of H₂S donors. b.End3 cells were treated with mitochondrial and non-mitochondrial H₂S donor compounds for 24 hours. **A:** The cellular viability was measured by the MTT assay. **B:** LDH release was detected by measuring the LDH activity in the cell culture supernatant. The non-mitochondrial H₂S donors are better tolerated by the cells: the mitochondrial H₂S donors reduce the cell survival at lower concentrations.

Next we studied the ROS-inhibitory effects of mitochondrial slow-release donors AP39 and AP123 against glucose induced ROS production. Both AP39 and AP123 significantly reduced hyperglycemia-induced increase in the mitochondrial membrane potential at low nanomolar concentrations (**Fig. 27**). Both compounds reduced the mitochondrial ROS production as detected by MitoSOX Red (**Fig. 27**) and also caused a slight decrease in the cellular ROS production as measured by CM-H₂DCFDA (**Fig. 27**). AP39 was more effective than AP123 that might be explained by the higher H₂S release of AP39. It is of note that a single treatment of these mitochondrial donors provided protection over a 3-day-long period at 1000-fold lower concentration than the previously reported cytoprotective concentration of H₂S using repeated administration [94].

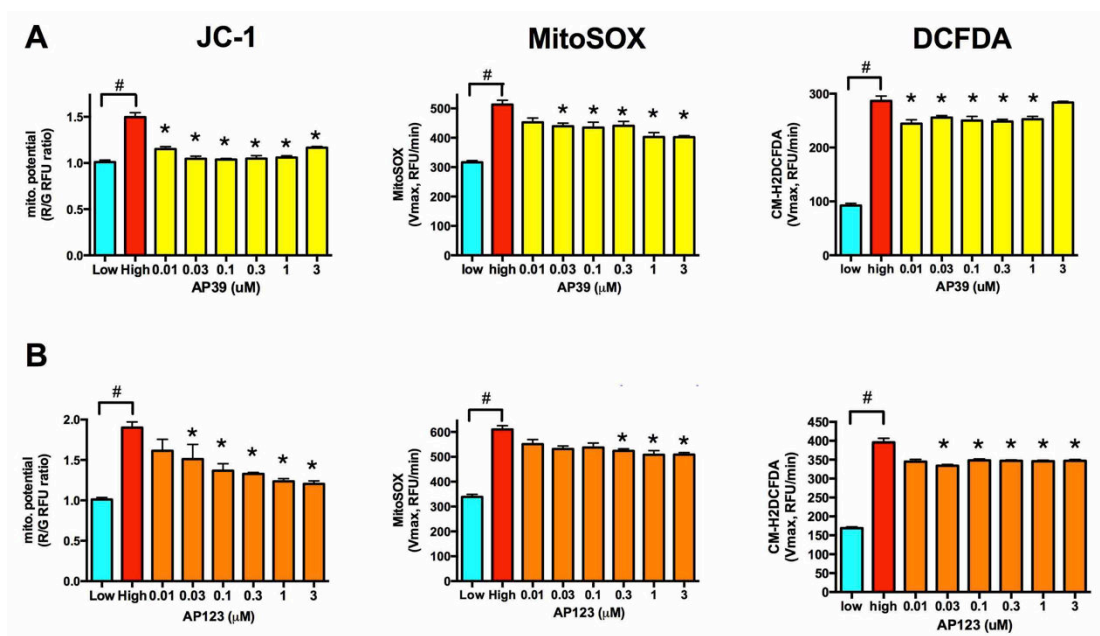


Fig. 27. Mitochondrial H₂S donors protect against ROS production in hyperglycemic endothelial cells. A-B: b.End3 endothelial cells were exposed to high extracellular glucose for 7 days with a single AP39 (A) or AP123 (B) treatment on the 4th day of hyperglycemia. The mitochondrial membrane potential was measured by JC-1, the mitochondrial superoxide production by MitoSOX Red, and the cellular ROS production by CM-H₂DCFDA. AP39 and AP123 restored the mitochondrial membrane potential and reduced the ROS production. (# $p < 0.05$ high glucose induced significant increase in mitochondrial membrane potential or ROS production. * $p < 0.05$ H₂S donor compounds significantly reduced the mitochondrial membrane potential or ROS production compared to hyperglycemic control cells.)

Mitochondrial dysfunction affects the cellular energy production in hyperglycemic endothelial cells and results in a decrease in the cellular ATP content after prolonged

exposure in b.End3 cells (**Fig. 28**). H₂S acts as an electron donor in the electron transport chain and it is shown to normalize the membrane potential and inhibit the mitochondrial ROS production in hyperglycemia suggesting that it may increase the ATP production in the mitochondria [94]. Thus, we tested whether the mitochondria-targeted H₂S donors affect the cellular energy level in hyperglycemia. Both AP39 and AP123 increased the cellular ATP content in a concentration-dependent manner (**Fig. 28**) supporting the hypothesis that H₂S-donor-mediated electron supplementation increases the mitochondrial ATP production [107]. Hyperglycemia did not induce changes in the cellular LDH activity in b.End3 endothelial cells (**Fig. 28**), but there was significant increase in the cellular MTT converting capacity (**Fig. 28**). This increase in the cellular MTT conversion was probably a compensatory activation of the citric acid cycle or an indicator of the OXPHOS stimulation. None of the compounds affected the cellular LDH activity (**Fig. 28**), but both compounds induced a significant decrease in the cellular MTT conversion (**Fig. 28**).

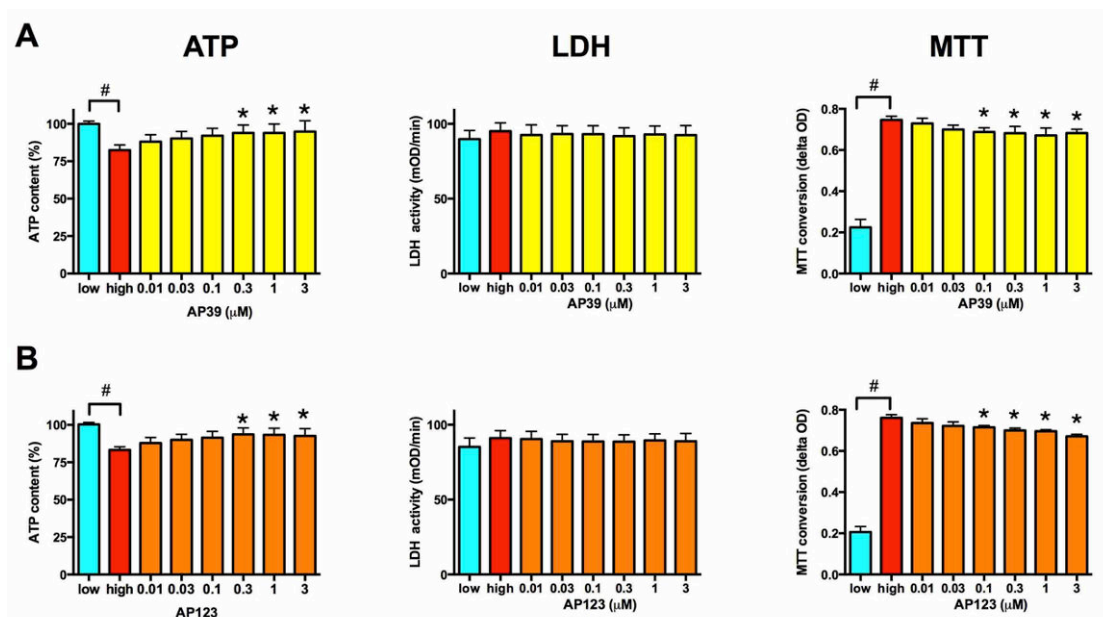


Fig. 28. Mitochondrial H₂S donors reduce the cellular hypermetabolism in hyperglycemic endothelial cells. *A-B*: b.End3 endothelial cells were exposed to high extracellular glucose for 7 days with a single AP39 (**A**) or AP123 (**B**) treatment on the 4th day of hyperglycemia. The MTT reducing capacity, the total cellular LDH activity and the cellular ATP content were measured on the 7th day. (# $p < 0.05$ high glucose induced significant changes in the cellular MTT reducing capacity and ATP content. * $p < 0.05$ H₂S donor compounds significantly reduced the MTT reduction and increased the cellular ATP content.)

To test the effect of the compounds on cellular bioenergetics, we performed metabolic profiling of b.End3 endothelial cells treated with AP39 or AP123 for 3 days using extracellular flux analysis (**Fig. 29**). Hyperglycemia induced subtle changes in the cellular metabolism at this stage and there is no detectable change in the basal OCR and ECAR (**Fig. 29C, G**), but the non-mitochondrial oxygen consumption is higher in the hyperglycemic cells: the residual OCR is elevated after blocking the mitochondria with oligomycin, FCCP and antimycin A (**Fig. 29A**). There was no detectable change in oxygen consumption linked to mitochondrial ATP-production, as measured by ATP synthase inhibition (**Fig. 29D**), but the mitochondrial H₂S donors induced significant increase in the respiratory capacity (**Fig. 29E**) that is in line with prior results showing that increased intra-mitochondrial H₂S production affects this measure [107]. The mitochondrial H₂S donors improve the coupling efficiency and significantly reduce the proton leak (**Fig. 29F**) that can explain the increased cellular ATP content in the cells (**Fig. 28**) without a measurable increase in oxygen consumption. There is no change in the anaerobic metabolism in cells treated with mitochondrial H₂S donors (**Fig. 29G**) that further confirms that the compounds do not inhibit mitochondrial respiration at nanomolar concentrations. The predominantly mitochondrial localization (**Fig. 25**) strongly suggests that there was no interference with anaerobic compensation following the inhibition of mitochondrial respiration (**Fig. 29H**).

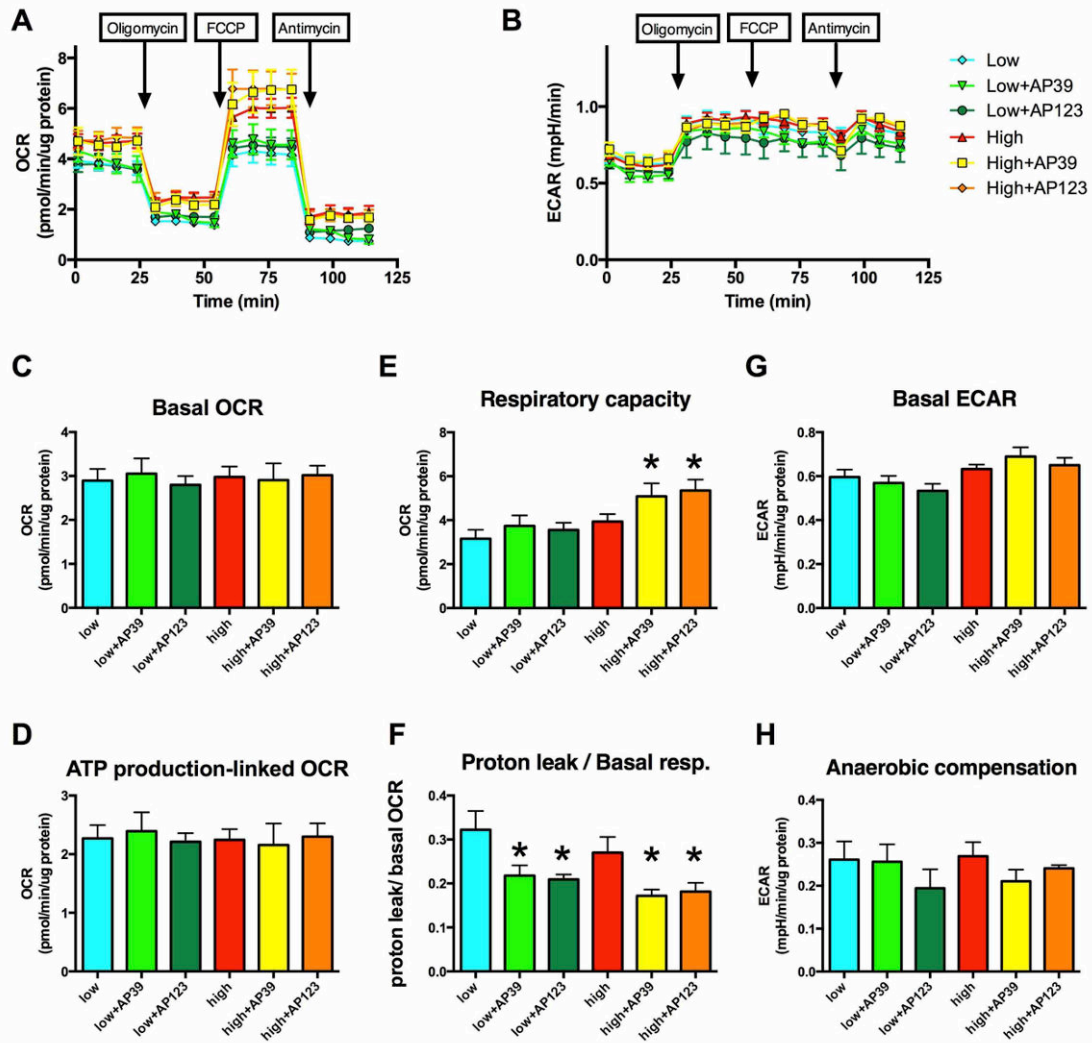


Fig. 29. Mitochondrial H_2S donors affect the cellular bioenergetics. *b.End3* cells exposed to 7-day-long hyperglycemia were treated with AP39 (30 nM) or AP123 (100nM) and the metabolic profile of the cells was studied by extracellular flux analysis. Sequential injections of Oligomycin (1 μ g/ml), FCCP (0.3 μ M) and antimycin A (2 μ g/ml) was used to measure **A**: the cellular oxygen consumption rate (OCR) and **B**: the extracellular acidification rate (ECAR). **C**: Basal oxygen consumption, **D**: ATP production linked oxygen consumption (determined by oligomycin injection), **E**: total respiratory capacity (determined following the addition of FCCP) and **F**: the proton leak/basal respiration was determined. **G**: Acid production of basal metabolism and **H**: acid production during anaerobic compensation was determined. AP39 and AP123 increase the respiratory capacity of the cells. ($n=3$, * $p<0.05$ compared to hyperglycemic control)

Mitochondrial H_2S oxidation is a complex process that requires three enzyme activities: 1) sulfide-quinone oxidoreductase (SQR) catalyses the two-electron oxidation of H_2S to the level of elemental sulfur by simultaneously reducing a cysteine disulfide such that a persulfide group is formed, 2) sulfur dioxygenase oxidises persulfides to sulfite, consuming molecular oxygen and water and 3) sulfur

transferase produces thiosulfate by transferring a second persulfide from SQR to sulfite [106]. During the first step of H₂S oxidation, the electrons are fed into the respiratory chain via the quinone pool (at the level of complex III). Oxygen consumption occurs only through the second step of H₂S oxidation, thus feeding of electrons from H₂S to the respiratory system does not necessarily increase the cellular oxygen consumption. To confirm that the action of mitochondrial H₂S donors increase the electron transfer, we performed a Complex II/III activity assay (**Fig. 30**). We blocked input from Complex I by rotenone and inhibited cytochrome c oxidation (Complex IV) by potassium cyanide. In the presence of substrate (succinate) Complex II transfers electrons to ubiquinone and Complex III to cytochrome c. The rate of cytochrome c reduction was measured in the absence or presence of AP39 or AP123. Both compounds induced a concentration-dependent increase in complex III activity at concentrations below 2.5 μM (**Fig. 30A, B**), but a decrease was detected at higher concentrations (5-10 μM). AP123 induced similar changes to AP39 but at twice as high concentration possibly due to its lower H₂S producing capacity. These results confirmed that the compounds directly affected the respiratory complex activities.

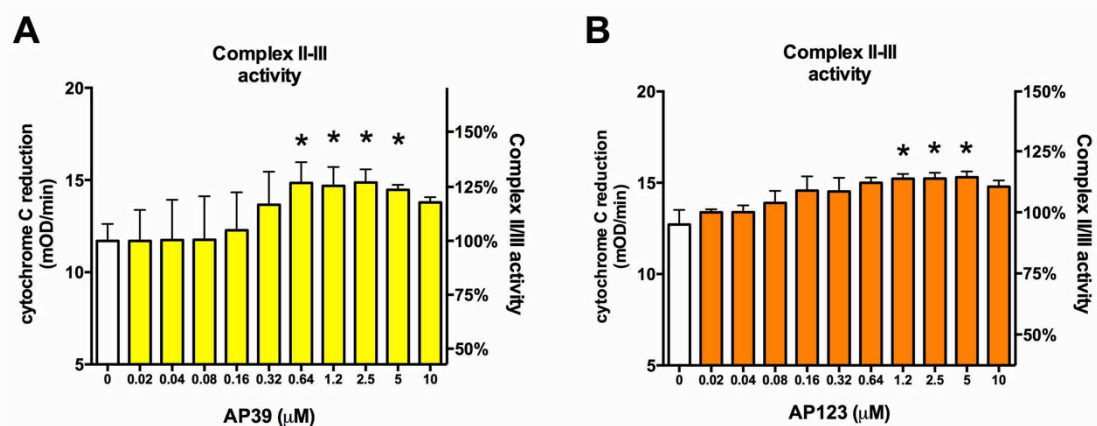


Fig. 30. Mitochondrial H₂S donors increase the respiratory Complex II/III activity. *A-B*: Cytochrome c reduction was monitored in bovine heart mitochondria following Complex I and IV blockade by rotenone and KCN, respectively. *A*: AP39 was added at 10 nM to 10 μM and complex II/III activity was measured kinetically, *B*: Mitochondria were treated with AP123 (10 nM to 10 μM) and the respiratory complex activity was monitored. (**p*<0.05, H₂S donors significantly increased the respiratory complex activity)

5. Discussion

5.1. Cell-based screening identifies currently approved drugs with repurposing potential and novel chemotypes as inhibitors of hyperglycemic endothelial ROS production

Diabetic endothelial dysfunction lies at the core of the development of diabetic complications (diabetic micro- and macrovascular disease, retinopathy, nephropathy and neuropathy) and the formation of reactive oxygen species (ROS) plays a key role in the development of tissue damage [179, 16]. Elevated blood glucose level plays a fundamental part in diabetic complications, still the mechanism, how this essential body fuel becomes an enemy, is controversial. Based on the predictive value of glucose concentration for diabetic complications [47] blood sugar cut-off values were chosen that identify patients at risk for complications [180-182], and values below the cut-off values were accepted as normal. In diabetic patients the improved glycemic control was proven to prevent the development of vascular complications [183-185, 41] confirming the pathogenic role of glucose. Thus, the maintenance of “normoglycemia” has become a widely accepted goal in diabetes management, but “glycemic control” by itself has not been able to decrease the incidence of diabetic complications [186] suggesting that additional therapeutic modalities might be necessary. Oxidative stress as a well-recognized contributor to the disease was proposed to connect hyperglycemia to diabetic damage [26] and it was suggested to serve as potential drug target in diabetes [187, 188].

Mitochondria are involved in the hyperglycemia-induced ROS production both as a source of oxidants and also as an activator of other sources of ROS generation in the cells [26]. They represent one of the most important sources of ROS generation in hyperglycemic endothelium, and while there are a number of molecular sources of mitochondrial ROS generation [87]. Glucose uptake occurs via facilitative transporters, thus high extracellular glucose concentration induces a similar rise in the intracellular glucose level. This leads to changes in the substrate availability for cellular metabolism and energy production [189] and it also induces ROS production in endothelial cells [15, 38]. The mitochondrial oxidative phosphorylation couples substrate oxidation to energy production, during which a low percentage (1-2%) of

oxygen is used for superoxide production [85]. The main sources of oxidants are complex III and complex I in the mitochondria [142], but since the respiratory complexes form supercomplexes [190] and there are changes in the relative amount of the respective respiratory complexes in diabetes [98, 99, 112], other complexes may also contribute to the oxidant production. The electrons used for ROS production will leave behind protons in the intermembrane space that may be released via the uncoupling proteins (UCP) to maintain the physiological membrane potential [191]. This amount of leak is relatively low compared to the measured ATP production/oxygen atom use (P/O) ratios that estimate approximately 20% basal leakage in the cells [191], but it also requires the neutralization of the oxidants and electron source to resupply the lost ones in the respiratory chain. The mitochondrial antioxidant defense system [192] can cope with the basal mitochondrial ROS production and the enzymes involved in the antioxidant defense are upregulated in diabetes [193], but for some reason the oxidant production is not properly counterbalanced in diabetes [141].

Mitochondrial superoxide, in concert with other sources of ROS and reactive nitrogen species (RNS), exerts deleterious effects via changes in gene transcription and initiation of post-translational protein modifications [87, 179, 16]. Some of the downstream processes involved in the hyperglycemic endothelial ROS production include inhibition of GAPDH, the activation of PKC isoforms, activation of the methylglyoxal pathway, activation of the hexosamine pathway, DNA damage and activation of the nuclear enzyme PARP, and mitochondrial and extramitochondrial protein modifications [83, 194, 125, 51, 87, 179, 16, 195].

Prior approaches to neutralize or inhibit ROS production in endothelial cells in diabetes to prevent diabetic complications. Antioxidant therapeutics were proposed to target the vasculature and have been shown beneficial in all diabetic complications [27]. Despite considerable evidence showing beneficial effects of antioxidants, results from large-scale clinical trials conclude that classic antioxidant scavengers may not be appropriate therapeutics in diabetes [196]. A possible explanation for the failure of vitamin C and E is that they can show pro-oxidant properties under certain circumstances [197-199], that suggests that specific inhibition or scavenging of glucose-induced ROS with low dose antioxidants is preferable to the liberal antioxidant use. Various natural antioxidants were also tested against diabetic

complications including the glutathione precursor N-acetylcysteine, coenzyme Q10, curcumin and sesamol and they all showed positive effects [200-202].

Significant efforts have also been directed to prevent the formation of ROS. One of the approaches involved re-balancing the glycolytic pathway in hyperglycemic cells via pharmacological activation of transketolase [203]. Several clinical drugs were tested to prevent diabetic activation of NADPH oxidase in preclinical studies including angiotensin I receptor blockers, statins and PPAR gamma ligands [153, 204-209]. Previous efforts found aldose reductase (a key enzyme of the polyol pathway) to serve as potential drug target and found that inhibition of aldose reductase may prevent the pathological changes that occur in response to high sorbitol levels [210]. Results of the clinical trials were less impressive than expected from preclinical studies, still the first aldose reductase inhibitor has been marketed in Asia for the treatment of diabetes complications [211]. Other potential approaches to reduce glucose-induced ROS generation include the inhibition of glyoxalase and the prevention of the down-regulation of mitochondrial uncoupling protein UCP3 [212, 213].

Following the discovery that mitochondrial superoxide is responsible for the induction of all ROS producing pathways in hyperglycemic endothelial cells, an intense search began for mitochondrial drug targets and inhibitors of mitochondrial superoxide generation [84, 83, 26]. Mitochondria-specific targeting moieties have been developed, like the triphenylphosphonium (TPP⁺) targeting group, which attains 100-500-fold accumulation in the mitochondria [175, 214], and linked to antioxidants or superoxide dismutase (SOD) mimetics [215, 216]. These molecules include the mitochondria-targeted ubiquinol (MitoQ) and the targeted piperidine nitroxide TEMPO (mitoTEMPO), that both proved beneficial in diabetes models [217-219]. Overexpression of mitochondrial SOD (MnSOD) was found to protect against diabetic retinopathy in a transgenic model, but long-term delivery of MnSOD is unresolved in humans [220]. In another phenotypic screen, which examined the OXPHOS-associated gene expression, the antihelmintic drug mebendazole and the Chinese herbal medicine deoxysappanone B emerged as inhibitors of mitochondrial ROS production [221]. The protective effect of these drugs might be a direct consequence of the normalization of the mitochondrial membrane potential or free radical scavenging.

In a further effort to identify compounds that reduce the mitochondrial ROS production but do not interfere with energy production, isolated mitochondria were used for high throughput screening and hit compounds were selected based on a dual output of ROS production and respiration rate [222, 223]. CN-POBS (N-cyclohexyl-4-(4-nitrophenoxy)benzenesulfonamide) was identified as a selective inhibitor of ROS production by the ubiquinone-binding site of complex I and S3QELs (“sequels”, selective suppressors of site III_{OQ} electron leak) were found to act as inhibitors of the outer ubiquinone binding site similar to terpestacin [224, 222, 223]. Unfortunately, there is no data about their action against hyperglycemia-induced ROS production. Statins also block the mitochondrial ROS production but they simultaneously reduce the mitochondrial respiration and may cause toxicity [221, 38]. H₂S, a further inhibitor of mitochondrial respiration, which is a known inhibitor of complex IV, turns out to act as stimulator of mitochondrial metabolism at low concentrations via electron donation [107]. Since H₂S supplementation via sodium sulfide inhibits the hyperglycemia-induced ROS production and endothelial dysfunction at low concentrations and long-term administration of H₂S proved effective against diabetic nephropathy and retinopathy in animal models [225, 226], here we tested novel mitochondria-targeted donor molecules [94, 35].

Finally, many of the currently used anti-diabetic medications have also been proven to possess mitochondrial targets and these targets might be partly responsible for their beneficial effects on endothelial cells and the vasculature. The biguanide metformin apart from activating AMPK also acts as a mild and transient inhibitor of respiratory complex I [161]. The sulfonylurea glibenclamide inhibits the mitochondrial ATP-sensitive potassium channel (mitoKATP), decreases the mitochondrial membrane potential and ROS production and increases the respiration rate [162, 163]. Thiazolidinediones (TZDs) also possess a specific mitochondrial target (mTOT, mitochondrial target of TZDs), which comprise of a recently identified protein complex. TZDs bind to a pyruvate carrier complex in the mitochondria and modulate the pyruvate entry into the mitochondria that may explain their antioxidant effect [164]. The discovery of these novel mitochondrial targets may support the significance of inhibition of mitochondrial ROS production in conjunction with glycemic control.

Drug re-purposing approach to find novel drugs against diabetic complications.

Drug reuse is a cost-effective approach in drug discovery that can provide novel therapeutics at an advanced speed [227, 228]. Drugs that are currently in clinical use or ever reached clinical trials in the past possess a large body of clinical or pharmacological information, which includes their known pharmacological effects and their safety or toxicity. Whether novel drug indication is limited by the prior indication of the compound depends on the applicable dosage, length of treatment and associated risk, thus approved or advanced clinical compounds are increasingly tested for drug repurposing [229]. Many currently used drugs have secondary, tertiary targets in the body and their side effects might be related to these [228]. Although beneficial secondary activities can be recognized in clinical use in related diseases, there is little chance to discover these activities in rare or unrelated syndromes [230-232].

So far, no systematic approach has been conducted to survey a wide variety of drugs, drug-like molecules and pharmacological agents for their potential ability to suppress mitochondrial ROS overproduction in hyperglycemic endothelial cells. Such a survey necessitated the development of a cell-based assay of hyperglycemic ROS production that is suitable for medium-throughput screening, and one that is coupled with the simultaneous evaluation of cell viability. Although cell-based screening assays in endothelial cells have previously been conducted, these assays were focusing on other outcome variables, such as identification of agents that inhibit angiogenesis [233, 234]. In addition, a handful of studies have conducted cell-based screening assays in non-endothelial cell systems, in order to identify cytoprotective agents [235, 146, 236-242]. For the current screening campaign, we have set up a mechanism-agnostic, cell-based approach, to identify compounds that inhibit hyperglycemia-induced ROS generation, in a way that they do not interfere with cell viability. We gave preference to compounds that remain effective with a shorter onset of action and work in a therapeutic regimen. The results of the screening and the subsequent hit confirmation have identified a handful of compounds (<20 compounds from the >6,000 compound library i.e. a <0.5% "hit rate") that met our criteria of significant inhibition of ROS production, without adversely affecting cell viability. For the current project, we have focused our investigations on the characterization of three compound groups: 1) paroxetine, a clinically widely used antidepressant agent, 2) glucocorticoid steroids,

which are in widespread general use and 3) novel mitochondrial H₂S donors that provide controlled release of the endogenous gasotransmitter H₂S. The mode of action of some other compounds may be of further interest: rottlerin and sirolimus are likely to act via uncoupling the mitochondria, while the mode of action for the microtubule polymerization inhibitors and the calcium channel blocker flunarizine and the antimetabolite thioguanosine remains to be elucidated in further studies.

5.2. The mode of action of select hit compounds

5.2.1. Paroxetine acts as mitochondrial superoxide scavenger

Prior clinical use of paroxetine. Paroxetine as a selective serotonin reuptake inhibitor (SSRI) antidepressant has been in clinical practice since 1992 [243]. Paroxetine is used to treat major depression, obsessive-compulsive disorder, panic disorder, social anxiety, posttraumatic stress and generalized anxiety disorders in adults. The recommended starting dose of paroxetine is 20 mg daily (orally), with a maximum dosage of 50 or 60 mg depending on indication. 20 mg daily dose of paroxetine results in a plasma level of ~130 nM (40 ng/ml) [244-246]. Paroxetine is generally a well-tolerated drug, and can be taken for years. Adverse effects of paroxetine are nausea and sexual dysfunction (ejaculatory disturbance). Paroxetine is relatively safe in overdose: patients survived paroxetine overdoses of up to 3600 mg [247, 248]. Paroxetine was tested for the treatment of diabetic neuropathy symptoms in 1990 and it showed positive effects within a 2 week-long treatment period [249]. Use of paroxetine was associated with a significant reduction in risk of myocardial infarction compared with use of other antidepressants and no antidepressant use in a case-control study of first myocardial infarction patients in 2003 [250]. However, these effects were never associated with the antioxidant property of paroxetine.

Paroxetine was also extensively used in long-term animal experiments in various neurological diseases including Huntington's disease, chronic social stress and amyloidosis at a dose of 1-20 mg/kg/day in mice for months [251-254]. (Up to 1 year long treatment periods is reported in mice with extended life span.) We used paroxetine at 10 mg/kg/day dose for 1 month in diabetic rats without noting any adverse effect [38]. Based on the safety of paroxetine, we anticipate that this

compound is theoretically amenable to potential clinical re-purposing for the experimental therapy of diabetic complications.

The mode of action of paroxetine against glucose-induced mitochondrial ROS production. Paroxetine emerged as a potent inhibitor of mitochondrial superoxide generation that shows an immediate effect but is also active for 3 days in the nanomolar concentration range. The rapid onset of action and the lack of modulation of mitochondrial gene expression by paroxetine suggested a direct mode of action, which was characterized as an inhibitor of mitochondrial ROS production. The inhibition of mitoSOX oxidation, but the lack of inhibition of DCFDA oxidation in the cell-based assays (**Fig. 7**) suggests that the mode of paroxetine may be at least partially preferential to mitochondrial sources of ROS, although the inhibition of the xantine-oxidase-derived ROS production suggests that paroxetine may also affect cytosolic ROS production as well. Characterization of additional selective serotonin reuptake inhibitors demonstrated that paroxetine is unique in its respect as an inhibitor of hyperglycemic ROS production. Partial and complete decomposition studies demonstrated that the primary site of the antioxidant action resides within the compound's sesamol moiety. The effects of paroxetine were not associated with any adverse changes in mitochondrial electron transport or mitochondrial function.

In accordance with its inhibitory effect on mitochondrial ROS production, paroxetine inhibited a variety of downstream responses that are typically associated with hyperglycemic ROS production in endothelial cells, such as indices of mitochondrial oxidative protein injury, as well as injury to the mitochondrial and nuclear DNA [**83, 194, 125, 203, 51, 87, 179, 16, 195, 94**]. The protective effect of paroxetine was also apparent against the development of hyperglycemic endothelial dysfunction in vascular rings, both in an *in vitro* model (vascular rings placed in elevated extracellular glucose concentration, followed by the measurement of endothelium-dependent relaxations) and in an *ex vivo* model. These reductionist models suggest that paroxetine may show protection against diabetic injury in more chronic, and more clinically relevant models of diabetes.

5.2.2. Glucocorticoids block the mitochondrial ROS production via UCP2 induction in microvascular endothelial cells

Glucocorticoid steroids, as major hyperglycemic hormones in the body, represent a contradictory group of drugs for drug re-use in diabetes, but the similar activity of glucocorticoid agonists and antagonists against mitochondrial ROS generation suggested a potential novel target of the disease in microvascular endothelial cells. We found that glucocorticoid steroids 1) reduce the mitochondrial membrane potential, 2) inhibit the mitochondrial ROS generation and 3) upregulate UCP2 that functions as the main regulator of the mitochondrial potential in microvascular endothelial cells.

Mitochondria produce higher levels of oxidants if the mitochondrial potential is elevated [31, 255]. In b.End3 microvascular endothelial cells, the increased mitochondrial membrane potential plays a crucial role in ROS generation, since the restoration of the mitochondrial membrane potential blocks the high glucose-induced mitochondrial superoxide production (Fig. 16-18). The lack of change in the ratios of individual mitochondrial respiratory complexes indirectly supports this phenomenon (Fig. 4). We found that UCP2 was a major controller of mitochondrial ROS production in microvascular endothelial cells, since UCP2 silencing by itself increased the mitochondrial membrane potential and ROS production (Fig. 22). Glucocorticoid steroids, that emerged as inhibitors of mitochondrial ROS production, upregulate UCP2 expression and this action may be responsible for the protective effect in hyperglycemic endothelial cells (Fig. 19-20) [38].

The primary function of uncoupling proteins UCP2 and UCP3 (uncoupling protein 3) is the limitation of free radical production in the cells [256] via both short-term and long-term controlling mechanisms. Redox regulation of UCP2 occurs via glutathionylation: under conditions associated with low ROS production the proton transferring function of UCP2 is blocked via glutathionylation, while UCP2 is deglutathionylated and activated by oxidative stress [32, 257]. ROS-induced UCP2 activation allows protons to be transferred back to the mitochondrial matrix and thereby leads to the decrease of the mitochondrial membrane potential. The diminished mitochondrial membrane potential decreases the electron transfer and

oxygen consumption leading to low oxidant production and UCP2 glutathionylation, which closes the channel and decreases the proton leak [257]. The function of the uncoupling proteins is also controlled at the transcriptional [258-262] and translational level [263, 157] via controlling the expression of the proteins. Regulation at this level seems to help adapt the cells to long-term stress. Thus, hyperglycemia itself induces UCP2 expression in some cell types, eg. in beta cells [264] and venous endothelial cells (Fig. 18) [34] and we also observed increased expression level in the muscle in diabetic mice [35]. Consistently, we found that the glucose-induced mitochondrial ROS production is modest in the EA.hy926 venous endothelial cells [38] compared to the microvascular endothelial cells, in which UCP2 expression is unaltered in hyperglycemia (Fig. 4).

Modulation of UCP2 has been recommended in diabetes complications [265], since the induction of UCP2 expression is safe: 1) the uncoupling function of the protein is redox regulated via reversible glutathionylation and 2) upregulation of UCP2 also occurs as an endogenous protective mechanism. Our results confirm that induction of UCP2 expression confers benefit against glucose-induced mitochondrial ROS production in microvascular endothelial cells. The functional benefit of uncoupling protein induction is also supported by the finding that overexpression of UCP3 (that shares functional similarity with UCP2 but shows distinct expression profile) is protective against glucose-induced damage in other cell types, eg. in neurons [212]. However, the regulation of UCP2 expression is a complex and incompletely understood process and upregulation of UCP2 expression has not been accomplished by pharmacological means. At the RNA level UCP2 expression is affected by micro RNAs (miRNA) at the 3' untranslated region of the gene: they either stabilize or destabilize the UCP2 transcript upon binding [261]. The expression of UCP2 can also be induced via blocking the heterogeneous nuclear ribonucleoprotein-K (hnRNP-K) mediated suppression as a mechanism involving this regulatory step has been described for angiopoietin-1 in endothelial cells [266]. This process has been suggested to occur at the posttranscriptional level (though it has not been confirmed by measuring the mRNA level of UCP2) and it may also involve a glucocorticoid-mediated phosphorylation step by Src tyrosine kinase [267]. We found that glucocorticoids increase the mRNA level of UCP2 (Fig. 18, 19), thus we suspect that the regulation occurs via the above mechanisms, especially, since they could explain

the cell-type restricted action of steroids. The microRNA expression profile of the microvascular endothelial cells differ from the macrovascular aortic or venous cells [28], and glucocorticoids induce robust changes in the miRNA expression in the cells [268-270]. Also, the heterogeneous nuclear ribonucleoprotein subtypes show cell or tissue specific expression pattern [271]. Interestingly, dexamethasone was reported to induce UCP3 expression in C2C12 muscle cells [156] via a glucocorticoid response element (GRE) located in the promoter region of the UCP3 gene. However, this mechanism is unlikely to be involved in the expression of UCP2, since its promoter region does not contain such sites and the glucocorticoid receptor (GR)-mediated actions occur universally in all cells, so it cannot explain the cell-type specific induction. At the translational level, UCP2 expression was reported to be affected by glutamine [157] and we found that availability of this amino acid stimulated the expression of UCP2 in endothelial cells and promoted its antioxidant effect but only if steroids induced the expression at the transcriptional level (**Fig. 20**).

In summary, UCP2 induction may represent a novel experimental therapeutic intervention in diabetic vascular complications. Direct repurposing of glucocorticoid steroids may not be possible due to their significant side effects that develop during chronic administration, but the UCP2-inducing pathway may be amenable to upregulation by other pharmacological means non affecting glucocorticoid receptors. Additionally, the short-term use of the glucocorticoid receptor antagonist mifepristone may be considered during short hyperglycemic episodes. Specific pharmacological tools that induce UCP2 expression in the microvasculature are expected to be shortly available and that they will allow the translation of this concept to clinical practice.

5.2.3. H₂S donors act as electron donors to the respiratory chain in endothelial cells

H₂S supplementation in diabetes. H₂S is an endogenously produced ‘gasotransmitter’ that plays key roles in regulating vascular tone, inflammation, cell death and proliferation as well as vascular protection [272-275]. Lower H₂S bioavailability has been reported in the diabetic vasculature in humans and it was associated with poor microcirculatory blood flow [276]. Impaired vascular H₂S synthesis or bioavailability

has been observed both in pharmacologically induced (streptozotocin diabetes [94]) and in genetically induced diabetes models (in Akita, db/db and NOD mice [277-279]).

The 'loss' of H₂S is thought to contribute to vascular endothelial dysfunction suggesting that approaches to increase H₂S bioavailability could be of therapeutic benefit in diabetic complications. One key mechanism by which H₂S is beneficial is by serving as an inorganic electron donor to the respiratory chain [107]. The oxidation of H₂S is a multi-step process and electron transfer to the respiratory chain may be dissociated from the subsequent steps of proton transfer and oxygen consumption [106]. Thus, unlike the main electron donors, nicotinamide adenine dinucleotide (NADH) and flavin adenine dinucleotide (FADH₂), H₂S can provide the respiratory chain with electrons only. This effect of H₂S is supported by our findings that exogenous H₂S, albeit at high concentrations, can normalize the mitochondrial membrane potential and reduce mitochondrial superoxide generation in hyperglycemic endothelial cells and also prevent the development of endothelial dysfunction in streptozotocin-induced diabetes [94, 280]. Furthermore, H₂S, in the form of inorganic salts (e.g. NaSH and Na₂S) have protective effects against diabetic retinopathy and nephropathy [225, 226, 281] and also has cardioprotective effects in diabetic models [282, 279, 283].

The positive effects of H₂S supplementation in diabetes were confirmed by several studies but long-term administration of H₂S remained a challenging issue [284, 94, 281, 285]. H₂S is volatile and has short half-life *in vivo*, thus for long-term treatment the use of donor molecules (prodrugs) is preferable as they release H₂S at a controlled rate. The administration of H₂S using its sodium salts is inconvenient in long-term diseases because it has a short half-life and lacks cellular targeting.

H₂S supplementation using natural products may represent an alternative approach for long-term treatment, though controlled H₂S release is more problematic with molecules of natural sources. Garlic is the most commonly used sulfur-rich nutrient that can provide H₂S using it either freshly or its extract as a dietary supplement. Garlic provides slower H₂S release than Na₂S [286]. Allicin (diallyl thiosulfinate) is the main source of H₂S in garlic, as it decomposes to various sulfur-containing compounds in aqueous solutions including diallyldisulfide (DADS) and diallyltrisulfide (DATS) [286-288]. DADS and DATS release H₂S in a thiol-dependent manner in cells, and they may deplete the cellular glutathione pool [289-

291]. While this chemical approach may help control the H₂S release, the loss of glutathione increases the risk of oxidative damage in a pro-oxidant state like diabetes and it may involve excessive H₂S release and toxicity **[292]**. Interestingly, the opposite effect of DADS, an increase in the cellular glutathione level was also reported after prolonged treatment periods **[293]** that may be directly caused by H₂S **[51]**. Overall, if thiol-dependent donors cause fluctuations in the glutathione pool and in H₂S levels, they may present a challenge in dosing and also incur an increased risk for oxidative damage. As a result, the beneficial effects of garlic were confirmed by multiple studies in diabetes models **[294-297]**, still garlic had no effect on endothelial function and oxidative stress in diabetic patients and no change was seen in the glutathione level in a recent pilot trial supporting the dosing difficulties of garlic-based dietary supplements **[298]**.

Several H₂S donor compounds have been developed over the last couple of years and various chemistries have been implicated but the control of H₂S generation is still not perfect **[299, 174, 288]**. A further problem may arise from the side effects caused by the by-products that are formed during H₂S release, thus in chronic diseases it is necessary to reduce the concentration of the donors as much as possible since very long treatment periods are anticipated. One option is to deliver the H₂S donors to specific cell types or subcellular compartments to minimize the off-target effects. The subset of cell types, that are involved in diabetic complications and should benefit from H₂S supplementation, includes capillary endothelial cells, mesangial cells, neurons and Schwann cells in peripheral nerves **[26]**. The glucose-induced damage is orchestrated by the mitochondria via superoxide generation that promotes all other oxidative stress pathways in diabetes **[26]**, thus mitochondrial oxidant production is the foremost target in the cells.

Mitochondria-targeted H₂S donors against hyperglycemic endothelial injury. We tested the efficacy of novel mitochondria-targeted H₂S donors against the glucose-induced oxidant production in endothelial cells. To accomplish mitochondria-specific drug delivery, a triphenylphosphonium targeting moiety is incorporated in the structures that allows potential-dependent drug accumulation **[175]**. It also assures that H₂S concentration is kept within a safe range, since the intra-mitochondrial drug concentration is higher, when the mitochondrial membrane potential is elevated, but lower when the potential is reduced using the same loading concentration of the drug.

Thus, normalization of the mitochondrial potential reduces the mitochondrial drug uptake. Also, a relatively stable supply of H₂S is maintained by the use of these compounds, since higher consumption of H₂S does not result in a drop in H₂S donors (eg. in metabolically active cells), since mitochondria are rapidly replenished with new donor molecules by the re-equilibration process. AP39 is a slow-release H₂S donor that was shown to accumulate in the mitochondria [36, 37] and protect against oxidative stress-induced mitochondrial DNA and protein damage in endothelial cells [300]. AP123, a structurally different mitochondrial H₂S donor that has similar molecular weight and solubility and also provides very slow, controlled H₂S release. It is difficult to determine the mitochondrial concentration of H₂S that might be associated with beneficial effects in the cells and various methodologies produced strikingly different results, but the amount to produce stimulatory effect on cellular bioenergetics is probably between 6 nM and 1 μM [301, 302, 107]. In contrast, a ~1000-fold higher concentration (100-300 μM exogenous H₂S) was necessary to normalize the mitochondrial membrane potential and decrease the oxidant production in endothelial cells exposed to high glucose concentrations when H₂S was supplemented using its sodium salts [94]. This huge difference might be explained by the fact that the donor compound was not targeted to mitochondria, thus the majority of H₂S was wasted because of extracellular consumption, low penetration or via extra-mitochondrial metabolism. The amount of H₂S that blocks complex IV and has inhibitory effect on the respiration is no more than 1 order of magnitude higher than its stimulatory concentration [176, 301, 302, 107] thus dosing remains a challenging issue. Furthermore, it is unclear whether exogenous H₂S supplementation affects the endogenous production of H₂S and whether the concentrations determined by prior assays truly reflect the beneficial amount of H₂S on the long term. Overall, both prior reports and our results suggest that mitochondria-specific delivery of H₂S can greatly reduce the therapeutic concentration of H₂S donors. We found that AP39 and AP123 were effective against hyperglycemic injury at >1000-fold lower concentrations than Na₂S in endothelial cells. We found that low nanomolar concentrations (30-300 nM) were cytoprotective in hyperglycemic endothelial cells, similar to the values previously reported for AP39 in other models [145, 300, 303, 304]. H₂S-mediated cytoprotection mostly depends on the mitochondrial effect of H₂S in endothelial cells, since it is associated with the normalization of the mitochondrial potential and

inhibition of mitochondrial ROS production. While the longer term efficacy of the compounds may suggest other mechanisms, including gene expression changes induced by the donor molecules, it is unlikely that the protection involves upregulation of H₂S biosynthetic enzymes as such effect has not been previously observed [305].

The antioxidant effects of the two mitochondrial H₂S donors (AP39 and AP123) are comparable but the effective concentration of AP39 is slightly lower than that of AP123 (**Fig. 27**). It might be explained by the slightly higher H₂S release from AP39: it also induced an increase in complex II/III activity at a lower concentration than AP123 (**Fig. 30**), and its lower toxic concentration: AP39 has a TC₅₀ of 7.8 μM while AP123's TC₅₀ is 16.7 μM (**Fig. 26**); concentrations far exceeding that required for cytoprotection (e.g. 10-300 nM, **Figs. 27**). Both AP39 and AP123 provide H₂S release for multiple days but AP39 is capable of releasing more H₂S than AP123 due to the structural differences in the H₂S releasing moiety (**Fig. 24**), which is evidenced by the toxic concentrations of the non-mitochondrial H₂S donors ADT-OH and HTB (69.5 μM and 165.5 μM, respectively). The lower therapeutic concentration achieved by the ester-linked mitochondrial targeting moiety possibly suggests lower risk of side effects caused by the metabolites of the drugs. The molecular mechanism of H₂S release from 1,2-dithiole-3-thione compounds are still unclear [287], but the mitochondrial redox environment may affect this process. Furthermore, H₂S generation from ADT-OH or AP39 can occur through multiple steps and each of these steps may be affected by various metabolites in the mitochondria. On the other hand, HTB compounds are more likely to liberate H₂S through a single step that is not affected by the metabolites, possibly allowing for better control of H₂S generation. Interestingly, HTB is the chosen H₂S donor moiety in many novel H₂S-releasing therapeutics including various non-steroidal anti-inflammatory drugs (NSAIDs) and some of them (eg. the naproxen derivative ATB-346) already reached clinical trial phases [299]. AP39 and AP123 showed no toxicity in animal experiments and we expect that they will be suitable to proceed to clinical trials in diseases associated with mitochondrial oxidative stress in the near future.

6. Conclusions

In conclusion, the current studies have utilized a cell-based screening method to identify a number of drugs and drug-like molecules that beneficially affect hyperglycemic ROS production in endothelial cells.

One of these compounds, the antidepressant paroxetine, has been tested in a variety of *in vitro* and *in vivo/ex vivo* models of hyperglycemic endothelial injury and diabetic vascular complications. We found that paroxetine shows effect at submicromolar concentrations and superoxide scavenging is involved in its mode of action against mitochondrial ROS. It is interesting to note that paroxetine has previously been shown to afford certain cardiovascular benefits in terms of protection from myocardial infarction in humans [250].

The antioxidant effect of mifepristone, a glucocorticoid receptor antagonist, is associated with mild mitochondrial uncoupling, which is achieved by induction of UCP2 expression. This compound was also found to be effective in a clinically relevant concentration range [306].

Mitochondrial slow release H₂S donors also provided protection against the prolonged low level oxidative stress induced by hyperglycemia in endothelial cells. They increase the electron transfer rate at respiratory complex III and have beneficial effect on cellular bioenergetics. These compounds showed positive effect in the nanomolar concentration range, which is more than two orders of magnitude lower than their maximum tolerated concentration, suggesting a safer alternative compared to non-targeted H₂S donors and natural sources [94].

The current results may lay the conceptual foundation for future exploratory clinical trials in patients with diabetes, with the potential ultimate goal of re-purposing for the experimental therapy of diabetic complications. However, such studies must be preceded by careful investigation of the safety profile of this compound in diabetic patients.

7. Summary

Introduction: Diabetic complications are responsible for the majority of expenses associated with diabetes treatment. Recently, mitochondrial superoxide production has been proposed to serve as the initiator of all other oxidative stress pathways in diabetic endothelial cells including the polyol pathway and advanced glycation endproduct (AGE) formation. Thus, inhibition of mitochondrial superoxide generation may protect against the endothelial injury and postpone the development of diabetic complications.

Aim: We aimed to identify compounds that block the glucose-induced mitochondrial superoxide production to find potential drug candidates for inhibiting the development of diabetic complications.

Methods: A comprehensive library of 6,766 drugs (comprising of clinical drugs and biologically active compounds) was tested against mitochondrial ROS production in hyperglycemic endothelial cells. Hit compounds were identified using the mitochondrial superoxide sensor MitoSOX dye to measure the ROS production. The mode of action of the most effective compounds and their protective effects were further characterized in secondary assays.

Results: Less than 0,5% of the drugs blocked the glucose-induced mitochondrial ROS production and the mechanism of action of hit compounds involved newly identified activities: 1) paroxetine reduced ROS via superoxide scavenging, 2) glucocorticoids induced the expression of uncoupling protein 2 (UCP2), 3) H₂S donors reduced the mitochondrial ROS via direct electron donation to the respiratory chain. The antioxidant activity of these drugs was associated with beneficial effects on cellular energy production and protection against diabetic vascular dysfunction *in vivo*.

Conclusions: Our results suggest that mitochondrial dysfunction can be directly addressed in endothelial cells by preventing or reducing the glucose-induced mitochondrial ROS production. The beneficial effect of the identified compounds and pathways may raise the potential of re-purposing of these approaches for the experimental therapy of diabetic cardiovascular complications.

Összefoglalás

Bevezetés: A cukorbetegség kezelési költségeinek döntő részéért a szövődmények felelősek. A diabeteses károsodásban központi szerepet játszik a mitokondriális szuperoxid termelés, azáltal, hogy aktiválja az összes további oxidatív stressz útvonalat az endothel sejtekben, így a poliol útvonalat és a késői glikációs végtermékek képzését is. A mitokondriális szuperoxid termelés gátlásától várható, hogy megakadályozza az endothel sejtek károsodását és késlelteti a cukorbetegség szövődmények kialakulását.

Cél: Olyan molekulák azonosítását tűztük ki célul, melyek csökkentik a magas glükóz koncentráció hatására kialakuló mitokondriális szuperoxid termelést, és potenciális gyógyszerjelöltek lehetnek a cukorbetegség szövődményeinek megelőzésében.

Módszerek: 6.766 molekulából álló (klinikai használatban álló gyógyszereket és biológiailag aktív anyagokat tartalmazó) molekula könyvtár szűrését végeztük el, hogy a szerek mitokondriális oxidáns termelésre kifejtett hatását megvizsgáljuk hyperglycemiás endothel sejtekben. A "hit" molekulák azonosítását a mitokondriális oxidáns termelés mérésével végeztük, a szuperoxid érzékeny MitoSOX festéket alkalmazva. A leghatásosabb szerek további vizsgálatát és hatásmechanizmusuk azonosítását szekunder vizsgálatok segítségével végeztük el.

Eredmények: A magas cukor hatására létrejövő mitokondriális oxidáns termelést kevesebb, mint a molekulák 0,5%-a csökkentette. A "hit-ek" antioxidáns hatásában újonnan megismert mechanizmusok játszottak szerepet: 1) a paroxetin direkt szabadgyökfogy szerepet tölt be, 2) a glükokortikoid szteroidok enyhe mitokondriális szétkapcsoló hatással bírnak az UCP2 fehérje szintézisének fokozása révén és 3) a hidrogén szulfid (H₂S) donor molekulák a légzési lánc elektron donoraiként csökkentik a szabadgyök termelést. Ezek a szerek, antioxidáns hatásukon túl, javítják a sejtek energiaforgalmát és a vaszkuláris endothel funkció javulását is eredményezik diabetesben.

Következtetés: Eredményeink azt mutatják, hogy a magas glükóz hatására kialakuló mitokondriális dysfunctio közvetlenül is gátolható az endothel sejtekben, a mitokondriális szabadgyök termelés gátlása révén. Az azonosított antioxidáns szerek pozitív hatásai felvetik ezen szerek kísérletes alkalmazásának lehetőségét diabetes cardiovascularis szövődményeiben.

8. References

1. Roglic G and World Health Organization. Global report on diabetes. World Health Organization, Geneva, Switzerland, 2016: 1-87.
2. Tamayo T, Brinks R, Hoyer A, Kuss OS, Rathmann W. (2016) The Prevalence and Incidence of Diabetes in Germany. *Dtsch Arztebl Int*, 113 (11): 177-82.
3. Ulrich S, Holle R, Wacker M, Stark R, Icks A, Thorand B, Peters A, Laxy M. (2016) Cost burden of type 2 diabetes in Germany: results from the population-based KORA studies. *BMJ Open*, 6 (11): e012527.
4. Hex N, Bartlett C, Wright D, Taylor M, Varley D. (2012) Estimating the current and future costs of Type 1 and Type 2 diabetes in the UK, including direct health costs and indirect societal and productivity costs. *Diabet Med*, 29 (7): 855-62.
5. Brown JB, Nichols GA, Glauber HS, Bakst AW. (1999) Type 2 diabetes: incremental medical care costs during the first 8 years after diagnosis. *Diabetes Care*, 22 (7): 1116-24.
6. Hadi HA and Suwaidi JA. (2007) Endothelial dysfunction in diabetes mellitus. *Vasc Health Risk Manag*, 3 (6): 853-76.
7. Georgescu A. (2011) Vascular dysfunction in diabetes: The endothelial progenitor cells as new therapeutic strategy. *World J Diabetes*, 2 (6): 92-7.
8. Esper RJ, Nordaby RA, Vilarino JO, Paragano A, Cacharron JL, Machado RA. (2006) Endothelial dysfunction: a comprehensive appraisal. *Cardiovasc Diabetol*, 5: 4.
9. Raitakari OT and Celermajer DS. (2000) Flow-mediated dilatation. *Br J Clin Pharmacol*, 50 (5): 397-404.
10. De Vriese AS, Verbeuren TJ, Van de Voorde J, Lameire NH, Vanhoutte PM. (2000) Endothelial dysfunction in diabetes. *Br J Pharmacol*, 130 (5): 963-74.
11. Montero D, Walther G, Perez-Martin A, Vicente-Salar N, Roche E, Vinet A. (2013) Vascular smooth muscle function in type 2 diabetes mellitus: a systematic review and meta-analysis. *Diabetologia*, 56 (10): 2122-33.
12. Artwohl M, Brunmair B, Furnsinn C, Holzenbein T, Rainer G, Freudenthaler A, Porod EM, Huttary N, Baumgartner-Parzer SM. (2007) Insulin does not

- regulate glucose transport and metabolism in human endothelium. *Eur J Clin Invest*, 37 (8): 643-50.
13. Bakker W, Eringa EC, Sipkema P, van Hinsbergh VW. (2009) Endothelial dysfunction and diabetes: roles of hyperglycemia, impaired insulin signaling and obesity. *Cell Tissue Res*, 335 (1): 165-89.
 14. Eelen G, de Zeeuw P, Simons M, Carmeliet P. (2015) Endothelial cell metabolism in normal and diseased vasculature. *Circ Res*, 116 (7): 1231-44.
 15. Quijano C, Castro L, Peluffo G, Valez V, Radi R. (2007) Enhanced mitochondrial superoxide in hyperglycemic endothelial cells: direct measurements and formation of hydrogen peroxide and peroxynitrite. *Am J Physiol Heart Circ Physiol*, 293 (6): H3404-14.
 16. Giacco F and Brownlee M. (2010) Oxidative stress and diabetic complications. *Circ Res*, 107 (9): 1058-70.
 17. Haj-Yehia AI, Nassar T, Assaf P, Nassar H, Anggard EE. (1999) Effects of the superoxide dismutase-mimic compound TEMPOL on oxidant stress-mediated endothelial dysfunction. *Antioxid Redox Signal*, 1 (2): 221-32.
 18. Coppey LJ, Gellett JS, Davidson EP, Dunlap JA, Lund DD, Yorek MA. (2001) Effect of antioxidant treatment of streptozotocin-induced diabetic rats on endoneurial blood flow, motor nerve conduction velocity, and vascular reactivity of epineurial arterioles of the sciatic nerve. *Diabetes*, 50 (8): 1927-37.
 19. Ceriello A. (2011) Diabetic complications: from oxidative stress to inflammatory cardiovascular disorders. *Medicographia*, 33 (1): 29-34.
 20. Maeda M, Hayashi T, Mizuno N, Hattori Y, Kuzuya M. (2015) Intermittent high glucose implements stress-induced senescence in human vascular endothelial cells: role of superoxide production by NADPH oxidase. *PLoS One*, 10 (4): e0123169.
 21. Galley HF and Webster NR. (2004) Physiology of the endothelium. *Br J Anaesth*, 93 (1): 105-13.
 22. Patrick V and Lepore J. Blood vessels and the endothelium, In: Warrell DA, Cox TM, Firth JD (editors.), *Oxford Textbook of Medicine*. 'Oxford University Press', Oxford, UK, 2010: 2593-2602.
 23. Bianconi E, Piovesan A, Facchin F, Beraudi A, Casadei R, Frabetti F, Vitale L, Pelleri MC, Tassani S, Piva F, Perez-Amodio S, Strippoli P, Canaider S.

- (2013) An estimation of the number of cells in the human body. *Ann Hum Biol*, 40 (6): 463-71.
24. Loomans CJ, de Koning EJ, Staal FJ, Rookmaaker MB, Verseyden C, de Boer HC, Verhaar MC, Braam B, Rabelink TJ, van Zonneveld AJ. (2004) Endothelial progenitor cell dysfunction: a novel concept in the pathogenesis of vascular complications of type 1 diabetes. *Diabetes*, 53 (1): 195-9.
 25. Rogers SC, Zhang X, Azhar G, Luo S, Wei JY. (2013) Exposure to high or low glucose levels accelerates the appearance of markers of endothelial cell senescence and induces dysregulation of nitric oxide synthase. *J Gerontol A Biol Sci Med Sci*, 68 (12): 1469-81.
 26. Brownlee M. (2005) The pathobiology of diabetic complications: a unifying mechanism. *Diabetes*, 54 (6): 1615-25.
 27. Calcutt NA, Cooper ME, Kern TS, Schmidt AM. (2009) Therapies for hyperglycaemia-induced diabetic complications: from animal models to clinical trials. *Nat Rev Drug Discov*, 8 (5): 417-29.
 28. McCall MN, Kent OA, Yu J, Fox-Talbot K, Zaiman AL, Halushka MK. (2011) MicroRNA profiling of diverse endothelial cell types. *BMC Med Genomics*, 4: 78.
 29. Kaiser N, Sasson S, Feener EP, Boukobza-Vardi N, Higashi S, Moller DE, Davidheiser S, Przybylski RJ, King GL. (1993) Differential regulation of glucose transport and transporters by glucose in vascular endothelial and smooth muscle cells. *Diabetes*, 42 (1): 80-9.
 30. Heilig CW, Concepcion LA, Riser BL, Freytag SO, Zhu M, Cortes P. (1995) Overexpression of glucose transporters in rat mesangial cells cultured in a normal glucose milieu mimics the diabetic phenotype. *J Clin Invest*, 96 (4): 1802-14.
 31. Korshunov SS, Skulachev VP, Starkov AA. (1997) High protonic potential actuates a mechanism of production of reactive oxygen species in mitochondria. *FEBS Lett*, 416 (1): 15-8.
 32. Mailloux RJ and Harper ME. (2011) Uncoupling proteins and the control of mitochondrial reactive oxygen species production. *Free Radic Biol Med*, 51 (6): 1106-15.

33. Mailloux RJ and Harper ME. (2012) Mitochondrial proticity and ROS signaling: lessons from the uncoupling proteins. *Trends Endocrinol Metab*, 23 (9): 451-8.
34. Koziel A, Woyda-Ploszczyca A, Kicinska A, Jarmuszkiewicz W. (2012) The influence of high glucose on the aerobic metabolism of endothelial EA.hy926 cells. *Pflugers Arch*, 464 (6): 657-69.
35. Gero D and Szabo C. (2016) Glucocorticoids Suppress Mitochondrial Oxidant Production via Upregulation of Uncoupling Protein 2 in Hyperglycemic Endothelial Cells. *PLoS One*, 11 (4): e0154813.
36. Busik JV, Mohr S, Grant MB. (2008) Hyperglycemia-induced reactive oxygen species toxicity to endothelial cells is dependent on paracrine mediators. *Diabetes*, 57 (7): 1952-65.
37. Engerman R, Bloodworth JM, Jr., Nelson S. (1977) Relationship of microvascular disease in diabetes to metabolic control. *Diabetes*, 26 (8): 760-9.
38. Gero D, Szoleczky P, Suzuki K, Modis K, Olah G, Coletta C, Szabo C. (2013) Cell-based screening identifies paroxetine as an inhibitor of diabetic endothelial dysfunction. *Diabetes*, 62 (3): 953-64.
39. Davidson SM and Yellon DM. (2006) Does hyperglycemia reduce proliferation or increase apoptosis? *Am J Physiol Heart Circ Physiol*, 291 (3): H1486; author reply H1487.
40. UK Prospective Diabetes Study (UKPDS) Group. (1998) Intensive blood-glucose control with sulphonylureas or insulin compared with conventional treatment and risk of complications in patients with type 2 diabetes (UKPDS 33) *Lancet*, 352 (9131): 837-53.
41. Cheng AY and Leiter LA. (2010) Glucose lowering and cardiovascular disease: what do we know and what should we do? *Eur J Cardiovasc Prev Rehabil*, 17 Suppl 1: S25-31.
42. Harris MI. Classification, Diagnostic Criteria, and Screening for Diabetes, In: Harris MI, Cowie CC, Stern MP, Boyko EJ, Reiber GE, Bennett PH (editors.), *Diabetes in America*. 1995: 15-36.
43. Si D, Bailie R, Wang Z, Weeramanthri T. (2010) Comparison of diabetes management in five countries for general and indigenous populations: an internet-based review. *BMC Health Serv Res*, 10: 169.

44. Powers MA, Bardsley J, Cypress M, Duker P, Funnell MM, Hess Fischl A, Maryniuk MD, Siminerio L, Vivian E. (2015) Diabetes Self-management Education and Support in Type 2 Diabetes: A Joint Position Statement of the American Diabetes Association, the American Association of Diabetes Educators, and the Academy of Nutrition and Dietetics. *Diabetes Care*, 38 (7): 1372-82.
45. Hammes HP, Feng Y, Pfister F, Brownlee M. (2011) Diabetic retinopathy: targeting vasoregression. *Diabetes*, 60 (1): 9-16.
46. WHO Expert Committee on Diabetes Mellitus. (1980) Second report. *World Health Organ Tech Rep Ser*, 646: 1-80.
47. Alberti KG and Zimmet PZ. (1998) Definition, diagnosis and classification of diabetes mellitus and its complications. Part 1: diagnosis and classification of diabetes mellitus provisional report of a WHO consultation. *Diabet Med*, 15 (7): 539-53.
48. Felig P, Wahren J, Hendler R. (1975) Influence of oral glucose ingestion on splanchnic glucose and gluconeogenic substrate metabolism in man. *Diabetes*, 24 (5): 468-75.
49. Bonora E and Muggeo M. (2001) Postprandial blood glucose as a risk factor for cardiovascular disease in Type II diabetes: the epidemiological evidence. *Diabetologia*, 44 (12): 2107-14.
50. Ihnat MA, Thorpe JE, Ceriello A. (2007) Hypothesis: the 'metabolic memory', the new challenge of diabetes. *Diabet Med*, 24 (6): 582-6.
51. Ihnat MA, Thorpe JE, Kamat CD, Szabo C, Green DE, Warnke LA, Lacza Z, Cselenyak A, Ross K, Shakir S, Piconi L, Kaltreider RC, Ceriello A. (2007) Reactive oxygen species mediate a cellular 'memory' of high glucose stress signalling. *Diabetologia*, 50 (7): 1523-31.
52. Horvath EM, Benko R, Kiss L, Muranyi M, Pek T, Fekete K, Barany T, Somlai A, Csordas A, Szabo C. (2009) Rapid 'glycaemic swings' induce nitrosative stress, activate poly(ADP-ribose) polymerase and impair endothelial function in a rat model of diabetes mellitus. *Diabetologia*, 52 (5): 952-61.
53. Skyler JS, Bergenstal R, Bonow RO, Buse J, Deedwania P, Gale EA, Howard BV, Kirkman MS, Kosiborod M, Reaven P, Sherwin RS, American Diabetes A, American College of Cardiology F, American Heart A. (2009) Intensive

- glycemic control and the prevention of cardiovascular events: implications of the ACCORD, ADVANCE, and VA diabetes trials: a position statement of the American Diabetes Association and a scientific statement of the American College of Cardiology Foundation and the American Heart Association. *Circulation*, 119 (2): 351-7.
54. Diabetes Control Complications Trial Research Group, Nathan DM, Genuth S, Lachin J, Cleary P, Crofford O, Davis M, Rand L, Siebert C. (1993) The effect of intensive treatment of diabetes on the development and progression of long-term complications in insulin-dependent diabetes mellitus. *N Engl J Med*, 329 (14): 977-86.
 55. Kowluru RA. (2003) Effect of reinstatement of good glycemic control on retinal oxidative stress and nitrate stress in diabetic rats. *Diabetes*, 52 (3): 818-23.
 56. Kowluru RA, Kanwar M, Kennedy A. (2007) Metabolic memory phenomenon and accumulation of peroxynitrite in retinal capillaries. *Exp Diabetes Res*, 2007: 21976.
 57. Galderisi A, Pirillo P, Moret V, Stocchero M, Gucciardi A, Perilongo G, Moretti C, Monciotti C, Giordano G, Baraldi E. (2017) Metabolomics reveals new metabolic perturbations in children with type 1 diabetes. *Pediatr Diabetes*.
 58. Padberg I, Peter E, Gonzalez-Maldonado S, Witt H, Mueller M, Weis T, Bethan B, Liebenberg V, Wiemer J, Katus HA, Rein D, Schatz P. (2014) A new metabolomic signature in type-2 diabetes mellitus and its pathophysiology. *PLoS One*, 9 (1): e85082.
 59. Li M, Wang X, Aa J, Qin W, Zha W, Ge Y, Liu L, Zheng T, Cao B, Shi J, Zhao C, Wang X, Yu X, Wang G, Liu Z. (2013) GC/TOFMS analysis of metabolites in serum and urine reveals metabolic perturbation of TCA cycle in db/db mice involved in diabetic nephropathy. *Am J Physiol Renal Physiol*, 304 (11): F1317-24.
 60. Sas KM, Karnovsky A, Michailidis G, Pennathur S. (2015) Metabolomics and diabetes: analytical and computational approaches. *Diabetes*, 64 (3): 718-32.
 61. Yuan W, Zhang J, Li S, Edwards JL. (2011) Amine metabolomics of hyperglycemic endothelial cells using capillary LC-MS with isobaric tagging. *J Proteome Res*, 10 (11): 5242-50.

62. Krutzfeldt A, Spahr R, Mertens S, Siegmund B, Piper HM. (1990) Metabolism of exogenous substrates by coronary endothelial cells in culture. *J Mol Cell Cardiol*, 22 (12): 1393-404.
63. Harjes U, Bensaad K, Harris AL. (2012) Endothelial cell metabolism and implications for cancer therapy. *Br J Cancer*, 107 (8): 1207-12.
64. Dagher Z, Ruderman N, Tornheim K, Ido Y. (2001) Acute regulation of fatty acid oxidation and amp-activated protein kinase in human umbilical vein endothelial cells. *Circ Res*, 88 (12): 1276-82.
65. Noyman I, Marikovsky M, Sasson S, Stark AH, Bernath K, Seger R, Madar Z. (2002) Hyperglycemia reduces nitric oxide synthase and glycogen synthase activity in endothelial cells. *Nitric Oxide*, 7 (3): 187-93.
66. Goveia J, Stapor P, Carmeliet P. (2014) Principles of targeting endothelial cell metabolism to treat angiogenesis and endothelial cell dysfunction in disease. *EMBO Mol Med*, 6 (9): 1105-20.
67. Yu J and Auwerx J. (2010) Protein deacetylation by SIRT1: an emerging key post-translational modification in metabolic regulation. *Pharmacol Res*, 62 (1): 35-41.
68. Ruderman NB, Xu XJ, Nelson L, Cacicedo JM, Saha AK, Lan F, Ido Y. (2010) AMPK and SIRT1: a long-standing partnership? *Am J Physiol Endocrinol Metab*, 298 (4): E751-60.
69. Zheng Z, Chen H, Li J, Li T, Zheng B, Zheng Y, Jin H, He Y, Gu Q, Xu X. (2012) Sirtuin 1-mediated cellular metabolic memory of high glucose via the LKB1/AMPK/ROS pathway and therapeutic effects of metformin. *Diabetes*, 61 (1): 217-28.
70. Canto C and Auwerx J. (2012) Targeting sirtuin 1 to improve metabolism: all you need is NAD(+)? *Pharmacol Rev*, 64 (1): 166-87.
71. Saha AK, Xu XJ, Lawson E, Deoliveira R, Brandon AE, Kraegen EW, Ruderman NB. (2010) Downregulation of AMPK accompanies leucine- and glucose-induced increases in protein synthesis and insulin resistance in rat skeletal muscle. *Diabetes*, 59 (10): 2426-34.
72. Saha AK, Xu XJ, Balon TW, Brandon A, Kraegen EW, Ruderman NB. (2011) Insulin resistance due to nutrient excess: is it a consequence of AMPK downregulation? *Cell Cycle*, 10 (20): 3447-51.

73. Rodgers JT, Lerin C, Haas W, Gygi SP, Spiegelman BM, Puigserver P. (2005) Nutrient control of glucose homeostasis through a complex of PGC-1 α and SIRT1. *Nature*, 434 (7029): 113-8.
74. Houtkooper RH, Pirinen E, Auwerx J. (2012) Sirtuins as regulators of metabolism and healthspan. *Nat Rev Mol Cell Biol*, 13 (4): 225-38.
75. Brownlee M. (2001) Biochemistry and molecular cell biology of diabetic complications. *Nature*, 414 (6865): 813-20.
76. Leopold JA, Zhang YY, Scribner AW, Stanton RC, Loscalzo J. (2003) Glucose-6-phosphate dehydrogenase overexpression decreases endothelial cell oxidant stress and increases bioavailable nitric oxide. *Arterioscler Thromb Vasc Biol*, 23 (3): 411-7.
77. Zhang Z, Yang Z, Zhu B, Hu J, Liew CW, Zhang Y, Leopold JA, Handy DE, Loscalzo J, Stanton RC. (2012) Increasing glucose 6-phosphate dehydrogenase activity restores redox balance in vascular endothelial cells exposed to high glucose. *PLoS One*, 7 (11): e49128.
78. Ramasamy R, Yan SF, Schmidt AM. (2011) Receptor for AGE (RAGE): signaling mechanisms in the pathogenesis of diabetes and its complications. *Ann N Y Acad Sci*, 1243: 88-102.
79. Menini S, Amadio L, Oddi G, Ricci C, Pesce C, Pugliese F, Giorgio M, Migliaccio E, Pelicci P, Iacobini C, Pugliese G. (2006) Deletion of p66Shc longevity gene protects against experimental diabetic glomerulopathy by preventing diabetes-induced oxidative stress. *Diabetes*, 55 (6): 1642-50.
80. Camici GG, Schiavoni M, Francia P, Bachschmid M, Martin-Padura I, Hersberger M, Tanner FC, Pelicci P, Volpe M, Anversa P, Luscher TF, Cosentino F. (2007) Genetic deletion of p66(Shc) adaptor protein prevents hyperglycemia-induced endothelial dysfunction and oxidative stress. *Proc Natl Acad Sci U S A*, 104 (12): 5217-22.
81. Giorgio M, Migliaccio E, Orsini F, Paolucci D, Moroni M, Contursi C, Pelliccia G, Luzi L, Minucci S, Marcaccio M, Pinton P, Rizzuto R, Bernardi P, Paolucci F, Pelicci PG. (2005) Electron transfer between cytochrome c and p66Shc generates reactive oxygen species that trigger mitochondrial apoptosis. *Cell*, 122 (2): 221-33.
82. Kumar S, Kim YR, Vikram A, Naqvi A, Li Q, Kassar M, Kumar V, Bachschmid MM, Jacobs JS, Kumar A, Irani K. (2017) Sirtuin1-regulated

- lysine acetylation of p66Shc governs diabetes-induced vascular oxidative stress and endothelial dysfunction. *Proc Natl Acad Sci U S A*, 114 (7): 1714-1719.
83. Nishikawa T, Edelstein D, Du XL, Yamagishi S, Matsumura T, Kaneda Y, Yorek MA, Beebe D, Oates PJ, Hammes HP, Giardino I, Brownlee M. (2000) Normalizing mitochondrial superoxide production blocks three pathways of hyperglycaemic damage. *Nature*, 404 (6779): 787-90.
 84. Nishikawa T, Edelstein D, Brownlee M. (2000) The missing link: a single unifying mechanism for diabetic complications. *Kidney Int Suppl*, 77: S26-30.
 85. Turrens JF. (2003) Mitochondrial formation of reactive oxygen species. *J Physiol*, 552 (Pt 2): 335-44.
 86. Rus DA, Sastre J, Vina J, Pallardo FV. (2007) Induction of mitochondrial xanthine oxidase activity during apoptosis in the rat mammary gland. *Front Biosci*, 12: 1184-9.
 87. Murphy MP. (2009) How mitochondria produce reactive oxygen species. *Biochem J*, 417 (1): 1-13.
 88. Kluge MA, Fetterman JL, Vita JA. (2013) Mitochondria and endothelial function. *Circ Res*, 112 (8): 1171-88.
 89. Dzbek J and Korzeniewski B. (2008) Control over the contribution of the mitochondrial membrane potential ($\Delta\Psi$) and proton gradient (ΔpH) to the protonmotive force (Δp). In silico studies. *J Biol Chem*, 283 (48): 33232-9.
 90. Kunz W, Gellerich FN, Schild L, Schonfeld P. (1988) Kinetic limitations in the overall reaction of mitochondrial oxidative phosphorylation accounting for flux-dependent changes in the apparent $\Delta G_{\text{exP}}/\Delta\mu_{\text{H}^+}$ ratio. *FEBS Lett*, 233 (1): 17-21.
 91. Mitchell P. (1961) Coupling of phosphorylation to electron and hydrogen transfer by a chemi-osmotic type of mechanism. *Nature*, 191: 144-8.
 92. Treberg JR, Quinlan CL, Brand MD. (2011) Evidence for two sites of superoxide production by mitochondrial NADH-ubiquinone oxidoreductase (complex I). *J Biol Chem*, 286 (31): 27103-10.
 93. Bleier L and Droese S. (2013) Superoxide generation by complex III: from mechanistic rationales to functional consequences. *Biochim Biophys Acta*, 1827 (11-12): 1320-31.

94. Suzuki K, Olah G, Modis K, Coletta C, Kulp G, Gero D, Szoleczky P, Chang T, Zhou Z, Wu L, Wang R, Papapetropoulos A, Szabo C. (2011) Hydrogen sulfide replacement therapy protects the vascular endothelium in hyperglycemia by preserving mitochondrial function. *Proc Natl Acad Sci U S A*, 108 (33): 13829-34.
95. Kadenbach B, Ramzan R, Wen L, Vogt S. (2010) New extension of the Mitchell Theory for oxidative phosphorylation in mitochondria of living organisms. *Biochim Biophys Acta*, 1800 (3): 205-12.
96. Nicholls DG and Ferguson SJ. *Bioenergetics 3*. 3rd ed. Academic Press, San Diego, Calif., 2002: 89-156.
97. Ramzan R, Staniek K, Kadenbach B, Vogt S. (2010) Mitochondrial respiration and membrane potential are regulated by the allosteric ATP-inhibition of cytochrome c oxidase. *Biochim Biophys Acta*, 1797 (9): 1672-80.
98. Ferreira FM, Palmeira CM, Seica R, Moreno AJ, Santos MS. (2003) Diabetes and mitochondrial bioenergetics: alterations with age. *J Biochem Mol Toxicol*, 17 (4): 214-22.
99. Munusamy S, Saba H, Mitchell T, Megyesi JK, Brock RW, Macmillan-Crow LA. (2009) Alteration of renal respiratory Complex-III during experimental type-1 diabetes. *BMC Endocr Disord*, 9: 2.
100. Gero D, Torregrossa R, Perry A, Waters A, Le-Trionnaire S, Whatmore JL, Wood M, Whiteman M. (2016) The novel mitochondria-targeted hydrogen sulfide (H₂S) donors AP123 and AP39 protect against hyperglycemic injury in microvascular endothelial cells in vitro. *Pharmacol Res*, 113 (Pt A): 186-198.
101. Lebovitz RM, Zhang H, Vogel H, Cartwright J, Jr., Dionne L, Lu N, Huang S, Matzuk MM. (1996) Neurodegeneration, myocardial injury, and perinatal death in mitochondrial superoxide dismutase-deficient mice. *Proc Natl Acad Sci U S A*, 93 (18): 9782-7.
102. Nishi H, Koga Y, Koyanagi T, Harada H, Imaizumi T, Toshima H, Sasazuki T, Kimura A. (1995) DNA typing of HLA class II genes in Japanese patients with dilated cardiomyopathy. *J Mol Cell Cardiol*, 27 (10): 2385-92.
103. Nomiya T, Tanaka Y, Piao L, Nagasaka K, Sakai K, Ogihara T, Nakajima K, Watada H, Kawamori R. (2003) The polymorphism of manganese

- superoxide dismutase is associated with diabetic nephropathy in Japanese type 2 diabetic patients. *J Hum Genet*, 48 (3): 138-41.
104. Vincent AM, Russell JW, Sullivan KA, Backus C, Hayes JM, McLean LL, Feldman EL. (2007) SOD2 protects neurons from injury in cell culture and animal models of diabetic neuropathy. *Exp Neurol*, 208 (2): 216-27.
 105. Szabo C, Biser A, Benko R, Bottinger E, Susztak K. (2006) Poly(ADP-ribose) polymerase inhibitors ameliorate nephropathy of type 2 diabetic *Leprdb/db* mice. *Diabetes*, 55 (11): 3004-12.
 106. Hildebrandt TM and Grieshaber MK. (2008) Three enzymatic activities catalyze the oxidation of sulfide to thiosulfate in mammalian and invertebrate mitochondria. *FEBS J*, 275 (13): 3352-61.
 107. Modis K, Coletta C, Erdelyi K, Papapetropoulos A, Szabo C. (2013) Intramitochondrial hydrogen sulfide production by 3-mercaptopyruvate sulfurtransferase maintains mitochondrial electron flow and supports cellular bioenergetics. *FASEB J*, 27 (2): 601-11.
 108. Jain SK, Bull R, Rains JL, Bass PF, Levine SN, Reddy S, McVie R, Bocchini JA. (2010) Low levels of hydrogen sulfide in the blood of diabetes patients and streptozotocin-treated rats causes vascular inflammation? *Antioxid Redox Signal*, 12 (11): 1333-7.
 109. Suzuki K, Sagara M, Aoki C, Tanaka S, Aso Y. (2017) Clinical Implication of Plasma Hydrogen Sulfide Levels in Japanese Patients with Type 2 Diabetes. *Intern Med*, 56 (1): 17-21.
 110. Yu T, Robotham JL, Yoon Y. (2006) Increased production of reactive oxygen species in hyperglycemic conditions requires dynamic change of mitochondrial morphology. *Proc Natl Acad Sci U S A*, 103 (8): 2653-8.
 111. Makino A, Scott BT, Dillmann WH. (2010) Mitochondrial fragmentation and superoxide anion production in coronary endothelial cells from a mouse model of type 1 diabetes. *Diabetologia*, 53 (8): 1783-94.
 112. Shenouda SM, Widlansky ME, Chen K, Xu G, Holbrook M, Tabit CE, Hamburg NM, Frame AA, Caiano TL, Kluge MA, Dues MA, Levit A, Kim B, Hartman ML, Joseph L, Shirihai OS, Vita JA. (2011) Altered mitochondrial dynamics contributes to endothelial dysfunction in diabetes mellitus. *Circulation*, 124 (4): 444-53.

113. Yu T, Jhun BS, Yoon Y. (2011) High-glucose stimulation increases reactive oxygen species production through the calcium and mitogen-activated protein kinase-mediated activation of mitochondrial fission. *Antioxid Redox Signal*, 14 (3): 425-37.
114. Wang W, Wang Y, Long J, Wang J, Haudek SB, Overbeek P, Chang BH, Schumacker PT, Danesh FR. (2012) Mitochondrial fission triggered by hyperglycemia is mediated by ROCK1 activation in podocytes and endothelial cells. *Cell Metab*, 15 (2): 186-200.
115. Larsen NB, Rasmussen M, Rasmussen LJ. (2005) Nuclear and mitochondrial DNA repair: similar pathways? *Mitochondrion*, 5 (2): 89-108.
116. Szczesny B, Brunyanski A, Olah G, Mitra S, Szabo C. (2014) Opposing roles of mitochondrial and nuclear PARP1 in the regulation of mitochondrial and nuclear DNA integrity: implications for the regulation of mitochondrial function. *Nucleic Acids Res*, 42 (21): 13161-73.
117. Santos JM, Tewari S, Goldberg AF, Kowluru RA. (2011) Mitochondrial biogenesis and the development of diabetic retinopathy. *Free Radic Biol Med*, 51 (10): 1849-60.
118. Gero D and Szabo C. (2008) Poly(ADP-ribose) polymerase: a new therapeutic target? *Curr Opin Anaesthesiol*, 21 (2): 111-21.
119. Paul BD and Snyder SH. (2012) H(2)S signalling through protein sulfhydration and beyond. *Nat Rev Mol Cell Biol*, 13 (8): 499-507.
120. Nguyen T, Nioi P, Pickett CB. (2009) The Nrf2-antioxidant response element signaling pathway and its activation by oxidative stress. *J Biol Chem*, 284 (20): 13291-5.
121. Xie L, Gu Y, Wen M, Zhao S, Wang W, Ma Y, Meng G, Han Y, Wang Y, Liu G, Moore PK, Wang X, Wang H, Zhang Z, Yu Y, Ferro A, Huang Z, Ji Y. (2016) Hydrogen Sulfide Induces Keap1 S-sulfhydration and Suppresses Diabetes-Accelerated Atherosclerosis via Nrf2 Activation. *Diabetes*, 65 (10): 3171-84.
122. Modis K, Ju Y, Ahmad A, Untereiner AA, Altaany Z, Wu L, Szabo C, Wang R. (2016) S-Sulfhydration of ATP synthase by hydrogen sulfide stimulates mitochondrial bioenergetics. *Pharmacol Res*, 113 (Pt A): 116-124.

123. Alpert E, Gruzman A, Riahi Y, Blejter R, Aharoni P, Weisinger G, Eckel J, Kaiser N, Sasson S. (2005) Delayed autoregulation of glucose transport in vascular endothelial cells. *Diabetologia*, 48 (4): 752-5.
124. Cohen G, Riahi Y, Alpert E, Gruzman A, Sasson S. (2007) The roles of hyperglycaemia and oxidative stress in the rise and collapse of the natural protective mechanism against vascular endothelial cell dysfunction in diabetes. *Arch Physiol Biochem*, 113 (4-5): 259-67.
125. Du X, Matsumura T, Edelstein D, Rossetti L, Zsengeller Z, Szabo C, Brownlee M. (2003) Inhibition of GAPDH activity by poly(ADP-ribose) polymerase activates three major pathways of hyperglycemic damage in endothelial cells. *J Clin Invest*, 112 (7): 1049-57.
126. Jarajapu YP and Grant MB. (2010) The promise of cell-based therapies for diabetic complications: challenges and solutions. *Circ Res*, 106 (5): 854-69.
127. Tepper OM, Galiano RD, Capla JM, Kalka C, Gagne PJ, Jacobowitz GR, Levine JP, Gurtner GC. (2002) Human endothelial progenitor cells from type II diabetics exhibit impaired proliferation, adhesion, and incorporation into vascular structures. *Circulation*, 106 (22): 2781-6.
128. Furchgott RF and Martin W. (1985) Interactions of endothelial cells and smooth muscle cells of arteries. *Chest*, 88 (4 Suppl): 210S-213S.
129. Ignarro LJ, Buga GM, Wood KS, Byrns RE, Chaudhuri G. (1987) Endothelium-derived relaxing factor produced and released from artery and vein is nitric oxide. *Proc Natl Acad Sci U S A*, 84 (24): 9265-9.
130. Ignarro LJ, Byrns RE, Buga GM, Wood KS. (1987) Endothelium-derived relaxing factor from pulmonary artery and vein possesses pharmacologic and chemical properties identical to those of nitric oxide radical. *Circ Res*, 61 (6): 866-79.
131. Furchgott RF and Vanhoutte PM. (1989) Endothelium-derived relaxing and contracting factors. *FASEB J*, 3 (9): 2007-18.
132. Beller CJ, Radovits T, Kosse J, Gero D, Szabo C, Szabo G. (2006) Activation of the peroxynitrite-poly(adenosine diphosphate-ribose) polymerase pathway during neointima proliferation: a new target to prevent restenosis after endarterectomy. *J Vasc Surg*, 43 (4): 824-30.

133. Gero D and Szabo C. (2006) Role of the peroxynitrite-poly (ADP-ribose) polymerase pathway in the pathogenesis of liver injury. *Curr Pharm Des*, 12 (23): 2903-10.
134. Radovits T, Seres L, Gero D, Lin LN, Beller CJ, Chen SH, Zotkina J, Berger I, Groves JT, Szabo C, Szabo G. (2007) The peroxynitrite decomposition catalyst FP15 improves ageing-associated cardiac and vascular dysfunction. *Mech Ageing Dev*, 128 (2): 173-81.
135. Alp NJ and Channon KM. (2004) Regulation of endothelial nitric oxide synthase by tetrahydrobiopterin in vascular disease. *Arterioscler Thromb Vasc Biol*, 24 (3): 413-20.
136. Pieper GM. (1997) Acute amelioration of diabetic endothelial dysfunction with a derivative of the nitric oxide synthase cofactor, tetrahydrobiopterin. *J Cardiovasc Pharmacol*, 29 (1): 8-15.
137. Pannirselvam M, Verma S, Anderson TJ, Triggle CR. (2002) Cellular basis of endothelial dysfunction in small mesenteric arteries from spontaneously diabetic (db/db -/-) mice: role of decreased tetrahydrobiopterin bioavailability. *Br J Pharmacol*, 136 (2): 255-63.
138. Hosoki R, Matsuki N, Kimura H. (1997) The possible role of hydrogen sulfide as an endogenous smooth muscle relaxant in synergy with nitric oxide. *Biochem Biophys Res Commun*, 237 (3): 527-31.
139. Coletta C, Papapetropoulos A, Erdelyi K, Olah G, Modis K, Panopoulos P, Asimakopoulou A, Gero D, Sharina I, Martin E, Szabo C. (2012) Hydrogen sulfide and nitric oxide are mutually dependent in the regulation of angiogenesis and endothelium-dependent vasorelaxation. *Proc Natl Acad Sci U S A*, 109 (23): 9161-6.
140. Szabo C. (2017) Hydrogen sulfide, an enhancer of vascular nitric oxide signaling: mechanisms and implications. *Am J Physiol Cell Physiol*, 312 (1): C3-C15.
141. Sharma K. (2015) Mitochondrial hormesis and diabetic complications. *Diabetes*, 64 (3): 663-72.
142. Lenaz G. (2001) The mitochondrial production of reactive oxygen species: mechanisms and implications in human pathology. *IUBMB Life*, 52 (3-5): 159-64.

143. Gero D, Szabo C, Whiteman M. (2015) Identification of potential drug targets for diabetic vascular complications by a forward chemical genomics approach. *Diabetic Medicine*, 32 (Suppl. 1): 73.
144. Thurnhofer S and Vetter W. (2007) Synthesis of (S)-(+)-enantiomers of food-relevant (n-5)-monoenoic acid saturated anteiso-fatty acids by a Wittig reaction. *Tetrahedron*, (63): 1140-1145.
145. Le Trionnaire S, Perry A, Szczesny B, Szabo C, Winyard PG, Whatmore JL, Wood ME, Whiteman M. (2014) The synthesis and functional evaluation of a mitochondria-targeted hydrogen sulfide donor, (10-oxo-10-(4-(3-thioxo-3H-1,2-dithiol-5-yl)phenoxy)decyl)triphenylphosphonium bromide (AP39). *Med. Chem. Commun.*, (5): 728-736.
146. Gero D, Modis K, Nagy N, Szoleczky P, Toth ZD, Dorman G, Szabo C. (2007) Oxidant-induced cardiomyocyte injury: identification of the cytoprotective effect of a dopamine 1 receptor agonist using a cell-based high-throughput assay. *Int J Mol Med*, 20 (5): 749-61.
147. Gero D, Szoleczky P, Modis K, Pribis JP, Al-Abed Y, Yang H, Chevan S, Billiar TR, Tracey KJ, Szabo C. (2013) Identification of pharmacological modulators of HMGB1-induced inflammatory response by cell-based screening. *PLoS One*, 8 (6): e65994.
148. Gero D and Szabo C. (2015) Nicotinamide adenine dinucleotide (NAD⁺) salvage plays critical role in bioenergetic recovery of posthypoxic cardiomyocytes. *Br J Pharmacol*.
149. Keij JF, Bell-Prince C, Steinkamp JA. (2000) Staining of mitochondrial membranes with 10-nonyl acridine orange, MitoFluor Green, and MitoTracker Green is affected by mitochondrial membrane potential altering drugs. *Cytometry*, 39 (3): 203-10.
150. Gero D, Szoleczky P, Chatzianastasiou A, Papapetropoulos A, Szabo C. (2014) Modulation of poly(ADP-ribose) polymerase-1 (PARP-1)-mediated oxidative cell injury by ring finger protein 146 (RNF146) in cardiac myocytes. *Mol Med*, 20: 313-28.
151. Modis K, Gero D, Erdelyi K, Szoleczky P, DeWitt D, Szabo C. (2012) Cellular bioenergetics is regulated by PARP1 under resting conditions and during oxidative stress. *Biochem Pharmacol*, 83 (5): 633-43.
152. Supino R. (1995) MTT assays. *Methods Mol Biol*, 43: 137-49.

153. Christ M, Bauersachs J, Liebetrau C, Heck M, Gunther A, Wehling M. (2002) Glucose increases endothelial-dependent superoxide formation in coronary arteries by NAD(P)H oxidase activation: attenuation by the 3-hydroxy-3-methylglutaryl coenzyme A reductase inhibitor atorvastatin. *Diabetes*, 51 (8): 2648-52.
154. Haas MJ, Horani MH, Parseghian SA, Mooradian AD. (2006) Statins prevent dextrose-induced endothelial barrier dysfunction, possibly through inhibition of superoxide formation. *Diabetes*, 55 (2): 474-9.
155. Kwon JW and Armbrust KL. (2004) Hydrolysis and photolysis of paroxetine, a selective serotonin reuptake inhibitor, in aqueous solutions. *Environ Toxicol Chem*, 23 (6): 1394-9.
156. Amat R, Solanes G, Giralt M, Villarroya F. (2007) SIRT1 is involved in glucocorticoid-mediated control of uncoupling protein-3 gene transcription. *J Biol Chem*, 282 (47): 34066-76.
157. Hurtaud C, Gelly C, Chen Z, Levi-Meyrueis C, Bouillaud F. (2007) Glutamine stimulates translation of uncoupling protein 2mRNA. *Cell Mol Life Sci*, 64 (14): 1853-60.
158. Nau PN, Van Natta T, Ralphe JC, Teneyck CJ, Bedell KA, Caldarone CA, Segar JL, Scholz TD. (2002) Metabolic adaptation of the fetal and postnatal ovine heart: regulatory role of hypoxia-inducible factors and nuclear respiratory factor-1. *Pediatr Res*, 52 (2): 269-78.
159. Marone JR, Falduto MT, Essig DA, Hickson RC. (1994) Effects of glucocorticoids and endurance training on cytochrome oxidase expression in skeletal muscle. *J Appl Physiol* (1985), 77 (4): 1685-90.
160. Rachamim N, Latter H, Malinin N, Asher C, Wald H, Garty H. (1995) Dexamethasone enhances expression of mitochondrial oxidative phosphorylation genes in rat distal colon. *Am J Physiol*, 269 (5 Pt 1): C1305-10.
161. Weber K, Bruck P, Mikes Z, Kupper JH, Klingenspor M, Wiesner RJ. (2002) Glucocorticoid hormone stimulates mitochondrial biogenesis specifically in skeletal muscle. *Endocrinology*, 143 (1): 177-84.
162. Scheller K and Sekeris CE. (2003) The effects of steroid hormones on the transcription of genes encoding enzymes of oxidative phosphorylation. *Exp Physiol*, 88 (1): 129-40.

163. Psarra AM and Sekeris CE. (2011) Glucocorticoids induce mitochondrial gene transcription in HepG2 cells: role of the mitochondrial glucocorticoid receptor. *Biochim Biophys Acta*, 1813 (10): 1814-21.
164. Minchenko AG. (1979) [Role of glucocorticoids in the mitochondrial DNA replication]. *Probl Endokrinol (Mosk)*, 25 (5): 52-6.
165. Lee SR, Kim HK, Song IS, Youm J, Dizon LA, Jeong SH, Ko TH, Heo HJ, Ko KS, Rhee BD, Kim N, Han J. (2013) Glucocorticoids and their receptors: insights into specific roles in mitochondria. *Prog Biophys Mol Biol*, 112 (1-2): 44-54.
166. Reinecke F, Smeitink JA, van der Westhuizen FH. (2009) OXPHOS gene expression and control in mitochondrial disorders. *Biochim Biophys Acta*, 1792 (12): 1113-21.
167. Stankov MV, Lucke T, Das AM, Schmidt RE, Behrens GM. (2010) Mitochondrial DNA depletion and respiratory chain activity in primary human subcutaneous adipocytes treated with nucleoside analogue reverse transcriptase inhibitors. *Antimicrob Agents Chemother*, 54 (1): 280-7.
168. Li K, Li Y, Shelton JM, Richardson JA, Spencer E, Chen ZJ, Wang X, Williams RS. (2000) Cytochrome c deficiency causes embryonic lethality and attenuates stress-induced apoptosis. *Cell*, 101 (4): 389-99.
169. Vempati UD, Han X, Moraes CT. (2009) Lack of cytochrome c in mouse fibroblasts disrupts assembly/stability of respiratory complexes I and IV. *J Biol Chem*, 284 (7): 4383-91.
170. Zhang J, Khvorostov I, Hong JS, Oktay Y, Vergnes L, Nuebel E, Wahjudi PN, Setoguchi K, Wang G, Do A, Jung HJ, McCaffery JM, Kurland IJ, Reue K, Lee WN, Koehler CM, Teitell MA. (2011) UCP2 regulates energy metabolism and differentiation potential of human pluripotent stem cells. *EMBO J*, 30 (24): 4860-73.
171. Ohkouchi S, Block GJ, Katsha AM, Kanehira M, Ebina M, Kikuchi T, Saijo Y, Nukiwa T, Prockop DJ. (2012) Mesenchymal stromal cells protect cancer cells from ROS-induced apoptosis and enhance the Warburg effect by secreting STC1. *Mol Ther*, 20 (2): 417-23.
172. Li L, Whiteman M, Guan YY, Neo KL, Cheng Y, Lee SW, Zhao Y, Baskar R, Tan CH, Moore PK. (2008) Characterization of a novel, water-soluble

- hydrogen sulfide-releasing molecule (GYY4137): new insights into the biology of hydrogen sulfide. *Circulation*, 117 (18): 2351-60.
173. Whiteman M, Li L, Rose P, Tan CH, Parkinson DB, Moore PK. (2010) The effect of hydrogen sulfide donors on lipopolysaccharide-induced formation of inflammatory mediators in macrophages. *Antioxid Redox Signal*, 12 (10): 1147-54.
 174. Whiteman M, Perry A, Zhou Z, Bucci M, Papapetropoulos A, Cirino G, Wood ME. (2015) Phosphinodithioate and Phosphoramidodithioate Hydrogen Sulfide Donors. *Handb Exp Pharmacol*, 230: 337-63.
 175. Murphy MP. (2008) Targeting lipophilic cations to mitochondria. *Biochim Biophys Acta*, 1777 (7-8): 1028-31.
 176. Nicholls P. (1975) Inhibition of cytochrome c oxidase by sulphide. *Biochem Soc Trans*, 3 (2): 316-9.
 177. Beauchamp RO, Jr., Bus JS, Popp JA, Boreiko CJ, Andjelkovich DA. (1984) A critical review of the literature on hydrogen sulfide toxicity. *Crit Rev Toxicol*, 13 (1): 25-97.
 178. Khan AA, Schuler MM, Prior MG, Yong S, Coppock RW, Florence LZ, Lillie LE. (1990) Effects of hydrogen sulfide exposure on lung mitochondrial respiratory chain enzymes in rats. *Toxicol Appl Pharmacol*, 103 (3): 482-90.
 179. Szabo C. (2009) Role of nitrosative stress in the pathogenesis of diabetic vascular dysfunction. *Br J Pharmacol*, 156 (5): 713-27.
 180. World Health Organization. Dept. of Noncommunicable Disease Surveillance. Definition, diagnosis and classification of diabetes mellitus and its complications: report of a WHO consultation. Part 1, Diagnosis and classification of diabetes mellitus. World Health Organization, Geneva, 1999: 1-59.
 181. World Health Organization. and International Diabetes Federation. Definition and diagnosis of diabetes mellitus and intermediate hyperglycaemia: report of a WHO/IDF consultation. World Health Organization, Geneva, 2006: 1-46.
 182. American Diabetes A. (2014) Standards of medical care in diabetes--2014. *Diabetes Care*, 37 Suppl 1: S14-80.
 183. Skyler JS. (2004) Effects of Glycemic Control on Diabetes Complications and on the Prevention of Diabetes. *Clinical Diabetes*, 22 (4): 162-166.

184. Action to Control Cardiovascular Risk in Diabetes Study Group, Gerstein HC, Miller ME, Byington RP, Goff DC, Jr., Bigger JT, Buse JB, Cushman WC, Genuth S, Ismail-Beigi F, Grimm RH, Jr., Probstfield JL, Simons-Morton DG, Friedewald WT. (2008) Effects of intensive glucose lowering in type 2 diabetes. *N Engl J Med*, 358 (24): 2545-59.
185. Brown SH and Abdelhafiz AH. (2009) Trials review: cardiovascular outcome with intensive glycemetic control and implications for patients with type 2 diabetes. *Postgrad Med*, 121 (5): 31-41.
186. McAlpine RR, Morris AD, Emslie-Smith A, James P, Evans JM. (2005) The annual incidence of diabetic complications in a population of patients with Type 1 and Type 2 diabetes. *Diabet Med*, 22 (3): 348-52.
187. Ceriello A and Testa R. (2009) Antioxidant anti-inflammatory treatment in type 2 diabetes. *Diabetes Care*, 32 Suppl 2: S232-6.
188. Wu Y, Tang L, Chen B. (2014) Oxidative stress: implications for the development of diabetic retinopathy and antioxidant therapeutic perspectives. *Oxid Med Cell Longev*, 2014: 752387.
189. Lu J, Xie G, Jia W, Jia W. (2013) Metabolomics in human type 2 diabetes research. *Front Med*, 7 (1): 4-13.
190. Lenaz G, Baracca A, Barbero G, Bergamini C, Dalmonte ME, Del Sole M, Faccioli M, Falasca A, Fato R, Genova ML, Sgarbi G, Solaini G. (2010) Mitochondrial respiratory chain super-complex I-III in physiology and pathology. *Biochim Biophys Acta*, 1797 (6-7): 633-40.
191. Brand MD. (2005) The efficiency and plasticity of mitochondrial energy transduction. *Biochem Soc Trans*, 33 (Pt 5): 897-904.
192. Rabilloud T, Heller M, Rigobello MP, Bindoli A, Aebersold R, Lunardi J. (2001) The mitochondrial antioxidant defence system and its response to oxidative stress. *Proteomics*, 1 (9): 1105-10.
193. Celik VK, Sahin ZD, Sari I, Bakir S. (2012) Comparison of oxidant/antioxidant, detoxification systems in various tissue homogenates and mitochondria of rats with diabetes induced by streptozocin. *Exp Diabetes Res*, 2012: 386831.
194. Garcia Soriano F, Virag L, Jagtap P, Szabo E, Mabley JG, Liaudet L, Marton A, Hoyt DG, Murthy KG, Salzman AL, Southan GJ, Szabo C. (2001) Diabetic

- endothelial dysfunction: the role of poly(ADP-ribose) polymerase activation. *Nat Med*, 7 (1): 108-13.
195. Madsen-Bouterse SA, Zhong Q, Mohammad G, Ho YS, Kowluru RA. (2010) Oxidative damage of mitochondrial DNA in diabetes and its protection by manganese superoxide dismutase. *Free Radic Res*, 44 (3): 313-21.
 196. Johansen JS, Harris AK, Rychly DJ, Ergul A. (2005) Oxidative stress and the use of antioxidants in diabetes: linking basic science to clinical practice. *Cardiovasc Diabetol*, 4: 5.
 197. Bowry VW, Ingold KU, Stocker R. (1992) Vitamin E in human low-density lipoprotein. When and how this antioxidant becomes a pro-oxidant. *Biochem J*, 288 (Pt 2): 341-4.
 198. Hunt JV, Bottoms MA, Mitchinson MJ. (1992) Ascorbic acid oxidation: a potential cause of the elevated severity of atherosclerosis in diabetes mellitus? *FEBS Lett*, 311 (2): 161-4.
 199. Young IS, Tate S, Lightbody JH, McMaster D, Trimble ER. (1995) The effects of desferrioxamine and ascorbate on oxidative stress in the streptozotocin diabetic rat. *Free Radic Biol Med*, 18 (5): 833-40.
 200. Tucker S, Ahl M, Bush A, Westaway D, Huang X, Rogers JT. (2005) Pilot study of the reducing effect on amyloidosis in vivo by three FDA pre-approved drugs via the Alzheimer's APP 5' untranslated region. *Curr Alzheimer Res*, 2 (2): 249-54.
 201. Kuhad A and Chopra K. (2008) Effect of sesamol on diabetes-associated cognitive decline in rats. *Exp Brain Res*, 185 (3): 411-20.
 202. Meng B, Li J, Cao H. (2012) Antioxidant and antiinflammatory activities of curcumin on diabetes mellitus and its complications. *Curr Pharm Des*, 19 (11): 2101-13.
 203. Hammes HP, Du X, Edelstein D, Taguchi T, Matsumura T, Ju Q, Lin J, Bierhaus A, Nawroth P, Hannak D, Neumaier M, Bergfeld R, Giardino I, Brownlee M. (2003) Benfotiamine blocks three major pathways of hyperglycemic damage and prevents experimental diabetic retinopathy. *Nat Med*, 9 (3): 294-9.
 204. Dorenkamp M, Riad A, Stiehl S, Spillmann F, Westermann D, Du J, Pauschinger M, Noutsias M, Adams V, Schultheiss HP, Tschope C. (2005) Protection against oxidative stress in diabetic rats: role of angiotensin AT(1)

- receptor and beta 1-adrenoceptor antagonism. *Eur J Pharmacol*, 520 (1-3): 179-87.
205. Tawfik HE, El-Remessy AB, Matragoon S, Ma G, Caldwell RB, Caldwell RW. (2006) Simvastatin improves diabetes-induced coronary endothelial dysfunction. *J Pharmacol Exp Ther*, 319 (1): 386-95.
 206. Vecchione C, Aretini A, Marino G, Bettarini U, Poulet R, Maffei A, Sbroglio M, Pastore L, Gentile MT, Notte A, Iorio L, Hirsch E, Tarone G, Lembo G. (2006) Selective Rac-1 inhibition protects from diabetes-induced vascular injury. *Circ Res*, 98 (2): 218-25.
 207. Hwang J, Kleinhenz DJ, Rupnow HL, Campbell AG, Thule PM, Sutliff RL, Hart CM. (2007) The PPARgamma ligand, rosiglitazone, reduces vascular oxidative stress and NADPH oxidase expression in diabetic mice. *Vascul Pharmacol*, 46 (6): 456-62.
 208. Piconi L, Corgnali M, Da Ros R, Assaloni R, Piliego T, Ceriello A. (2008) The protective effect of rosuvastatin in human umbilical endothelial cells exposed to constant or intermittent high glucose. *J Diabetes Complications*, 22 (1): 38-45.
 209. Van Linthout S, Spillmann F, Lorenz M, Meloni M, Jacobs F, Egorova M, Stangl V, De Geest B, Schultheiss HP, Tschöpe C. (2009) Vascular-protective effects of high-density lipoprotein include the downregulation of the angiotensin II type 1 receptor. *Hypertension*, 53 (4): 682-7.
 210. Tang WH, Martin KA, Hwa J. (2012) Aldose reductase, oxidative stress, and diabetic mellitus. *Front Pharmacol*, 3: 87.
 211. Grewal AS, Bhardwaj S, Pandita D, Lather V, Sekhon BS. (2016) Updates on Aldose Reductase Inhibitors for Management of Diabetic Complications and Non-diabetic Diseases. *Mini Rev Med Chem*, 16 (2): 120-62.
 212. Vincent AM, Olzmann JA, Brownlee M, Sivitz WI, Russell JW. (2004) Uncoupling proteins prevent glucose-induced neuronal oxidative stress and programmed cell death. *Diabetes*, 53 (3): 726-34.
 213. Schlotterer A, Kukudov G, Bozorgmehr F, Hutter H, Du X, Oikonomou D, Ibrahim Y, Pfisterer F, Rabbani N, Thornalley P, Sayed A, Fleming T, Humpert P, Schwenger V, Zeier M, Hamann A, Stern D, Brownlee M, Bierhaus A, Nawroth P, Morcos M. (2009) *C. elegans* as model for the study of high glucose- mediated life span reduction. *Diabetes*, 58 (11): 2450-6.

214. Frantz MC and Wipf P. (2010) Mitochondria as a target in treatment. *Environ Mol Mutagen*, 51 (5): 462-75.
215. Kagan VE, Wipf P, Stoyanovsky D, Greenberger JS, Borisenko G, Belikova NA, Yanamala N, Samhan Arias AK, Tungekar MA, Jiang J, Tyurina YY, Ji J, Klein-Seetharaman J, Pitt BR, Shvedova AA, Bayir H. (2009) Mitochondrial targeting of electron scavenging antioxidants: Regulation of selective oxidation vs random chain reactions. *Adv Drug Deliv Rev*, 61 (14): 1375-85.
216. Apostolova N, Rocha M, Rovira-Llopis S, Banuls C, Falcon R, Castello R, Hernandez-Mijares A, Victor VM. (2014) Mitochondria-targeted antioxidants as a therapeutic strategy for protecting endothelium in cardiovascular diseases. *Curr Med Chem*, 21 (25): 2989-3006.
217. Chacko BK, Reily C, Srivastava A, Johnson MS, Ye Y, Ulasova E, Agarwal A, Zinn KR, Murphy MP, Kalyanaraman B, Darley-Usmar V. (2010) Prevention of diabetic nephropathy in Ins2(+/-)(Akita) mice by the mitochondria-targeted therapy MitoQ. *Biochem J*, 432 (1): 9-19.
218. Shahzad K, Bock F, Dong W, Wang H, Kopf S, Kohli S, Al-Dabet MM, Ranjan S, Wolter J, Wacker C, Biemann R, Stoyanov S, Reymann K, Soderkvist P, Gross O, Schwenger V, Pahernik S, Nawroth PP, Grone HJ, Madhusudhan T, Isermann B. (2015) Nlrp3-inflammasome activation in non-myeloid-derived cells aggravates diabetic nephropathy. *Kidney Int*, 87 (1): 74-84.
219. Qi H, Casalena G, Shi S, Yu L, Ebefors K, Sun Y, Zhang W, D'Agati V, Schlondorff D, Haraldsson B, Bottinger E, Daehn I. (2017) Glomerular Endothelial Mitochondrial Dysfunction Is Essential and Characteristic of Diabetic Kidney Disease Susceptibility. *Diabetes*, 66 (3): 763-778.
220. Kanwar M, Chan PS, Kern TS, Kowluru RA. (2007) Oxidative damage in the retinal mitochondria of diabetic mice: possible protection by superoxide dismutase. *Invest Ophthalmol Vis Sci*, 48 (8): 3805-11.
221. Wagner BK, Kitami T, Gilbert TJ, Peck D, Ramanathan A, Schreiber SL, Golub TR, Mootha VK. (2008) Large-scale chemical dissection of mitochondrial function. *Nat Biotechnol*, 26 (3): 343-51.
222. Orr AL, Ashok D, Sarantos MR, Shi T, Hughes RE, Brand MD. (2013) Inhibitors of ROS production by the ubiquinone-binding site of mitochondrial

- complex I identified by chemical screening. *Free Radic Biol Med*, 65: 1047-59.
223. Orr AL, Vargas L, Turk CN, Baaten JE, Matzen JT, Dardov VJ, Attle SJ, Li J, Quackenbush DC, Goncalves RL, Perevoshchikova IV, Petrassi HM, Meeusen SL, Ainscow EK, Brand MD. (2015) Suppressors of superoxide production from mitochondrial complex III. *Nat Chem Biol*, 11 (11): 834-6.
224. Jung HJ, Shim JS, Lee J, Song YM, Park KC, Choi SH, Kim ND, Yoon JH, Mungai PT, Schumacker PT, Kwon HJ. (2010) Terpestacin inhibits tumor angiogenesis by targeting UQCRB of mitochondrial complex III and suppressing hypoxia-induced reactive oxygen species production and cellular oxygen sensing. *J Biol Chem*, 285 (15): 11584-95.
225. Si YF, Wang J, Guan J, Zhou L, Sheng Y, Zhao J. (2013) Treatment with hydrogen sulfide alleviates streptozotocin-induced diabetic retinopathy in rats. *Br J Pharmacol*, 169 (3): 619-31.
226. Safar MM and Abdelsalam RM. (2015) H₂S donors attenuate diabetic nephropathy in rats: Modulation of oxidant status and polyol pathway. *Pharmacol Rep*, 67 (1): 17-23.
227. Serbedzija G, Phil M, Grau D. (2005) Innovative Strategies for Drug Repurposing. *Drug Discovery & Development*, 8 (5).
228. Thayer AM. (2012) Drug Repurposing. *Chemical & Engineering News*, 90 (40): 15-25.
229. Tari L, Vo N, Liang S, Patel J, Baral C, Cai J. (2013) Identifying novel drug indications through automated reasoning. *PLoS One*, 7 (7): e40946.
230. Ekins S and Williams AJ. (2011) Finding promiscuous old drugs for new uses. *Pharm Res*, 28 (8): 1785-91.
231. Muthyala R. (2011) Orphan/rare drug discovery through drug repositioning. *Drug Discovery Today: Therapeutic Strategies*, 8 (3-4): 71-76.
232. Xu K and Cote TR. (2011) Database identifies FDA-approved drugs with potential to be repurposed for treatment of orphan diseases. *Brief Bioinform*, 12 (4): 341-5.
233. Evensen L, Micklem DR, Link W, Lorens JB. (2010) A novel imaging-based high-throughput screening approach to anti-angiogenic drug discovery. *Cytometry A*, 77 (1): 41-51.

234. Hada K, Suda A, Asoh K, Tsukuda T, Hasegawa M, Sato Y, Ogawa K, Kuramoto S, Aoki Y, Shimma N, Ishikawa T, Koyano H. (2012) Angiogenesis inhibitors identified by cell-based high-throughput screening: synthesis, structure-activity relationships and biological evaluation of 3-[(E)-styryl]benzamides that specifically inhibit endothelial cell proliferation. *Bioorg Med Chem*, 20 (4): 1442-60.
235. Degterev A, Huang Z, Boyce M, Li Y, Jagtap P, Mizushima N, Cuny GD, Mitchison TJ, Moskowitz MA, Yuan J. (2005) Chemical inhibitor of nonapoptotic cell death with therapeutic potential for ischemic brain injury. *Nat Chem Biol*, 1 (2): 112-9.
236. Xu Y, Shi Y, Ding S. (2008) A chemical approach to stem-cell biology and regenerative medicine. *Nature*, 453 (7193): 338-44.
237. Modis K, Gero D, Nagy N, Szoleczky P, Toth ZD, Szabo C. (2009) Cytoprotective effects of adenosine and inosine in an in vitro model of acute tubular necrosis. *Br J Pharmacol*, 158 (6): 1565-78.
238. Zhang B, Au Q, Yoon IS, Tremblay MH, Yip G, Zhou Y, Barber JR, Ng SC. (2009) Identification of small-molecule HSF1 amplifiers by high content screening in protection of cells from stress induced injury. *Biochem Biophys Res Commun*, 390 (3): 925-30.
239. An WF and Tolliday N. (2010) Cell-based assays for high-throughput screening. *Mol Biotechnol*, 45 (2): 180-6.
240. Pieper AA, Xie S, Capota E, Estill SJ, Zhong J, Long JM, Becker GL, Huntington P, Goldman SE, Shen CH, Capota M, Britt JK, Kotti T, Ure K, Brat DJ, Williams NS, MacMillan KS, Naidoo J, Melito L, Hsieh J, De Brabander J, Ready JM, McKnight SL. (2010) Discovery of a proneurogenic, neuroprotective chemical. *Cell*, 142 (1): 39-51.
241. Guo S, Olm-Shipman A, Walters A, Urciuoli WR, Devito S, Nadtochiy SM, Wojtovich AP, Brookes PS. (2012) A cell-based phenotypic assay to identify cardioprotective agents. *Circ Res*, 110 (7): 948-57.
242. Szoleczky P, Modis K, Nagy N, Dori Toth Z, DeWitt D, Szabo C, Gero D. (2012) Identification of agents that reduce renal hypoxia-reoxygenation injury using cell-based screening: purine nucleosides are alternative energy sources in LLC-PK1 cells during hypoxia. *Arch Biochem Biophys*, 517 (1): 53-70.

243. Magnussen I, Tonder K, Engbaek F. (1982) Paroxetine, a Potent Selective Long-Acting Inhibitor of Synaptosomal 5-HT Uptake in Mice. *Journal of Neural Transmission*, 55: 217-226.
244. Preskorn S. (1994) Targeted pharmacotherapy in depression management: comparative pharmacokinetics of fluoxetine, paroxetine and sertraline. *Int Clin Psychopharmacol*, 9 Suppl 3: 13-9.
245. Preskorn SH. Basic Neuropharmacology of SSRIs, In: Preskorn SH (editors.), *Clinical Pharmacology of SSRIs*. Professional Communications, Inc., 1996: 1-255.
246. Burke MJ and Preskorn HS. Therapeutic drug monitoring of antidepressants, In: Preskorn HS, Feighner JP, Stanga CY, Ross R (editors.), *Antidepressants: past, present, and future*. Springer Verlag Berlin, New York, 2004: 88-114.
247. Velez LI, Shepherd G, Roth BA, Benitez FL. (2004) Serotonin syndrome with elevated paroxetine concentrations. *Ann Pharmacother*, 38 (2): 269-72.
248. Gupta AK, Verma P, Praharaj SK, Roy D, Singh A. (2005) Paroxetine overdose. *Indian J Psychiatry*, 47 (3): 167-8.
249. Sindrup SH, Gram LF, Broesen K, Eshoj O, Mogensen EF. (1990) The selective serotonin reuptake inhibitor paroxetine is effective in the treatment of diabetic neuropathy symptoms. *Pain*, 42 (2): 135-44.
250. Sauer WH, Berlin JA, Kimmel SE. (2003) Effect of antidepressants and their relative affinity for the serotonin transporter on the risk of myocardial infarction. *Circulation*, 108 (1): 32-6.
251. Beracochea D, Deslandes A, Jaffard R. (1994) [Comparison of the effects of tianeptine and paroxetine on amnesic deficits induced by prolonged alcohol drinking in mice]. *Encephale*, 20 (1): 13-6.
252. Duan W, Guo Z, Jiang H, Ladenheim B, Xu X, Cadet JL, Mattson MP. (2004) Paroxetine retards disease onset and progression in Huntingtin mutant mice. *Ann Neurol*, 55 (4): 590-4.
253. Nelson RL, Guo Z, Halagappa VM, Pearson M, Gray AJ, Matsuoka Y, Brown M, Martin B, Iyun T, Maudsley S, Clark RF, Mattson MP. (2007) Prophylactic treatment with paroxetine ameliorates behavioral deficits and retards the development of amyloid and tau pathologies in 3xTgAD mice. *Exp Neurol*, 205 (1): 166-76.

254. Scharf SH, Sterlemann V, Liebl C, Muller MB, Schmidt MV. (2013) Chronic social stress during adolescence: Interplay of paroxetine treatment and ageing. *Neuropharmacology*.
255. Suski JM, Lebiezinska M, Bonora M, Pinton P, Duszynski J, R. WM. Relation Between Mitochondrial Membrane Potential and ROS Formation, In: Palmeira CMaMAJ (editors.), *Mitochondrial Bioenergetics: Methods and Protocols* Springer Science+Business Media, LLC (Humana Press), New York City, 2012: 183-205.
256. Rousset S, Alves-Guerra MC, Mozo J, Miroux B, Cassard-Doulcier AM, Bouillaud F, Ricquier D. (2004) The biology of mitochondrial uncoupling proteins. *Diabetes*, 53 Suppl 1: S130-5.
257. Mailloux RJ, Seifert EL, Bouillaud F, Aguer C, Collins S, Harper ME. (2011) Glutathionylation acts as a control switch for uncoupling proteins UCP2 and UCP3. *J Biol Chem*, 286 (24): 21865-75.
258. Berraondo B, Marti A, Duncan JS, Trayhurn P, Martinez JA. (2000) Up-regulation of muscle UCP2 gene expression by a new beta3-adrenoceptor agonist, trectadrine, in obese (cafeteria) rodents, but down-regulation in lean animals. *Int J Obes Relat Metab Disord*, 24 (2): 156-63.
259. Martin-Oliva D, Aguilar-Quesada R, O'Valle F, Munoz-Gamez JA, Martinez-Romero R, Garcia Del Moral R, Ruiz de Almodovar JM, Villuendas R, Piris MA, Oliver FJ. (2006) Inhibition of poly(ADP-ribose) polymerase modulates tumor-related gene expression, including hypoxia-inducible factor-1 activation, during skin carcinogenesis. *Cancer Res*, 66 (11): 5744-56.
260. Chan SH, Wu CA, Wu KL, Ho YH, Chang AY, Chan JY. (2009) Transcriptional upregulation of mitochondrial uncoupling protein 2 protects against oxidative stress-associated neurogenic hypertension. *Circ Res*, 105 (9): 886-96.
261. Chen X, Wang K, Chen J, Guo J, Yin Y, Cai X, Guo X, Wang G, Yang R, Zhu L, Zhang Y, Wang J, Xiang Y, Weng C, Zen K, Zhang J, Zhang CY. (2009) In vitro evidence suggests that miR-133a-mediated regulation of uncoupling protein 2 (UCP2) is an indispensable step in myogenic differentiation. *J Biol Chem*, 284 (8): 5362-9.

262. Chen XL, Tang WX, Tang XH, Qin W, Gong M. (2014) Downregulation of uncoupling protein-2 by genipin exacerbates diabetes-induced kidney proximal tubular cells apoptosis. *Ren Fail*, 36 (8): 1298-303.
263. Pecqueur C, Alves-Guerra MC, Gelly C, Levi-Meyrueis C, Couplan E, Collins S, Ricquier D, Bouillaud F, Miroux B. (2001) Uncoupling protein 2, in vivo distribution, induction upon oxidative stress, and evidence for translational regulation. *J Biol Chem*, 276 (12): 8705-12.
264. Chan CB, Saleh MC, Koshkin V, Wheeler MB. (2004) Uncoupling protein 2 and islet function. *Diabetes*, 53 Suppl 1: S136-42.
265. Souza BM, Assmann TS, Kliemann LM, Gross JL, Canani LH, Crispim D. (2011) The role of uncoupling protein 2 (UCP2) on the development of type 2 diabetes mellitus and its chronic complications. *Arq Bras Endocrinol Metabol*, 55 (4): 239-48.
266. Tahir TA, Singh H, Brindle NP. (2014) The RNA binding protein hnRNP-K mediates post-transcriptional regulation of uncoupling protein-2 by angiopoietin-1. *Cell Signal*, 26 (7): 1379-84.
267. Yang S, Roselli F, Patchev AV, Yu S, Almeida OF. (2013) Non-receptor-tyrosine kinases integrate fast glucocorticoid signaling in hippocampal neurons. *J Biol Chem*, 288 (33): 23725-39.
268. Smith LK, Shah RR, Cidlowski JA. (2010) Glucocorticoids modulate microRNA expression and processing during lymphocyte apoptosis. *J Biol Chem*, 285 (47): 36698-708.
269. Hu Z, Shen WJ, Cortez Y, Tang X, Liu LF, Kraemer FB, Azhar S. (2013) Hormonal regulation of microRNA expression in steroid producing cells of the ovary, testis and adrenal gland. *PLoS One*, 8 (10): e78040.
270. Li T, Li H, Li T, Fan J, Zhao RC, Weng X. (2014) MicroRNA expression profile of dexamethasone-induced human bone marrow-derived mesenchymal stem cells during osteogenic differentiation. *J Cell Biochem*, 115 (10): 1683-91.
271. Kamma H, Portman DS, Dreyfuss G. (1995) Cell type-specific expression of hnRNP proteins. *Exp Cell Res*, 221 (1): 187-96.
272. Whiteman M, Le Trionnaire S, Chopra M, Fox B, Whatmore J. (2011) Emerging role of hydrogen sulfide in health and disease: critical appraisal of biomarkers and pharmacological tools. *Clin Sci (Lond)*, 121 (11): 459-88.

273. Whiteman M and Winyard PG. (2011) Hydrogen sulfide and inflammation: the good, the bad, the ugly and the promising. *Expert Rev Clin Pharmacol*, 4 (1): 13-32.
274. Wang R. (2012) Physiological implications of hydrogen sulfide: a whiff exploration that blossomed. *Physiol Rev*, 92 (2): 791-896.
275. Dunn WR, Alexander SP, Ralevic V, Roberts RE. (2016) Effects of hydrogen sulphide in smooth muscle. *Pharmacol Ther*, 158: 101-13.
276. Yusuf M, Kwong Huat BT, Hsu A, Whiteman M, Bhatia M, Moore PK. (2005) Streptozotocin-induced diabetes in the rat is associated with enhanced tissue hydrogen sulfide biosynthesis. *Biochem Biophys Res Commun*, 333 (4): 1146-52.
277. Brancaleone V, Roviezzo F, Vellecco V, De Gruttola L, Bucci M, Cirino G. (2008) Biosynthesis of H₂S is impaired in non-obese diabetic (NOD) mice. *Br J Pharmacol*, 155 (5): 673-80.
278. Kundu S, Pushpakumar SB, Tyagi A, Coley D, Sen U. (2013) Hydrogen sulfide deficiency and diabetic renal remodeling: role of matrix metalloproteinase-9. *Am J Physiol Endocrinol Metab*, 304 (12): E1365-78.
279. Peake BF, Nicholson CK, Lambert JP, Hood RL, Amin H, Amin S, Calvert JW. (2013) Hydrogen sulfide preconditions the db/db diabetic mouse heart against ischemia-reperfusion injury by activating Nrf2 signaling in an Erk-dependent manner. *Am J Physiol Heart Circ Physiol*, 304 (9): H1215-24.
280. Szabo C. (2012) Roles of hydrogen sulfide in the pathogenesis of diabetes mellitus and its complications. *Antioxid Redox Signal*, 17 (1): 68-80.
281. van den Born JC, Hammes HP, Greffrath W, van Goor H, Hillebrands JL, Complications DGIRTGDM. (2016) Gasotransmitters in Vascular Complications of Diabetes. *Diabetes*, 65 (2): 331-45.
282. Zhong X, Wang L, Wang Y, Dong S, Leng X, Jia J, Zhao Y, Li H, Zhang X, Xu C, Yang G, Wu L, Wang R, Lu F, Zhang W. (2012) Exogenous hydrogen sulfide attenuates diabetic myocardial injury through cardiac mitochondrial protection. *Mol Cell Biochem*, 371 (1-2): 187-98.
283. Lambert JP, Nicholson CK, Amin H, Amin S, Calvert JW. (2014) Hydrogen sulfide provides cardioprotection against myocardial/ischemia reperfusion injury in the diabetic state through the activation of the RISK pathway. *Med Gas Res*, 4 (1): 20.

284. Szabo C. (2010) Gaseotransmitters: new frontiers for translational science. *Sci Transl Med*, 2 (59): 59ps54.
285. Xie L, Gu Y, Wen M, Zhao S, Wang W, Ma Y, Meng G, Han Y, Wang Y, Liu G, Moore PK, Wang X, Wang H, Zhang Z, Yu Y, Ferro A, Huang Z, Ji Y. (2016) Hydrogen sulfide induces keap1 S-sulphydration and suppresses diabetes-accelerated atherosclerosis via Nrf2 activation. *Diabetes*.
286. Liang D, Wu H, Wong MW, Huang D. (2015) Diallyl Trisulfide Is a Fast H₂S Donor, but Diallyl Disulfide Is a Slow One: The Reaction Pathways and Intermediates of Glutathione with Polysulfides. *Org Lett*, 17 (17): 4196-9.
287. Zhao Y, Pacheco A, Xian M. (2015) Medicinal Chemistry: Insights into the Development of Novel H₂S Donors. *Handb Exp Pharmacol*, 230: 365-88.
288. Zheng Y, Ji X, Ji K, Wang B. (2015) Hydrogen sulfide prodrugs-a review. *Acta Pharm Sin B*, 5 (5): 367-77.
289. Benavides GA, Squadrito GL, Mills RW, Patel HD, Isbell TS, Patel RP, Darley-Usmar VM, Doeller JE, Kraus DW. (2007) Hydrogen sulfide mediates the vasoactivity of garlic. *Proc Natl Acad Sci U S A*, 104 (46): 17977-82.
290. Lemar KM, Aon MA, Cortassa S, O'Rourke B, Muller CT, Lloyd D. (2007) Diallyl disulphide depletes glutathione in *Candida albicans*: oxidative stress-mediated cell death studied by two-photon microscopy. *Yeast*, 24 (8): 695-706.
291. Caro AA, Adlong LW, Crocker SJ, Gardner MW, Luikart EF, Gron LU. (2012) Effect of garlic-derived organosulfur compounds on mitochondrial function and integrity in isolated mouse liver mitochondria. *Toxicol Lett*, 214 (2): 166-74.
292. Truong DH, Eghbal MA, Hindmarsh W, Roth SH, O'Brien PJ. (2006) Molecular mechanisms of hydrogen sulfide toxicity. *Drug Metab Rev*, 38 (4): 733-44.
293. Filomeni G, Aquilano K, Rotilio G, Ciriolo MR. (2005) Glutathione-related systems and modulation of extracellular signal-regulated kinases are involved in the resistance of AGS adenocarcinoma gastric cells to diallyl disulfide-induced apoptosis. *Cancer Res*, 65 (24): 11735-42.
294. Ahmad MS and Ahmed N. (2006) Antiglycation properties of aged garlic extract: possible role in prevention of diabetic complications. *J Nutr*, 136 (3 Suppl): 796S-799S.

295. Shiju TM, Rajesh NG, Viswanathan P. (2013) Renoprotective effect of aged garlic extract in streptozotocin-induced diabetic rats. *Indian J Pharmacol*, 45 (1): 18-23.
296. Bayan L, Koulivand PH, Gorji A. (2014) Garlic: a review of potential therapeutic effects. *Avicenna J Phytomed*, 4 (1): 1-14.
297. Supakul L, Pintana H, Apaijai N, Chattipakorn S, Shinlapawittayatorn K, Chattipakorn N. (2014) Protective effects of garlic extract on cardiac function, heart rate variability, and cardiac mitochondria in obese insulin-resistant rats. *Eur J Nutr*, 53 (3): 919-28.
298. Atkin M, Laight D, Cummings MH. (2016) The effects of garlic extract upon endothelial function, vascular inflammation, oxidative stress and insulin resistance in adults with type 2 diabetes at high cardiovascular risk. A pilot double blind randomized placebo controlled trial. *J Diabetes Complications*, 30 (4): 723-7.
299. Wallace JL and Wang R. (2015) Hydrogen sulfide-based therapeutics: exploiting a unique but ubiquitous gasotransmitter. *Nat Rev Drug Discov*, 14 (5): 329-45.
300. Szczesny B, Modis K, Yanagi K, Coletta C, Le Trionnaire S, Perry A, Wood ME, Whiteman M, Szabo C. (2014) AP39, a novel mitochondria-targeted hydrogen sulfide donor, stimulates cellular bioenergetics, exerts cytoprotective effects and protects against the loss of mitochondrial DNA integrity in oxidatively stressed endothelial cells in vitro. *Nitric Oxide*, 41: 120-30.
301. Goubern M, Andriamihaja M, Nubel T, Blachier F, Bouillaud F. (2007) Sulfide, the first inorganic substrate for human cells. *FASEB J*, 21 (8): 1699-706.
302. Lagoutte E, Mimoun S, Andriamihaja M, Chaumontet C, Blachier F, Bouillaud F. (2010) Oxidation of hydrogen sulfide remains a priority in mammalian cells and causes reverse electron transfer in colonocytes. *Biochim Biophys Acta*, 1797 (8): 1500-11.
303. Ahmad A, Olah G, Szczesny B, Wood ME, Whiteman M, Szabo C. (2016) AP39, A Mitochondrially Targeted Hydrogen Sulfide Donor, Exerts Protective Effects in Renal Epithelial Cells Subjected to Oxidative Stress in Vitro and in Acute Renal Injury in Vivo. *Shock*, 45 (1): 88-97.

304. Chatzianastasiou A, Bibli SI, Andreadou I, Efentakis P, Kaludercic N, Wood ME, Whiteman M, Di Lisa F, Daiber A, Manolopoulos VG, Szabo C, Papapetropoulos A. (2016) Cardioprotection by H₂S donors: nitric oxide-dependent and -independent mechanisms. *J Pharmacol Exp Ther.*
305. Ikeda K, Marutani E, Hirai S, Wood ME, Whiteman M, Ichinose F. (2015) Mitochondria-targeted hydrogen sulfide donor AP39 improves neurological outcomes after cardiac arrest in mice. *Nitric Oxide*, 49: 90-6.
306. Wang JD, Shi WL, Zhang GQ, Bai XM. (1994) Tissue and serum levels of steroid hormones and RU 486 after administration of mifepristone. *Contraception*, 49 (3): 245-53.

9. Bibliography of the candidate's publications

I. List of original publications **within the topic of the PhD thesis:**

1. Gero D, Szoleczky P, Suzuki K, Modis K, Olah G, Coletta C, Szabo C
Cell-Based Screening Identifies Paroxetine as an Inhibitor of Diabetic Endothelial Dysfunction
DIABETES 62:(3) 953-964. (2013)

2. Gerö D, Szabo C
Glucocorticoids suppress mitochondrial oxidant production via upregulation of uncoupling protein 2 in hyperglycemic endothelial cells
PLOS ONE 11:(4) e0154813. (2016)

3. Suzuki K, Olah G, Modis K, Coletta C, Kulp G, Gero D, Szoleczky P, Chang T, Zhou Z, Wu L, Wang R, Papapetropoulos A, Szabo C
Hydrogen sulfide replacement therapy protects the vascular endothelium in hyperglycemia by preserving mitochondrial function
PROCEEDINGS OF THE NATIONAL ACADEMY OF SCIENCES OF THE UNITED STATES OF AMERICA 108:(33) 13829-13834. (2011)

4. Gerö D, Torregrossa R, Perry A, Waters A, Le-Trionnaire S, Whatmore JL, Wood M, Whiteman M
The novel mitochondria-targeted hydrogen sulfide (H₂S) donors AP123 and AP39 protect against hyperglycemic injury in microvascular endothelial cells in vitro
PHARMACOLOGICAL RESEARCH 113:(Part A) 186-198. (2016)

II. List of the candidate's publications **unrelated to the topic of the PhD thesis:**

1. Ahmad A, Gerö D, Olah G, Szabo C
Effect of endotoxemia in mice genetically deficient in cystathionine-γ-lyase, cystathionine-β-synthase or 3-mercaptopyruvate sulfurtransferase
INTERNATIONAL JOURNAL OF MOLECULAR MEDICINE 38:(6) 1683-1692. (2016)

2. Druzhyna N, Szczesny B, Olah G, Módis K, Asimakopoulou A, Pavlidou A, Szoleczky P, Gerő D, Yanagi K, Törő G, López-García I, Myrianthopoulos V, Mikros E, Zatarain JR, Chao C, Papapetropoulos A, Hellmich MR, Szabo C
Screening of a composite library of clinically used drugs and well-characterized pharmacological compounds for cystathionine β -synthase inhibition identifies benserazide as a drug potentially suitable for repurposing for the experimental therapy of colon cancer

PHARMACOLOGICAL RESEARCH 113:(Part A) 18-37. (2016)

3. López-García I, Gerő D, Szczesny B, Szoleczky P, Olah G, Módis K, Zhang K, Gao J, Wu P, Sowers LC, DeWitt D, Prough DS, Szabo C
Development of a stretch-induced neurotrauma model for medium-throughput screening in vitro: identification of rifampicin as a neuroprotectant

BRITISH JOURNAL OF PHARMACOLOGY 176: (2) 284-300. (2018)

4. Rios ECS, Soriano FG, Olah G, Gerő D, Szczesny B, Szabo C
Hydrogen sulfide modulates chromatin remodeling and inflammatory mediator production in response to endotoxin, but does not play a role in the development of endotoxin tolerance

JOURNAL OF INFLAMMATION-LONDON 13:(1) 10. (2016)

5. Gero D, Szabo C
Salvage of nicotinamide adenine dinucleotide plays a critical role in the bioenergetic recovery of post-hypoxic cardiomyocytes

BRITISH JOURNAL OF PHARMACOLOGY 172:(20) 4817-4832. (2015)

6. Olah G, Szczesny B, Brunyanszki A, Lopez-Garcia IA, Gero D, Radak Z, Szabo C
Differentiation-Associated Downregulation of Poly(ADP-Ribose) Polymerase-1 Expression in Myoblasts Serves to Increase Their Resistance to Oxidative Stress

PLOS ONE 10:(7) e0134227. (2015)

7. Pribis JP, Al-Abed Y, Yang H, Gero D, Xu H, Montenegro MF , Bauer E M , Kim S, Chavan SS, Cai C, Li T, Szoleczky P, Szabo C, Tracey KJ , Billiar TR

The HIV Protease Inhibitor Saquinavir Inhibits HMGB1-Driven Inflammation by Targeting the Interaction of Cathepsin V with TLR4/MyD88

MOLECULAR MEDICINE 21:(1) 749-757. (2015)

8. Yang H, Wang H, Ju Z, Ragab AA, Lundbäck P, Long W, Valdes-Ferrer SI, He M, Pribis JP, Li J, Lu B, Gero D, Szabo C, Antoine DJ, Harris HE, Golenbock DT, Meng J, Roth J, Chavan SS, Andersson U, Billiar TR, Tracey KJ, Al-Abed Y

MD-2 is required for disulfide HMGB1-dependent TLR4 signaling

JOURNAL OF EXPERIMENTAL MEDICINE 212:(1) 5-14. (2015)

9. Gero D, Szoleczky P, Chatzianastasiou A, Papapetropoulos A, Szabo C

Modulation of poly(ADP-ribose) polymerase-1 (PARP-1)-mediated oxidative cell injury by ring finger protein 146 (RNF146) in cardiac myocytes.

MOLECULAR MEDICINE 20: 313-328. (2014)

10. Gero D, Szoleczky P, Modis K, Pribis JP, Al-Abed Y, Yang H, Chavan S, Billiar TR, Tracey KJ, Szabo C

Identification of pharmacological modulators of HMGB1-induced inflammatory response by cell-based screening.

PLOS ONE 8:(6) e65994. (2013)

11. Módis K, Gerő D, Stangl R, Rosero O, Szijártó A, Lotz G, Mohácsik P, Szoleczky P, Coletta C, Szabó C

Adenosine and inosine exert cytoprotective effects in an in vitro model of liver ischemia-reperfusion injury

INTERNATIONAL JOURNAL OF MOLECULAR MEDICINE 31:(2) 437-446. (2013)

12. Coletta C, Papapetropoulos A, Erdelyi K, Olah G, Modis K, Panopoulos P, Asimakopoulou A, Gero D, Sharina I, Martin E, Szabo C

Hydrogen sulfide and nitric oxide are mutually dependent in the regulation of angiogenesis and endothelium-dependent vasorelaxation.

PROCEEDINGS OF THE NATIONAL ACADEMY OF SCIENCES OF THE UNITED STATES OF AMERICA 109:(23) 9161-9166. (2012)

13. Modis K, Gero D, Erdelyi K, Szoleczky P, DeWitt D, Szabo C
Cellular bioenergetics is regulated by PARP1 under resting conditions and during oxidative stress.

BIOCHEMICAL PHARMACOLOGY 83:(5) 633-643. (2012)

14. Szoleczky P, Modis K, Nagy N, Dori Toth Z, DeWitt D, Szabo C, Gero D
Identification of agents that reduce renal hypoxia-reoxygenation injury using cell-based screening: purine nucleosides are alternative energy sources in LLC-PK1 cells during hypoxia.

ARCHIVES OF BIOCHEMISTRY AND BIOPHYSICS 517:(1) 53-70. (2012)

15. Bartha E, Solti I, Szabo A, Olah G, Magyar K, Szabados E, Kalai T, Hideg K, Toth K, Gero D, Szabo C, Sumegi B, Halmosi R
Regulation of kinase cascade activation and heat shock protein expression by poly(ADP-ribose) polymerase inhibition in doxorubicin-induced heart failure

JOURNAL OF CARDIOVASCULAR PHARMACOLOGY 58:(4) 380-391. (2011)

16. Olah G, Finnerty CC, Sbrana E, Elijah I, Gero D, Herndon DN, Szabo C
Increased poly(ADP-ribosyl)ation in skeletal muscle tissue of pediatric patients with severe burn injury: prevention by propranolol treatment

SHOCK 36:(1) 18-23. (2011)

17. Olah G, Modis K, Gero D, Suzuki K, Dewitt D, Traber DL, Szabo C
Cytoprotective effect of gamma-tocopherol against tumor necrosis factor alpha induced cell dysfunction in L929 cells

INTERNATIONAL JOURNAL OF MOLECULAR MEDICINE 28:(5) 711-720. (2011)

18. Stangl R, Szíjártó A, Ónody P, Tamás J, Tátrai M, Hegedüs V, Blázovics A, Lotz G, Kiss A, Módis K, Gerő D, Szabó C, Kupcsulik P, Harsányi L

Reduction of liver ischemia-reperfusion injury via glutamine pretreatment

JOURNAL OF SURGICAL RESEARCH 166:(1) 95-103. (2011)

19. Szabo G, Veres G, Radovits T, Gero D, Modis K, Miesel-Groschel C, Horkay F, Karck M, Szabo C

Cardioprotective effects of hydrogen sulfide

NITRIC OXIDE-BIOLOGY AND CHEMISTRY 25:(2) 201-210. (2011)

20. Ozsvári B, Puskas LG, Nagy LI, Kanizsai I, Gyuris M, Madacsi R, Feher LZ, Gero D, Szabo C

A cell-microelectronic sensing technique for the screening of cytoprotective compounds

INTERNATIONAL JOURNAL OF MOLECULAR MEDICINE 25:(4) 525-530. (2010)

21. Modis K, Gero D, Nagy N, Szoleczky P, Toth ZD, Szabo C

Cytoprotective effects of adenosine and inosine in an in vitro model of acute tubular necrosis.

BRITISH JOURNAL OF PHARMACOLOGY 158:(6) 1565-1578. (2009)

22. Gerő D, Szabo C

Poly (ADP-ribose) polymerase: a new therapeutic target?

CURRENT OPINION IN ANAESTHESIOLOGY 21:(2) 111-121. (2008)

23. Horváth EM, Benko R, Gero D, Kiss L, Szabó C

Treatment with insulin inhibits poly(ADP-ribose)polymerase activation in a rat model of endotoxemia

LIFE SCIENCES 82:(3-4) 205-209. (2008)

24. Radovits T, Gerő D, Lin LN, Loganathan S, Hoppe-Tichy T, Szabó C, Karck M, Sakurai H, Szabó G

Improvement of Aging-Associated Cardiovascular Dysfunction by the Orally Administered Copper(II)-Aspirinate Complex

REJUVENATION RESEARCH 11:(5) 945-956. (2008)

25. Gero D, Modis K, Nagy N, Szoleczky P, Toth ZD, Dorman G, Szabo C
Oxidant-induced cardiomyocyte injury: identification of the cytoprotective effect of a dopamine 1 receptor agonist using a cell-based high-throughput assay.
INTERNATIONAL JOURNAL OF MOLECULAR MEDICINE 20:(5) 749-761. (2007)
26. Radovits T, Zotkina J, Lin LN, Bomicke T, Arif R, Gero D, Horvath EM, Karck M, Szabo C, Szabo G
Poly(ADP-Ribose) polymerase inhibition improves endothelial dysfunction induced by hypochlorite
EXPERIMENTAL BIOLOGY AND MEDICINE 232:(9) 1204-1212. (2007)
27. Radovits T, Lin LN, Zotkina J, Gero D, Szabo C, Karck M, Szabo G
Poly(ADP-ribose) polymerase inhibition improves endothelial dysfunction induced by reactive oxidant hydrogen peroxide in vitro
EUROPEAN JOURNAL OF PHARMACOLOGY 564:(1-3) 158-166. (2007)
28. Radovits T, Seres L, Gero D, Berger I, Szabo C, Karck M, Szabo G
Single dose treatment with PARP-inhibitor INO-1001 improves aging-associated cardiac and vascular dysfunction
EXPERIMENTAL GERONTOLOGY 42:(7) 676-685. (2007)
29. Radovits T, Seres L, Gero D, Lin LN, Beller CJ, Chen SH, Zotkina J, Berger I, Groves JT, Szabo C, Szabo G
The peroxynitrite decomposition catalyst FP15 improves ageing-associated cardiac and vascular dysfunction.
MECHANISMS OF AGEING AND DEVELOPMENT 128:(2) 173-181. (2007)
30. Szijarto A, Batmunkh E, Hahn O, Mihály Z, Kreiss A, Kiss A, Lotz G, Schaff Z, Váli L, Blazovics A, Gero D, Szabó C, Kupcsulik P
Effect of PJ-34-PARP inhibitor on rat liver microcirculation and antioxidant status
JOURNAL OF SURGICAL RESEARCH 142:(1) 72-80. (2007)

31. Szijártó A, Hahn O, Batmunkh E, Stangl R, Kiss A, Lotz G, Schaff Z, Váli L, Blázovics A, Gero D, Szabó C, Kupcsulik P, Harsányi L

Short-term alanyl-glutamine dipeptide pretreatment in liver ischemia-reperfusion model: Effects on microcirculation and antioxidant status in rats

CLINICAL NUTRITION 26:(5) 640-648. (2007)

32. Beller CJ, Kosse J, Radovits T, Gero D, Krempien R, Gross ML, Berger I, Hagl S, Szabo C, Szabo G

Poly(ADP-ribose) polymerase inhibition combined with irradiation: a dual treatment concept to prevent neointimal hyperplasia after endarterectomy.

INTERNATIONAL JOURNAL OF RADIATION ONCOLOGY BIOLOGY PHYSICS 66:(3) 867-875. (2006)

33. Beller CJ, Radovits T, Kosse J, Gero D, Szabo C, Szabo G

Activation of the peroxynitrite-poly(adenosine diphosphate-ribose) polymerase pathway during neointima proliferation: a new target to prevent restenosis after endarterectomy

JOURNAL OF VASCULAR SURGERY 43:(4) 824-830. (2006)

34. Gero D, Szabo C

Role of the peroxynitrite-poly (ADP-ribose) polymerase pathway in the pathogenesis of liver injury

CURRENT PHARMACEUTICAL DESIGN 12:(23) 2903-2910. (2006)

35. Kiss L, Chen M, Gero D, Modis K, Lacza Z, Szabo C

Effects of 7-ketocholesterol on the activity of endothelial poly(ADP-ribose) polymerase and on endothelium-dependent relaxant function

INTERNATIONAL JOURNAL OF MOLECULAR MEDICINE 18:(6) 1113-1117. (2006)

36. Lacza Z, Pankotai E, Csordás A, Gero D, Kiss L, Horváth EM, Kollai M, Busija DW, Szabó C

Mitochondrial NO and reactive nitrogen species production: Does mtNOS exist?

NITRIC OXIDE-BIOLOGY AND CHEMISTRY 14:(2 SPEC. ISS.) 162-168. (2006)

37. Molnár A, Tóth A, Bagi Z, Papp Z, Édes I, Vaszily M, Galajda Z, Papp JG, Varró A, Szűts V, Lacza Z, Gerő D, Szabó C
Activation of the poly(ADP-ribose) polymerase pathway in human heart failure
MOLECULAR MEDICINE 12:(7-8) 143-152. (2006)

38. Szabo G, Stumpf N, Radovits T, Sonnenberg K, Gero D, Hagl S, Szabo C, Bahrle S
Effects of inosine on reperfusion injury after heart transplantation
EUROPEAN JOURNAL OF CARDIO-THORACIC SURGERY 30:(1) 96-102. (2006)

39. Szabo G, Bahrle S, Sivanandam V, Stumpf N, Gero D, Berger I, Beller C, Hagl S, Szabo C, Dengler TJ
Immunomodulatory effects of poly(ADP-ribose) polymerase inhibition contribute to improved cardiac function and survival during acute cardiac rejection
JOURNAL OF HEART AND LUNG TRANSPLANTATION 25:(7) 794-804. (2006)

40. Tóth-Zsámboki E, Horváth E, Vargová K, Pankotai E, Murthy K, Zsengellér Z, Bárányi T, Pék T, Fekete K, Kiss RG, Préda I, Lacza Z, Gerő D, Szabó C
Activation of poly(ADP-ribose) polymerase by myocardial ischemia and coronary reperfusion in human circulating leukocytes
MOLECULAR MEDICINE 12:(9-10) 221-228. (2006)

41. Su X, Hu Q, Kristan JM, Costa C, Shen Y, Gero D, Matis LA, Wang Y
Significant role for Fas in the pathogenesis of autoimmune diabetes
JOURNAL OF IMMUNOLOGY 164:(5) 2523-2532. (2000)

10. Acknowledgements

Domokos Gero received funding from the People Programme (Marie Curie Actions) of the European Union's Seventh Framework Programme under the grant agreement number 628100 (FP7/2007/2013/628100). The current work was also supported by a grant from the Juvenile Diabetes Foundation (Award# 17-2010-542) to Csaba Szabo and by a grant from the Medical Research Council (MR/M022706/1) to Matthew Whiteman and Mark E. Wood.

11. Supplementary material

Suppl. Table 1. List of genes analyzed by the mouse mitochondrial energy metabolism PCR array (part 1/2). The genes associated with mitochondrial energy production are listed with their gene symbol, full gene name Unigene identifier and NCBI accession number and respective position on the plate.

Position	UniGene	RefSeq	Gene Symbol	Description
A01	Mm.276721	NM_029609	Lhpp	Phospholysine phosphohistidine inorganic pyrophosphate phosphatase
A02	Mm.273271	NM_138652	Atp12a	ATPase, H+/K+ transporting, nongastric, alpha polypeptide
A03	Mm.12821	NM_018731	Atp4a	ATPase, H+/K+ exchanging, gastric, alpha polypeptide
A04	Mm.154039	NM_009724	Atp4b	ATPase, H+/K+ exchanging, beta polypeptide
A05	Mm.276137	NM_007505	Atp5a1	ATP synthase, H+ transporting, mitochondrial F1 complex, alpha subunit 1
A06	Mm.238973	NM_016774	Atp5b	ATP synthase, H+ transporting mitochondrial F1 complex, beta subunit
A07	Mm.12677	NM_020615	Atp5c1	ATP synthase, H+ transporting, mitochondrial F1 complex, gamma polypeptide 1
A08	Mm.278560	NM_025313	Atp5d	ATP synthase, H+ transporting, mitochondrial F1 complex, delta subunit
A09	Mm.251152	NM_009725	Atp5f1	ATP synthase, H+ transporting, mitochondrial F0 complex, subunit B1
A10	Mm.371547	NM_007506	Atp5g1	ATP synthase, H+ transporting, mitochondrial F0 complex, subunit c1 (subunit 9)
A11	Mm.10314	NM_026468	Atp5g2	ATP synthase, H+ transporting, mitochondrial F0 complex, subunit C2 (subunit 9)
A12	Mm.2966	NM_175015	Atp5g3	ATP synthase, H+ transporting, mitochondrial F0 complex, subunit C3 (subunit 9)
B01	Mm.371641	NM_027862	Atp5h	ATP synthase, H+ transporting, mitochondrial F0 complex, subunit d
B02	Mm.353	NM_016755	Atp5j	ATP synthase, H+ transporting, mitochondrial F0 complex, subunit F
B03	Mm.133551	NM_020582	Atp5j2	ATP synthase, H+ transporting, mitochondrial F0 complex, subunit F2
B04	Mm.41	NM_138597	Atp5o	ATP synthase, H+ transporting, mitochondrial F1 complex, subunit
B05	Mm.1158	NM_011596	Atp6v0a2	ATPase, H+ transporting, lysosomal V0 subunit A2
B06	Mm.19298	NM_175406	Atp6v0d2	ATPase, H+ transporting, lysosomal V0 subunit D2
B07	Mm.178798	NM_133699	Atp6v1c2	ATPase, H+ transporting, lysosomal V1 subunit C2
B08	Mm.159369	NM_029121	Atp6v1e2	ATPase, H+ transporting, lysosomal V1 subunit E2
B09	Mm.114424	NM_177397	Atp6v1g3	ATPase, H+ transporting, lysosomal V1 subunit G3
B10	Mm.358700	NM_025784	Bcs1l	BCS1-like (yeast)
B11	Mm.151940	NM_199008	Cox11	COX11 homolog, cytochrome c oxidase assembly protein (yeast)
B12	Mm.386758	NM_009941	Cox4i1	Cytochrome c oxidase subunit IV isoform 1
C01	Mm.196668	NM_053091	Cox4i2	Cytochrome c oxidase subunit IV isoform 2
C02	Mm.273403	NM_007747	Cox5a	Cytochrome c oxidase, subunit Va
C03	Mm.180182	NM_009942	Cox5b	Cytochrome c oxidase, subunit Vb
C04	Mm.43415	NM_007748	Cox6a1	Cytochrome c oxidase, subunit VI a, polypeptide 1
C05	Mm.43824	NM_009943	Cox6a2	Cytochrome c oxidase, subunit VI a, polypeptide 2
C06	Mm.400	NM_025628	Cox6b1	Cytochrome c oxidase, subunit VIb polypeptide 1
C07	Mm.29625	NM_183405	Cox6b2	Cytochrome c oxidase subunit VIb polypeptide 2
C08	Mm.548	NM_053071	Cox6c	Cytochrome c oxidase, subunit VIc
C09	Mm.152627	NM_009945	Cox7a2	Cytochrome c oxidase, subunit VIIa 2
C10	Mm.30072	NM_009187	Cox7a2l	Cytochrome c oxidase subunit VIIa polypeptide 2-like
C11	Mm.197728	NM_025379	Cox7b	Cytochrome c oxidase subunit VIIb
C12	Mm.14022	NM_007750	Cox8a	Cytochrome c oxidase, subunit VIIIA
D01	Mm.660	NM_001039049	Cox8c	Cytochrome c oxidase, subunit VIIIC
D02	Mm.29196	NM_025567	Cyc1	Cytochrome c-1

Suppl. Table 1. List of genes analyzed by the mouse mitochondrial energy metabolism PCR array (part 2/2). The genes associated with mitochondrial energy production are listed with their gene symbol, full gene name Unigene identifier and NCBI accession number and respective position on the plate.

Position	UniGene	RefSeq	Gene Symbol	Description
D03	Mm.34869	NM_019443	Ndufa1	NADH dehydrogenase (ubiquinone) 1 alpha subcomplex, 1
D04	Mm.248778	NM_024197	Ndufa10	NADH dehydrogenase (ubiquinone) 1 alpha subcomplex 10
D05	Mm.279823	NM_027244	Ndufa11	NADH dehydrogenase (ubiquinone) 1 alpha subcomplex 11
D06	Mm.29867	NM_010885	Ndufa2	NADH dehydrogenase (ubiquinone) 1 alpha subcomplex, 2
D07	Mm.17851	NM_025348	Ndufa3	NADH dehydrogenase (ubiquinone) 1 alpha subcomplex, 3
D08	Mm.415865	NM_010886	Ndufa4	NADH dehydrogenase (ubiquinone) 1 alpha subcomplex, 4
D09	Mm.275780	NM_026614	Ndufa5	NADH dehydrogenase (ubiquinone) 1 alpha subcomplex, 5
D10	Mm.27570	NM_025987	Ndufa6	NADH dehydrogenase (ubiquinone) 1 alpha subcomplex, 6 (B14)
D11	Mm.29513	NM_023202	Ndufa7	NADH dehydrogenase (ubiquinone) 1 alpha subcomplex, 7 (B14.5a)
D12	Mm.19834	NM_026703	Ndufa8	NADH dehydrogenase (ubiquinone) 1 alpha subcomplex, 8
E01	Mm.347976	NM_028177	Ndufab1	NADH dehydrogenase (ubiquinone) 1, alpha/beta subcomplex, 1
E02	Mm.1129	NM_026684	Ndufb10	NADH dehydrogenase (ubiquinone) 1 beta subcomplex, 10
E03	Mm.29415	NM_026612	Ndufb2	NADH dehydrogenase (ubiquinone) 1 beta subcomplex, 2
E04	Mm.2033	NM_025597	Ndufb3	NADH dehydrogenase (ubiquinone) 1 beta subcomplex 3
E05	Mm.379154	NM_026610	Ndufb4	NADH dehydrogenase (ubiquinone) 1 beta subcomplex 4
E06	Mm.28058	NM_025316	Ndufb5	NADH dehydrogenase (ubiquinone) 1 beta subcomplex, 5
E07	Mm.1103	NM_001033305	Ndufb6	NADH dehydrogenase (ubiquinone) 1 beta subcomplex, 6
E08	Mm.29683	NM_025843	Ndufb7	NADH dehydrogenase (ubiquinone) 1 beta subcomplex, 7
E09	Mm.2060	NM_026061	Ndufb8	NADH dehydrogenase (ubiquinone) 1 beta subcomplex 8
E10	Mm.322294	NM_023172	Ndufb9	NADH dehydrogenase (ubiquinone) 1 beta subcomplex, 9
E11	Mm.331007	NM_025523	Ndufc1	NADH dehydrogenase (ubiquinone) 1, subcomplex unknown, 1
E12	Mm.334031	NM_024220	Ndufc2	NADH dehydrogenase (ubiquinone) 1, subcomplex unknown, 2
F01	Mm.290791	NM_145518	Ndufs1	NADH dehydrogenase (ubiquinone) Fe-S protein 1
F02	Mm.21669	NM_153064	Ndufs2	NADH dehydrogenase (ubiquinone) Fe-S protein 2
F03	Mm.30113	NM_026688	Ndufs3	NADH dehydrogenase (ubiquinone) Fe-S protein 3
F04	Mm.253142	NM_010887	Ndufs4	NADH dehydrogenase (ubiquinone) Fe-S protein 4
F05	Mm.42805	NM_001030274	Ndufs5	NADH dehydrogenase (ubiquinone) Fe-S protein 5
F06	Mm.29897	NM_010888	Ndufs6	NADH dehydrogenase (ubiquinone) Fe-S protein 6
F07	Mm.28712	NM_029272	Ndufs7	NADH dehydrogenase (ubiquinone) Fe-S protein 7
F08	Mm.44227	NM_144870	Ndufs8	NADH dehydrogenase (ubiquinone) Fe-S protein 8
F09	Mm.29842	NM_133666	Ndufv1	NADH dehydrogenase (ubiquinone) flavoprotein 1
F10	Mm.2206	NM_028388	Ndufv2	NADH dehydrogenase (ubiquinone) flavoprotein 2
F11	Mm.28349	NM_030087	Ndufv3	NADH dehydrogenase (ubiquinone) flavoprotein 3
F12	Mm.182340	NM_026936	Oxa1l	Oxidase assembly 1-like
G01	Mm.28897	NM_026438	Ppa1	Pyrophosphatase (inorganic) 1
G02	Mm.210305	NM_146141	Ppa2	Pyrophosphatase (inorganic) 2
G03	Mm.158231	NM_023281	Sdha	Succinate dehydrogenase complex, subunit A, flavoprotein (Fp)
G04	Mm.246965	NM_023374	Sdhb	Succinate dehydrogenase complex, subunit B, iron sulfur (Ip)
G05	Mm.198138	NM_025321	Sdhc	Succinate dehydrogenase complex, subunit C, integral membrane protein
G06	Mm.10406	NM_025848	Sdhd	Succinate dehydrogenase complex, subunit D, integral membrane protein
G07	Mm.379119	NM_025650	Uqcr11	Ubiquinol-cytochrome c reductase, complex III subunit XI
G08	Mm.335460	NM_025407	Uqcr1	Ubiquinol-cytochrome c reductase core protein 1
G09	Mm.334206	NM_025899	Uqcr2	Ubiquinol cytochrome c reductase core protein 2
G10	Mm.181933	NM_025710	Uqcrfs1	Ubiquinol-cytochrome c reductase, Rieske iron-sulfur polypeptide 1
G11	Mm.181721	NM_025641	Uqcrh	Ubiquinol-cytochrome c reductase hinge protein
G12	Mm.251621	NM_025352	Uqcrq	Ubiquinol-cytochrome c reductase, complex III subunit VII

Suppl. Table 2.: Comparison of gene expression profiles of b.END3 endothelial cells exposed to hyperglycemia and normoglycemic cells analyzed by the mouse mitochondrial energy metabolism gene expression array (part 1/2). Total RNA was isolated from b.End3 cells exposed to hyperglycemia or normoglycemia for 7 days using TRIzol® reagent. 2 µg RNA was treated with DNase (Epicentre, Madison, WI) and reverse transcription was carried out using High Capacity cDNA Archive kit (Applied Biosystems, Foster City, CA). 1 µg RNA was used for gene expression measurements using the mouse mitochondrial energy real-time PCR array (SABiosciences Frederick, MD) on CFX96 thermo cycler (Biorad, Hercules, CA). Threshold cycle (C_T) values determined by CFX Manager were used to calculate expression changes with the RT² Profiler™ PCR Array Data Analysis tool supplied with the array. (Significant differences are shown in bold.)

Gene Symbol	Gene name	fold change	T-TEST	fold up- or down-regulation
		high glc /low glc	p value	high glc/ low glc
Lhpp	Phospholysine phosphohistidine inorganic pyrophosphate phosphatase	0.55	0.104956	-1.83
Atp12a	ATPase, H+/K+ transporting, nongastric, alpha polypeptide	1.16	0.495906	1.16
Atp4a	ATPase, H+/K+ exchanging, gastric, alpha polypeptide	1.08	0.404976	1.08
Atp4b	ATPase, H+/K+ exchanging, beta polypeptide	0.51	0.011622	-1.97
Atp5a1	ATP synthase, H+ transporting, mitochondrial F1 complex, alpha subunit 1	0.91	0.081448	-1.10
Atp5b	ATP synthase, H+ transporting mitochondrial F1 complex, beta subunit	1.09	0.272205	1.09
Atp5c1	ATP synthase, H+ transporting, mitochondrial F1 complex, gamma polypeptide 1	0.92	0.058275	-1.08
Atp5d	ATP synthase, H+ transporting, mitochondrial F1 complex, delta subunit	1.03	0.633547	1.03
Atp5f1	ATP synthase, H+ transporting, mitochondrial F0 complex, subunit B1	1.01	0.757150	1.01
Atp5g1	ATP synthase, H+ transporting, mitochondrial F0 complex, subunit c1 (subunit 9)	1.18	0.266908	1.18
Atp5g2	ATP synthase, H+ transporting, mitochondrial F0 complex, subunit C2 (subunit 9)	1.00	0.872486	-1.00
Atp5g3	ATP synthase, H+ transporting, mitochondrial F0 complex, subunit C3 (subunit 9)	1.00	0.931517	1.00
Atp5h	ATP synthase, H+ transporting, mitochondrial F0 complex, subunit d	0.87	0.003010	-1.14
Atp5j	ATP synthase, H+ transporting, mitochondrial F0 complex, subunit F	0.86	0.016573	-1.16
Atp5j2	ATP synthase, H+ transporting, mitochondrial F0 complex, subunit F2	0.89	0.036442	-1.12
Atp5o	ATP synthase, H+ transporting, mitochondrial F1 complex, O subunit	1.03	0.607019	1.03
Atp6v0a2	ATPase, H+ transporting, lysosomal V0 subunit A2	0.93	0.191990	-1.08
Atp6v0d2	ATPase, H+ transporting, lysosomal V0 subunit D2	1.40	0.402090	1.40
Atp6v1c2	ATPase, H+ transporting, lysosomal V1 subunit C2	1.35	0.195736	1.35
Atp6v1e2	ATPase, H+ transporting, lysosomal V1 subunit E2	1.30	0.191061	1.30
Atp6v1g3	ATPase, H+ transporting, lysosomal V1 subunit G3	1.16	0.495906	1.16
Bcs1l	BCS1-like (yeast)	1.02	0.745362	1.02
Cox11	COX11 homolog, cytochrome c oxidase assembly protein (yeast)	0.99	0.846831	-1.01
Cox4i1	Cytochrome c oxidase subunit IV isoform 1	1.02	0.740261	1.02
Cox4i2	Cytochrome c oxidase subunit IV isoform 2	1.29	0.014383	1.29
Cox5a	Cytochrome c oxidase, subunit Va	0.92	0.399742	-1.09
Cox5b	Cytochrome c oxidase, subunit Vb	0.94	0.155015	-1.06
Cox6a1	Cytochrome c oxidase, subunit VI a, polypeptide 1	1.12	0.170281	1.12
Cox6a2	Cytochrome c oxidase, subunit VI a, polypeptide 2	0.72	0.341071	-1.40
Cox6b1	Cytochrome c oxidase, subunit VI b polypeptide 1	0.94	0.072654	-1.07
Cox6b2	Cytochrome c oxidase subunit VI b polypeptide 2	0.83	0.058137	-1.20
Cox6c	Cytochrome c oxidase, subunit VIc	0.90	0.107180	-1.11
Cox7a2	Cytochrome c oxidase, subunit VIIa 2	0.91	0.062870	-1.10
Cox7a2l	Cytochrome c oxidase subunit VIIa polypeptide 2-like	0.92	0.233821	-1.08
Cox7b	Cytochrome c oxidase subunit VIIb	0.90	0.013969	-1.12
Cox8a	Cytochrome c oxidase, subunit VIIla	0.99	0.667824	-1.02
Cox8c	Cytochrome c oxidase, subunit VIIlc	1.16	0.495906	1.16
Cyc1	Cytochrome c-1	1.09	0.110352	1.09

Suppl. Table 2.: Comparison of gene expression profiles of b.END3 endothelial cells exposed to hyperglycemia and normoglycemic cells analyzed by the mouse mitochondrial energy metabolism gene expression array (part 2/2). Total RNA was isolated from b.End3 cells exposed to hyperglycemia or normoglycemia for 7 days using TRIzol® reagent. 2 µg RNA was treated with DNase (Epicentre, Madison, WI) and reverse transcription was carried out using High Capacity cDNA Archive kit (Applied Biosystems, Foster City, CA). 1 µg RNA was used for gene expression measurements using the mouse mitochondrial energy real-time PCR array (SABiosciences Frederick, MD) on CFX96 thermo cycler (Biorad, Hercules, CA). Threshold cycle (C_T) values determined by CFX Manager were used to calculate expression changes with the RT² Profiler™ PCR Array Data Analysis tool supplied with the array. (Significant differences are shown in bold.)

Gene Symbol	Gene name	fold change	T-TEST	fold up- or down-regulation
		high glc /low glc	p value	high glc/ low glc
Ndufa1	NADH dehydrogenase (ubiquinone) 1 alpha subcomplex, 1	0.88	0.128230	-1.13
Ndufa10	NADH dehydrogenase (ubiquinone) 1 alpha subcomplex 10	1.01	0.792812	1.01
Ndufa11	NADH dehydrogenase (ubiquinone) 1 alpha subcomplex 11	1.14	0.589318	1.14
Ndufa2	NADH dehydrogenase (ubiquinone) 1 alpha subcomplex, 2	0.89	0.020925	-1.12
Ndufa3	NADH dehydrogenase (ubiquinone) 1 alpha subcomplex, 3	1.02	0.734265	1.02
Ndufa4	NADH dehydrogenase (ubiquinone) 1 alpha subcomplex, 4	0.98	0.660552	-1.02
Ndufa5	NADH dehydrogenase (ubiquinone) 1 alpha subcomplex, 5	0.91	0.060937	-1.10
Ndufa6	NADH dehydrogenase (ubiquinone) 1 alpha subcomplex, 6 (B14)	0.91	0.072746	-1.10
Ndufa7	NADH dehydrogenase (ubiquinone) 1 alpha subcomplex, 7 (B14.5a)	1.02	0.204352	1.02
Ndufa8	NADH dehydrogenase (ubiquinone) 1 alpha subcomplex, 8	0.82	0.032735	-1.22
Ndufab1	NADH dehydrogenase (ubiquinone) 1, alpha/beta subcomplex, 1	0.61	0.221531	-1.63
Ndufb10	NADH dehydrogenase (ubiquinone) 1 beta subcomplex, 10	1.46	0.242469	1.46
Ndufb2	NADH dehydrogenase (ubiquinone) 1 beta subcomplex, 2	0.94	0.150036	-1.07
Ndufb3	NADH dehydrogenase (ubiquinone) 1 beta subcomplex 3	0.97	0.209182	-1.03
Ndufb4	NADH dehydrogenase (ubiquinone) 1 beta subcomplex 4	1.02	0.396472	1.02
Ndufb5	NADH dehydrogenase (ubiquinone) 1 beta subcomplex, 5	0.64	0.113494	-1.55
Ndufb6	NADH dehydrogenase (ubiquinone) 1 beta subcomplex, 6	1.12	0.006489	1.12
Ndufb7	NADH dehydrogenase (ubiquinone) 1 beta subcomplex, 7	0.83	0.077174	-1.20
Ndufb8	NADH dehydrogenase (ubiquinone) 1 beta subcomplex 8	0.98	0.491799	-1.02
Ndufb9	NADH dehydrogenase (ubiquinone) 1 beta subcomplex, 9	1.01	0.717582	1.01
Ndufc1	NADH dehydrogenase (ubiquinone) 1, subcomplex unknown, 1	0.95	0.144298	-1.05
Ndufc2	NADH dehydrogenase (ubiquinone) 1, subcomplex unknown, 2	0.90	0.294585	-1.11
Ndufs1	NADH dehydrogenase (ubiquinone) Fe-S protein 1	1.01	0.760374	1.01
Ndufs2	NADH dehydrogenase (ubiquinone) Fe-S protein 2	1.03	0.380073	1.03
Ndufs3	NADH dehydrogenase (ubiquinone) Fe-S protein 3	1.20	0.001463	1.20
Ndufs4	NADH dehydrogenase (ubiquinone) Fe-S protein 4	1.01	0.804763	1.01
Ndufs5	NADH dehydrogenase (ubiquinone) Fe-S protein 5	0.80	0.231159	-1.26
Ndufs6	NADH dehydrogenase (ubiquinone) Fe-S protein 6	0.94	0.359973	-1.07
Ndufs7	NADH dehydrogenase (ubiquinone) Fe-S protein 7	1.12	0.177052	1.12
Ndufs8	NADH dehydrogenase (ubiquinone) Fe-S protein 8	0.99	0.969348	-1.01
Ndufv1	NADH dehydrogenase (ubiquinone) flavoprotein 1	1.00	0.995208	-1.00
Ndufv2	NADH dehydrogenase (ubiquinone) flavoprotein 2	0.83	0.058661	-1.21
Ndufv3	NADH dehydrogenase (ubiquinone) flavoprotein 3	0.86	0.174471	-1.17
Oxa11	Oxidase assembly 1-like	1.07	0.074985	1.07
Ppa1	Pyrophosphatase (inorganic) 1	1.41	0.005336	1.41
Ppa2	Pyrophosphatase (inorganic) 2	0.86	0.008473	-1.16
Sdha	Succinate dehydrogenase complex, subunit A, flavoprotein (Fp)	1.00	0.975468	1.00
Sdhb	Succinate dehydrogenase complex, subunit B, iron sulfur (Ip)	1.14	0.047328	1.14
Sdhc	Succinate dehydrogenase complex, subunit C, membrane protein	1.16	0.020830	1.16
Sdhd	Succinate dehydrogenase complex, subunit D, membrane protein	0.91	0.010970	-1.10
Uqcr11	Ubiquinol-cytochrome c reductase, complex III subunit XI	0.94	0.079199	-1.06
Uqcrcl	Ubiquinol-cytochrome c reductase core protein 1	1.09	0.150281	1.09
Uqcrc2	Ubiquinol cytochrome c reductase core protein 2	1.07	0.157631	1.07
Uqcrfs1	Ubiquinol-cytochrome c reductase, Rieske iron-sulfur polypeptide 1	1.01	0.881551	1.01
Uqcrh	Ubiquinol-cytochrome c reductase hinge protein	0.81	0.002055	-1.23
Uqcrg	Ubiquinol-cytochrome c reductase, complex III subunit VII	1.12	0.209514	1.12

Suppl. Table 3. Hit confirmation of hyperglycemia-induced mitochondrial ROS production screen (part 1/4)

Compounds that decreased the mitochondrial ROS production by 25% (ROS score > 1) but did not affect the viability (Viability score > -1) were re-tested at 10 μ M in replicates (results shown in *italic*). Compounds were categorized as toxic compounds (TOX) if reduced the viability by 10%, confirmed hits (CONF. HIT) if showed ROS production decreasing activity without affecting the viability, or non-confirmed (NON CONF.) if the average decrease in ROS production was less than 10% in the hit confirmation.

Compound Name	Biological Activity	Compound Source Library	Change in mitoROS production (%)	ROS score	ROS production MEAN \pm SEM	Viability MEAN \pm SEM	Result
I. adrenergic compounds							
naphazoline hydrochloride	adrenergic vasoconstrictor	P	-40	1.589	-9 \pm 5	86 \pm 3	TOX
xylazine	alpha-2-adrenergic agonist, sedative	F	-27	1.069	-8 \pm 2	92 \pm 2	NON CONF.
prazosin	alpha 1-blocker	F	-31	1.247	-11 \pm 3	116 \pm 1	CONF. HIT
alprenolol	beta blocker	F	-27	1.068	-8 \pm 2	91 \pm 1	NON CONF.
celiprolol HCl	beta blocker	P	-25	1.016	-11 \pm 2	71 \pm 2	TOX
acetobutol hydrochloride	beta 1 antagonist	P	-31	1.240	-13 \pm 2	93 \pm 4	CONF. HIT
pergolide mesylate	dopaminergic agonist	P	-31	1.224	-4 \pm 2	95 \pm 1	NON CONF.
bromocryptine mesylate	dopaminergic, prolactin inhibitor	P	-26	1.044	-2 \pm 2	95 \pm 1	NON CONF.
II. antimicrobial and antihelmintic agents, etc.							
ampicillin trihydrate	antibiotics, beta lactam	P	-25	1.003	-9 \pm 1	87 \pm 4	TOX
cefadroxil	antibiotics, bacterial transpeptidase inhibitor	P	-29	1.146	-3 \pm 1	97 \pm 1	NON CONF.
clindamycin hydrochloride	antibiotics, ribosomal protein synthesis inhibitor	P	-29	1.171	-1 \pm 3	89 \pm 5	TOX
tetracycline hydrochloride	antibiotics	N	-27	1.092	-19 \pm 3	105 \pm 3	CONF. HIT
thiamphenicol glycinate	antibiotics	F	-28	1.116	-9 \pm 3	80 \pm 10	TOX
sisomicin sulfate	antibiotics, ribosomal protein synthesis inhibitor	P	-30	1.209	-2 \pm 1	92 \pm 3	NON CONF.
carbadox	antibiotics, inhibits DNA synthesis	P	-28	1.137	-2 \pm 3	93 \pm 1	NON CONF.
sulfachlorpyridazine	antibiotics, sulfanilamide	U	-32	1.285	-7 \pm 3	97 \pm 2	NON CONF.
fenbendazole	anthelmintic benzimidazole	F	-29	1.152	-24 \pm 4	76 \pm 4	TOX
oxfendazole	anthelmintic, benzimidazole	F	-25	1.007	-13 \pm 2	98 \pm 2	CONF. HIT
ivermectin B1a	antihelmintic, GABAergic	P	-34	1.369	-4 \pm 4	109 \pm 8	NON CONF.
ivermectin	antiparasitic agents, also a GABA agonist	F	-26	1.032	-61 \pm 3	6 \pm 1	TOX
itraconazole	antifungal, triazole cytochrome P450 oxidase inhibitor	F	-34	1.363	-46 \pm 1	55 \pm 8	TOX
glimepiride	sulfonylurea anti-diabetic drug	F	-28	1.117	-33 \pm 2	100 \pm 2	CONF. HIT
III. antidepressants							
paroxetine HCl	antidepressant SSRI	F, U, P, L, B, T	-35	1.397	-50 \pm 4	96 \pm 2	CONF. HIT
paroxetine maleate	antidepressant SSRI	B	-33	1.332			
methyl-paroxetine	antidepressant SSRI	B	-32	1.260			
amoxapine	antidepressant tricyclic	F, U	-31	1.242	-36 \pm 1	71 \pm 2	TOX
sibutramine HCl	antiobesity agent, neurotransmitter (serotonin, norepinephrine) reuptake inhibitor	P	-32	1.298	-6 \pm 3	95 \pm 2	NON CONF.

Suppl. Table 3. Hit confirmation of hyperglycemia-induced mitochondrial ROS production screen (part 2/4).

Compounds that decreased the mitochondrial ROS production by 25% (ROS score > 1) but did not affect the viability (Viability score > -1) were re-tested at 10 μ M in replicates (results shown in *italic*). Compounds were categorized as toxic compounds (TOX) if reduced the viability by 10%, confirmed hits (CONF. HIT) if showed ROS production decreasing activity without affecting the viability, or non-confirmed (NON CONF.) if the average decrease in ROS production was less than 10% in the hit confirmation.

Compound Name	Biological Activity	Compound Source Library	Change in mitoROS production (%)	ROS score	ROS production MEAN \pm SEM	Viability MEAN \pm SEM	Result
IV. anti-inflammatory agents (steroids, NSAIDs, etc.)							
betamethasone	glucocorticoid steroid	L	-30	1.203	<i>-15\pm5</i>	<i>132\pm9</i>	<i>CONF. HIT</i>
budesonide	glucocorticoid steroid	U,P,L	-39	1.569	<i>-23\pm4</i>	<i>111\pm1</i>	<i>CONF. HIT</i>
dexamethasone	glucocorticoid steroid	U	-23	0.905	<i>-16\pm5</i>	<i>100\pm4</i>	<i>CONF. HIT</i>
flunisolide	glucocorticoid steroid	U	-25	1.002	<i>-25\pm6</i>	<i>112\pm2</i>	<i>CONF. HIT</i>
flurandrenolide	glucocorticoid steroid	U	-28	1.112	<i>-19\pm3</i>	<i>110\pm1</i>	<i>CONF. HIT</i>
6-alpha-methylprednisolone	glucocorticoid steroid	P	-39	1.547	<i>-17\pm1</i>	<i>102\pm1</i>	<i>CONF. HIT</i>
triamcinolone	glucocorticoid steroid	P	-26	1.049	<i>-11\pm2</i>	<i>104\pm2</i>	<i>CONF. HIT</i>
acetylsalicylic acid	NSAID	L	-27	1.091	<i>-9\pm3</i>	<i>99\pm3</i>	<i>NON CONF.</i>
piroxicam	NSAID, highly selective inhibitor of COX-1	P	-30	1.198	<i>-13\pm2</i>	<i>93\pm0</i>	<i>CONF. HIT</i>
tenoxicam	NSAID, COX inhibitor	P	-33	1.304	<i>-7\pm3</i>	<i>95\pm1</i>	<i>NON CONF.</i>
D-panthenol	antiinflammatory agent, provitamin of B5	P	-58	2.328	<i>-8\pm3</i>	<i>99\pm3</i>	<i>NON CONF.</i>
sirolimus	immunosuppressant, with antifungal activity	U	-26	1.046	<i>-60\pm4</i>	<i>103\pm1</i>	<i>CONF. HIT</i>
rolipram	PDE4-inhibitor, antiinflammatory	F	-26	1.025	<i>5\pm5</i>	<i>103\pm3</i>	<i>NON CONF.</i>
V. antimetabolites							
thioguanosine	antimetabolite	P	-42	1.675	<i>-28\pm0</i>	<i>150\pm4</i>	<i>CONF. HIT</i>
azaguanine-8	antimetabolite purine	P	-37	1.487	<i>-40\pm2</i>	<i>84\pm2</i>	<i>TOX</i>
cytarabin	antimetabolite, chemotherapy agent	U	-27	1.072	<i>-23\pm2</i>	<i>84\pm3</i>	<i>TOX</i>
L-4 chlorophenylalanine	antimetabolite	N	-32	1.278	<i>-3\pm5</i>	<i>95\pm4</i>	<i>NON CONF.</i>
VI. calcium channel inhibitors, calcium related compounds							
diltiazem hydrochloride	calcium channel blocker, (L-Type)	P	-30	1.210	<i>-11\pm1</i>	<i>86\pm4</i>	<i>TOX</i>
flunarizine	calcium channel blocker	U	-28	1.116	<i>-31\pm6</i>	<i>93\pm3</i>	<i>CONF. HIT</i>
loperamide hydrochloride	calcium channel antagonist	P	-26	1.057	<i>5\pm2</i>	<i>84\pm3</i>	<i>TOX</i>
manidipine	calcium channel blocker	F	-31	1.238	<i>-22\pm3</i>	<i>89\pm2</i>	<i>TOX</i>
nifedipine	calcium channel blocker	U	-26	1.035	<i>-26\pm1</i>	<i>88\pm5</i>	<i>TOX</i>
niguldipine	calcium channel blocker	F	-25	1.011	<i>-66\pm5</i>	<i>0.00</i>	<i>TOX</i>
perhexiline maleate	calcium channel blocker, mitochondrial carnitine palmitoyltransferase-1 inhibitor	P	-27	1.097	<i>-1\pm2</i>	<i>70\pm4</i>	<i>TOX</i>
pimozide	calcium channel inhibitor, caspase-3 inhibitor	T	-48	1.904	<i>5\pm3</i>	<i>91\pm4</i>	<i>NON CONF.</i>

Suppl. Table 3. Hit confirmation of hyperglycemia-induced mitochondrial ROS production screen (part 3/4).

Compounds that decreased the mitochondrial ROS production by 25% (ROS score > 1) but did not affect the viability (Viability score > -1) were re-tested at 10 μ M in replicates (results shown in *italic*). Compounds were categorized as toxic compounds (TOX) if reduced the viability by 10%, confirmed hits (CONF. HIT) if showed ROS production decreasing activity without affecting the viability, or non-confirmed (NON CONF.) if the average decrease in ROS production was less than 10% in the hit confirmation.

Compound Name	Biological Activity	Compound Source Library	Change in mitoROS production (%)	ROS score	ROS production MEAN \pm SEM	Viability MEAN \pm SEM	Result
VII. GABAergic mediators, inhibitors							
carisoprodol	GABA A receptor activator, centrally acting muscle relaxant	P	-31	1.220	-5 \pm 5	98 \pm 1	NON CONF.
thiocolchicoside	GABA agonist, muscle relaxant	P	-30	1.192	7 \pm 5	99 \pm 2	NON CONF.
gabazine	GABA antagonist	P	-37	1.461	-4 \pm 1	96 \pm 1	NON CONF.
VIII. Glutamatergic mediators, inhibitors							
l-BCP	glutamatergic, selective potentiator of AMPA-mediated responses	T	-34	1.379	-21 \pm 3	96 \pm 3	CONF. HIT
IX. cholinergic mediators, muscle relaxants							
neostigmine	parasympathomimetic that acts as a reversible acetylcholinesterase inhibitor	U	-29	1.150	-15 \pm 3	94 \pm 2	CONF. HIT
procyclidine HCl	muscle relaxant, muscarinic antagonist, blocks of central cholinergic receptors M1, M2 and M4	P	-27	1.063	-3 \pm 4	100 \pm 3	NON CONF.
X. microtubular agents							
colchicine	microtubular agent	K, U	-28	1.11	-29 \pm 5	95 \pm 1	CONF. HIT
nocodazole	microtubule inhibitor	T	-25	1.00	-35 \pm 2	92 \pm 4	CONF. HIT
XI. mitochondrial respiratory chain inhibitors							
roflumetinolol	uncoupling agent, inhibits PKC isoforms	N	-38	1.503	-35 \pm 3	96 \pm 2	CONF. HIT
XII. retinoids							
acitretin	retinoid, nuclear receptor regulator	P	-27	1.073	-25 \pm 4	81 \pm 2	TOX
tretinon	retinoid, used in acute promyelocytic leukemia	U	-34	1.341	-26 \pm 1	108 \pm 4	CONF. HIT

Suppl. Table 3. Hit confirmation of hyperglycemia-induced mitochondrial ROS production screen (part 4/4).

Compounds that decreased the mitochondrial ROS production by 25% (ROS score > 1) but did not affect the viability (Viability score > -1) were re-tested at 10 μ M in replicates (results shown in *italic*). Compounds were categorized as toxic compounds (TOX) if reduced the viability by 10%, confirmed hits (CONF. HIT) if showed ROS production decreasing activity without affecting the viability, or non-confirmed (NON CONF.) if the average decrease in ROS production was less than 10% in the hit confirmation.

Compound Name	Biological Activity	Compound Source Library	Change in mitoROS production (%)	ROS score	ROS production MEAN \pm SEM	Viability MEAN \pm SEM	Result
XIII. various compounds							
A) clinical drugs							
bromhexine	mucolytic agent	F	-28	1.122	<i>7\pm5</i>	<i>93\pm4</i>	NON CONF.
dimenhydrinate	H1 histamine antagonist	P	-33	1.333	<i>-13\pm3</i>	<i>89\pm1</i>	TOX
promethazine	H1 receptor antagonist	F	-27	1.075	<i>1\pm4</i>	<i>87\pm1</i>	TOX
suloctidil	platelet inhibiting agent, vasodilator	P	-32	1.277	<i>-4\pm1</i>	<i>70\pm3</i>	TOX
cisapride	5-HT antagonist, peristaltic stimulant	P	-35	1.402	<i>-4\pm1</i>	<i>90\pm1</i>	NON CONF.
racecadotril	antidiarrheal drug, enkephalinase inhibitor	F	-25	1.011	<i>-1\pm5</i>	<i>102\pm1</i>	NON CONF.
canrenone	aldosterone antagonist	F	-26	1.045	<i>-7\pm3</i>	<i>97\pm5</i>	NON CONF.
hydroflumethiazide	diuretics, Na ⁺ Cl ⁻ transport inhibitor, carbonic anhydrase inhibitor, cAMP PDE inhibitor	P	-41	1.629	<i>-7\pm4</i>	<i>90\pm1</i>	TOX
sulfinpyrazone	uricosuric, inhibitor of the urate anion transporter, also CFTR and COX inhibitor	P	-26	1.022	<i>-19\pm3</i>	<i>80\pm5</i>	TOX
B) natural products							
cytidine 5'-monophosphate	pyrimidine base	N	-28	1.121	<i>-12\pm4</i>	<i>84\pm8</i>	TOX
5-hydroxy-3'-methoxyflavone	cytotoxic flavonoid from Miliusa balansae, may reduce respiratory burst	N	-26	1.052	<i>6\pm4</i>	<i>113\pm2</i>	NON CONF.
L(+) citrulline	amino acid, participates in urea cycle	N	-25	1.005	<i>-13\pm1</i>	<i>100\pm3</i>	CONF. HIT
C) compounds for research use only							
chrysene-1,4-quinone	mutagenic agent	P	-31	1.240	<i>-12\pm2</i>	<i>51\pm2</i>	TOX
chromanol 293B	I _K blocker. Also blocks I _{CFTR}	T	-30	1.213	<i>1\pm1</i>	<i>104\pm3</i>	NON CONF.
SG 209	K ⁺ channel opener	T	-35	1.405	<i>0\pm4</i>	<i>94\pm8</i>	NON CONF.
ivachtin	caspase-3 inhibitor	T	-27	1.067	<i>5\pm5</i>	<i>86\pm3</i>	TOX

Suppl. Table 4. Comparison of gene expression profiles of b.END3 endothelial cells exposed to hyperglycemia with paroxetine treatment or vehicle analyzed by the mouse mitochondrial energy metabolism gene expression array (part 1/2). Gene expression changes were analyzed with mitochondrial energy array in bEND.3 cells exposed to hyperglycemia for 7 days and treated with paroxetine (10 μ M) or vehicle for 3 days as described for **Suppl. Table 2. (Significant differences are shown in bold. Please note, that we could not confirm significant changes in Lhpp expression in subsequent tests and the C_T values of Cox6a2 were above 35. Statistically significant, but less than 1.2-fold change in gene expression was not followed up.)**

Gene Symbol	Gene name	fold change	T-TEST	fold up- or down-regulation
		high+PRX /high glc	p value	high+PRX /high glc
Lhpp	Phospholysine phosphohistidine inorganic pyrophosphate phosphatase	1.49	0.013856	1.49
Atp12a	ATPase, H ⁺ /K ⁺ transporting, nongastric, alpha polypeptide	1.30	0.181013	1.30
Atp4a	ATPase, H ⁺ /K ⁺ exchanging, gastric, alpha polypeptide	1.06	0.738769	1.06
Atp4b	ATPase, H ⁺ /K ⁺ exchanging, beta polypeptide	1.01	0.962724	1.01
Atp5a1	ATP synthase, H ⁺ transporting, mitochondrial F1 complex, alpha subunit 1	1.04	0.586647	1.04
Atp5b	ATP synthase, H ⁺ transporting, mitochondrial F1 complex, beta subunit	1.02	0.907093	1.02
Atp5c1	ATP synthase, H ⁺ transporting, mitochondrial F1 complex, gamma polypeptide 1	1.13	0.068191	1.13
Atp5d	ATP synthase, H ⁺ transporting, mitochondrial F1 complex, delta subunit	1.06	0.595067	1.06
Atp5f1	ATP synthase, H ⁺ transporting, mitochondrial F0 complex, subunit B1	1.01	0.806560	1.01
Atp5g1	ATP synthase, H ⁺ transporting, mitochondrial F0 complex, subunit c1 (subunit 9)	0.84	0.495957	-1.20
Atp5g2	ATP synthase, H ⁺ transporting, mitochondrial F0 complex, subunit C2 (subunit 9)	1.07	0.184877	1.07
Atp5g3	ATP synthase, H ⁺ transporting, mitochondrial F0 complex, subunit C3 (subunit 9)	0.93	0.384719	-1.07
Atp5h	ATP synthase, H ⁺ transporting, mitochondrial F0 complex, subunit d	1.15	0.025099	1.15
Atp5j	ATP synthase, H ⁺ transporting, mitochondrial F0 complex, subunit F	1.12	0.015634	1.12
Atp5j2	ATP synthase, H ⁺ transporting, mitochondrial F0 complex, subunit F2	1.12	0.194507	1.12
Atp5o	ATP synthase, H ⁺ transporting, mitochondrial F1 complex, O subunit	1.08	0.421280	1.08
Atp6v0a2	ATPase, H ⁺ transporting, lysosomal V0 subunit A2	1.06	0.012648	1.06
Atp6v0d2	ATPase, H ⁺ transporting, lysosomal V0 subunit D2	0.86	0.362030	-1.17
Atp6v1c2	ATPase, H ⁺ transporting, lysosomal V1 subunit C2	1.04	0.963301	1.04
Atp6v1e2	ATPase, H ⁺ transporting, lysosomal V1 subunit E2	1.04	0.916908	1.04
Atp6v1g3	ATPase, H ⁺ transporting, lysosomal V1 subunit G3	1.30	0.181013	1.30
Bcs1l	BCS1-like (yeast)	1.01	0.872749	1.01
Cox11	COX11 homolog, cytochrome c oxidase assembly protein (yeast)	0.96	0.322245	-1.05
Cox4i1	Cytochrome c oxidase subunit IV isoform 1	1.13	0.476330	1.13
Cox4i2	Cytochrome c oxidase subunit IV isoform 2	1.07	0.116874	1.07
Cox5a	Cytochrome c oxidase, subunit Va	1.08	0.515839	1.08
Cox5b	Cytochrome c oxidase, subunit Vb	1.07	0.194962	1.07
Cox6a1	Cytochrome c oxidase, subunit VI a, polypeptide 1	0.87	0.071195	-1.15
Cox6a2	Cytochrome c oxidase, subunit VI a, polypeptide 2	2.61	0.001383	2.61
Cox6b1	Cytochrome c oxidase, subunit VIb polypeptide 1	1.11	0.062478	1.11
Cox6b2	Cytochrome c oxidase subunit VIb polypeptide 2	1.30	0.236259	1.30
Cox6c	Cytochrome c oxidase, subunit VIc	1.13	0.263812	1.13
Cox7a2	Cytochrome c oxidase, subunit VIIa 2	1.19	0.164027	1.19
Cox7a2l	Cytochrome c oxidase subunit VIIa polypeptide 2-like	1.01	0.856668	1.01
Cox7b	Cytochrome c oxidase subunit VIIb	1.13	0.207663	1.13
Cox8a	Cytochrome c oxidase, subunit VIIIA	1.15	0.151049	1.15
Cox8c	Cytochrome c oxidase, subunit VIIIC	1.30	0.181013	1.30
Cyc1	Cytochrome c-1	0.94	0.186497	-1.06

Suppl. Table 4. Comparison of gene expression profiles of b.END3 endothelial cells exposed to hyperglycemia with paroxetine treatment or vehicle analyzed by the mouse mitochondrial energy metabolism gene expression array (part 2/2). Gene expression changes were analyzed with mitochondrial energy array in bEND.3 cells exposed to hyperglycemia for 7 days and treated with paroxetine (10 μ M) or vehicle for 3 days as described for **Suppl. Table 2. (Significant differences are shown in bold. Please note, that we could not confirm significant changes in Lhpp expression in subsequent tests and the C_T values of Cox6a2 were above 35. Statistically significant, but less than 1.2-fold change in gene expression was not followed up.)**

Gene Symbol	Gene name	fold change	T-TEST	fold up- or down-regulation
		high+PRX /high glc	p value	high+PRX /high glc
Ndufa1	NADH dehydrogenase (ubiquinone) 1 alpha subcomplex, 1	1.19	0.021836	1.19
Ndufa10	NADH dehydrogenase (ubiquinone) 1 alpha subcomplex 10	1.08	0.135229	1.08
Ndufa11	NADH dehydrogenase (ubiquinone) 1 alpha subcomplex 11	0.82	0.814655	-1.22
Ndufa2	NADH dehydrogenase (ubiquinone) 1 alpha subcomplex, 2	1.08	0.108171	1.08
Ndufa3	NADH dehydrogenase (ubiquinone) 1 alpha subcomplex, 3	1.08	0.062500	1.08
Ndufa4	NADH dehydrogenase (ubiquinone) 1 alpha subcomplex, 4	1.04	0.635004	1.04
Ndufa5	NADH dehydrogenase (ubiquinone) 1 alpha subcomplex, 5	1.02	0.754086	1.02
Ndufa6	NADH dehydrogenase (ubiquinone) 1 alpha subcomplex, 6 (B14)	1.23	0.052835	1.23
Ndufa7	NADH dehydrogenase (ubiquinone) 1 alpha subcomplex, 7 (B14.5a)	1.04	0.143405	1.04
Ndufa8	NADH dehydrogenase (ubiquinone) 1 alpha subcomplex, 8	0.96	0.701452	-1.04
Ndufab1	NADH dehydrogenase (ubiquinone) 1, alpha/beta subcomplex, 1	1.35	0.062480	1.35
Ndufb10	NADH dehydrogenase (ubiquinone) 1 beta subcomplex, 10	0.91	0.619764	-1.10
Ndufb2	NADH dehydrogenase (ubiquinone) 1 beta subcomplex, 2	1.04	0.558614	1.04
Ndufb3	NADH dehydrogenase (ubiquinone) 1 beta subcomplex 3	0.96	0.597986	-1.04
Ndufb4	NADH dehydrogenase (ubiquinone) 1 beta subcomplex 4	1.04	0.074337	1.04
Ndufb5	NADH dehydrogenase (ubiquinone) 1 beta subcomplex, 5	1.07	0.874418	1.07
Ndufb6	NADH dehydrogenase (ubiquinone) 1 beta subcomplex, 6	1.04	0.419691	1.04
Ndufb7	NADH dehydrogenase (ubiquinone) 1 beta subcomplex, 7	1.16	0.080872	1.16
Ndufb8	NADH dehydrogenase (ubiquinone) 1 beta subcomplex 8	1.03	0.664122	1.03
Ndufb9	NADH dehydrogenase (ubiquinone) 1 beta subcomplex, 9	1.01	0.856513	1.01
Ndufc1	NADH dehydrogenase (ubiquinone) 1, subcomplex unknown, 1	1.09	0.176985	1.09
Ndufc2	NADH dehydrogenase (ubiquinone) 1, subcomplex unknown, 2	0.97	0.794978	-1.03
Ndufs1	NADH dehydrogenase (ubiquinone) Fe-S protein 1	1.10	0.152897	1.10
Ndufs2	NADH dehydrogenase (ubiquinone) Fe-S protein 2	1.01	0.750776	1.01
Ndufs3	NADH dehydrogenase (ubiquinone) Fe-S protein 3	1.03	0.604331	1.03
Ndufs4	NADH dehydrogenase (ubiquinone) Fe-S protein 4	0.99	0.801664	-1.01
Ndufs5	NADH dehydrogenase (ubiquinone) Fe-S protein 5	1.07	0.324852	1.07
Ndufs6	NADH dehydrogenase (ubiquinone) Fe-S protein 6	1.14	0.125132	1.14
Ndufs7	NADH dehydrogenase (ubiquinone) Fe-S protein 7	1.03	0.835572	1.03
Ndufs8	NADH dehydrogenase (ubiquinone) Fe-S protein 8	0.88	0.437864	-1.14
Ndufv1	NADH dehydrogenase (ubiquinone) flavoprotein 1	1.05	0.551239	1.05
Ndufv2	NADH dehydrogenase (ubiquinone) flavoprotein 2	1.11	0.294270	1.11
Ndufv3	NADH dehydrogenase (ubiquinone) flavoprotein 3	1.23	0.292898	1.23
Oxa11	Oxidase assembly 1-like	1.15	0.066023	1.15
Ppa1	Pyrophosphatase (inorganic) 1	0.95	0.313819	-1.05
Ppa2	Pyrophosphatase (inorganic) 2	1.19	0.054890	1.19
Sdha	Succinate dehydrogenase complex, subunit A, flavoprotein (Fp)	1.02	0.719138	1.02
Sdhb	Succinate dehydrogenase complex, subunit B, iron sulfur (Ip)	1.00	0.961844	-1.00
Sdhc	Succinate dehydrogenase complex, subunit C, membrane protein	1.11	0.084638	1.11
Sdhd	Succinate dehydrogenase complex, subunit D, membrane protein	1.03	0.747767	1.03
Uqcr11	Ubiquinol-cytochrome c reductase, complex III subunit XI	1.10	0.118082	1.10
Uqcr1	Ubiquinol-cytochrome c reductase core protein 1	0.99	0.429415	-1.01
Uqcr2	Ubiquinol cytochrome c reductase core protein 2	1.01	0.924818	1.01
Uqcrfs1	Ubiquinol-cytochrome c reductase, Rieske iron-sulfur polypeptide 1	1.11	0.067253	1.11
Uqcrh	Ubiquinol-cytochrome c reductase hinge protein	1.11	0.269416	1.11
Uqcrq	Ubiquinol-cytochrome c reductase, complex III subunit VII	1.09	0.194837	1.09